

https://dspace.org/

Analysis of the dynamic power requirements for controllable energy storage on photovoltaic microgrid

Horonga, Nyasha

2016

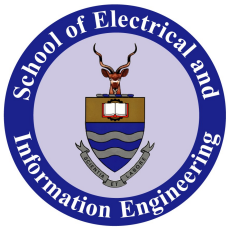
http://hdl.handle.net/10539/22674

Horonga, Nyasha (2016) Analysis of the dynamic power requirements for controllable energy storage on photovoltaic microgrid, University of the Witwatersrand, Johannesburg, <http://hdl.handle.net/10539/22674>

Downloaded from a DSpace repository. https://dspace.org/

ANALYSIS OF THE DYNAMIC POWER REQUIREMENTS FOR

CONTROLLABLE ENERGY STORAGE ON PHOTOVOLTAIC MICROGRID



Nyasha Horonga

School of Electrical and Information Engineering

University of the Witwatersrand

A dissertation submitted to the Facaulty of Engineering and the Built Environment, University of the Witwatersrand in fulfilment of the requirements of the degree of

Master of science in Engineering

September 2016

Declaration

I, **Nyasha Horonga**, declare that this dissertation titled, **ANALYSIS OF THE DYNAMIC POWER REQUIREMENTS FOR CONTROLLABLE ENERGY STORAGE ON PHOTOVOLTAIC MICROGRID** and the work presented in it are my own. I confirm that:

- This work was done wholly or mainly while in candidature for a research degree at this University.
- Where any part of this dissertation has previously been submitted for a degree or any other qualification at this University or any other institution, this has been clearly stated.
- Where I have consulted the published work of others, this is always clearly attributed.
- Where I have quoted from the work of others, the source is always given. With the exception of such quotations, this dissertation is entirely my own work.
- I have acknowledged all main sources of help.
- Where the dissertation is based on work done by myself jointly with others, I have made clear exactly what was done by others and what I have contributed myself.

Signed:

Date:

I would like to dedicate this dissertation to my loving parents, my fiancee Zanele Njazi and my siblings Simbarashe, Tapiwanashe, Cynthia and Tonderai

Our premise is that many of the circumstances that seem to block us in our daily lives may only appear to do so based on a framework of assumption we carry with us. Draw a different frame around the same set of circumstances and new pathways come into view

The Art of Possibility - R.S. Zander

Acknowledgements

The author would like to thank the ALSTOM chair for clean energy system technology for funding the research. Most of all the Author would like to thank the Supervisor Prof W.A. Cronje and the University of the Witwatersrand Energy group for their continued support during the course of the research.
Special thanks to W. Doorsamy and Dr M. Shuma-iwisi for their valuable inputs.

Abstract

Standalone microgrid studies are being done because an expansion of the existing utility grids to supply power to remote communities is not feasible. Standalone microgrids can be considered as one of the solutions for remote communities because power can be generated close to these communities and it minimizes cost related to power transmission. Renewable energy sources with large fluctuations are frequently the source of power for these standalone microgrids. The fluctuating nature of these renewable sources can often lead to frequent blackouts. This research is aimed at minimizing power fluctuations using controllable energy storage systems. This MSc focuses on the analysis of the ramp rate and delay time requirements for controllable energy storage system used in standalone PV microgrids. Measured insolation data and recorded load demand data for typical domestic appliances are used in this study to analyze ramp rates present. The ramp rates are then used to determine the range of energy storage ramp rate and delay time required to maintain the microgrid voltage within the standardized range of 1pu±5%. From the recorded data it has been observed that PV power can be sampled from at least 1-second intervals without losing important information. The 1 second averaged ramp rates obtained from the insolation data measurements have been found to have the highest value of 0.12pu/sec. However, this ramp rate increases to 0.3pu/sec when the allowable microgrid voltage band is narrow (1pu±5%). These insolation ramp rates are very low compared to the ramp rates of typical loads that can be connected to a microgrid. This means that, if the energy storage system is specified to meet the load ramp rate requirements, it will be able to respond to the fluctuating PV power. The results obtained from the simulations confirm that energy storage system ramp rate plays an important role in the stability of a standalone microgrid. The minimum allowable energy storage ramp rate was found to be 8.15pu/sec for load transients with a ramp time of 20ms. This value is 28 times the energy storage ramp rate required to cancel out insolation fluctuations. This further confirms that energy storage system ramp rates must be specified using the load demand data. The maximum allowable delay time was also found to be 0.53s to maintain the microgrid voltage within the standardized range of 1pu±5%. This delay time is applicable when canceling out only the insolation fluctuations. To cancel out load transient power fluctuations, there should be no delay time.

Contents

Contents vi

List of Figures ix

Acronyms 1

Symbols 2

Important Definitions 3

1 Introduction 4

1.1 Introduction 4

1.2 Research objectives 9

1.3 Research assumptions 10

1.4 Research Methodology 12

1.5 Dissertation Overview 12

2 Literature Review 14

2.1 Introduction 14

2.2 Highlights on the importance of standalone microgrids 15

2.3 Current situation in microgrids 16

2.3.1 Diakha Madina standalone microgrid in Senegal 16

2.3.2 Olosho-Oibor standalone microgrid in Kenya 17

2.3.3 Akkan standalone microgrid in Morocco 17

2.3.4 Discussion on the microgrid examples . . . 18
2.4 Current studies on variability of PV sources . . . 18
2.4.1 Size of the PV array . . . 19
2.4.2 Centralized vs distributed . . . 20
2.4.3 Local cloud pattern . . . 20
2.5 Methods for reductions of power fluctuations on microgrid . . . 21
2.6 Potential energy storage systems for a microgrid . . . 22
2.7 Gap in knowledge . . . 25
2.8 Summary . . . 25

3 Energy Resource and Load Data Analysis 27
3.1 Introduction . . . 27
3.2 PV source and load data analysis . . . 28
3.3 Data set validation . . . 30
3.4 Analysis of PV data variations . . . 32
3.5 Analysis of load demand variations . . . 34
3.6 Summary . . . 43

4 Microgrid Simulations 45
4.1 Introduction . . . 45
4.2 Microgrid model . . . 46
4.3 Microgrid model validation . . . 47
4.4 Simplified PV source inverter model . . . 48
4.5 Energy storage model . . . 51
4.6 Requirements for reliable operation of a collocated standalone microgrid . . . 55
4.7 Simulations of a standalone microgrid without a controllable energy storage system . . . 55
4.8 Simulations of a standalone microgrid with a controllable energy storage present . . . 60
4.8.1 Simulation with constant load . . . 61

4.8.2 Simulation with a varying load 63
4.9 Summary 63

5 Discussion of Simulation Results **64**
5.1 Introduction 64
5.2 Discussion of Simulation Results 64
5.3 Summary 72

6 Conclusions and Recommendations **73**
6.1 Conclusions 73
6.1.1 Findings from PV source and load demand ramp rate analysis . . . 74
6.1.2 Findings from the microgrid simulations 75
6.2 Recommendations 76

References **78**

A Data Measurements **i**
A.1 Introduction i
A.2 PV Data Measurements i
A.3 Determining The Sampling Rate ii
A.4 Using Nyquist' Sampling Theorem ii
A.5 Using Graphical Method iii
A.6 Conclusion ix

B Ramp Rate Analysis MATLAB Code **x**
B.1 Introduction x
B.2 MATLAB Code x

C Publications **xx**
C.1 Introduction xx

List of Figures

1.1 Electricity access regional aggregates [1]. 5

1.2 Globally installed capacities of Wind and PV as at December 2013 [2]. . . . 6

1.3 Power triangle showing power angle θ. Most appliances have a power angle less than 45°. 11

2.1 A diagram showing different energy storage technologies together with their power and energy capabilities [3]. 23

2.2 The dynamic characteristic the study will focus on. t_1 is the response time while P_m/t_2 is the ramp rate. 24

3.1 A single line schematic example of a three-phase low voltage standalone microgrid system. 28

3.2 Normalized measured insolation (W/m^2) obtained at the Chamber of mines building (Wits University). The insolation values were normalized to the insolation peak for the 2 days shown in this figure. The data was sampled at 40ms intervals. 30

3.3 Normalized measured power demand for the Genmin building (Wits University). The power demand values were normalized to the Genmin building load peak for the 2 days shown in this figure. The original data was sampled at 100ms intervals and re-sampled at 1 second intervals. 31

3.4 PV inverter output overlaid on the insolation data. 32

3.5 An extract of the data in figure 3.4. 33

3.6 Ramp rates for the insolation data recorded on the roof of Chamber of mines building at the University of the Witwatersrand. 34
3.7 Insolation data overlaid on the ramp rate data. 35
3.8 Circuit diagram used to measure the ramp rate of typical house appliances that can be connected to a microgrid. 37
3.9 The experimental setup used to measure the ramp rate for household appliances 38
3.10 Measured power required by a laptop charger few seconds after closing the switch. 39
3.11 Measured power consumed by a light bulb during the first 2 seconds. 39
3.12 Measured power consumed by a 1.5kW rated microwave during the first 30 seconds. 40
3.13 Measured power consumed by a 2kW rated heater during the first 1 second. 40
3.14 Measured power consumed by a 68W rated fridge during the first 1 second. 41

4.1 Simulation circuit for a standalone microgrid with a current and a voltage source modeling a PV source + inverter and an energy storage+ inverter respectively. 46
4.2 Power flow through a power line. 49
4.3 V-I curve illustrating the operation of a simplified grid-forming PV inverter used. 51
4.4 A block diagram showing the operation of the grid-forming PV inverter. . . 52
4.5 A flow diagram for the basic energy storage controller used in the simulations. 53
4.6 A system block diagram showing the required inputs and how it is connected to the microgrid. 54
4.7 A Simulink® model of a standalone microgrid without a controllable energy storage. 56
4.8 A Simulink® block diagram showing the simplified PV inverter controller used in the simulation. 57

4.9 The simulated voltage of a standalone microgrid without a controllable energy storage. 58
4.10 The simulated voltages showing the effects of adding load on a standalone microgrid without controllable energy storage 59
4.11 A standalone microgrid Simulink® model used to determine the controllable energy storage ideal response. 60
4.12 A Simulink® block diagram of the energy storage controller. 61
4.13 Response of an ideal energy storage to a standalone microgrid with a fluctuating source and a constant resistive load. 61
4.14 Response of an energy storage system to a standalone microgrid with a fluctuating source and a varying resistive load. 62
4.15 An extract of the data in figure 4.14 clearly showing that the energy storage must match that of a load with faster dynamics. 62

5.1 Effects of energy storage delay time on the microgrid voltage. 66
5.2 Effects of ramp rate on the microgrid voltage. Increasing the ramp rate of the energy storage would result in a stable microgrid. 67
5.3 Effects of delay time on the magnitude of voltage swells and voltage sags caused by PV panel power fluctuations 68
5.4 The effects of energy storage system ramp rate on the voltage of a standalone microgrid with loads with a ramp time of 20ms and above. 69
5.5 The effects of energy storage system ramp rate on a standalone microgrid with a PV source and a constant load. 70
5.6 The graphs show that an increase in the energy required by the load can result in insufficient charging time for the energy storage system to fully charge at least once in a 24hr period. Normal operation requires the state of charge of the energy storage 50% at the beginning of each day. 71

6.1 System block diagram of the microgrid testbed that will be used in this study. 77

6.2 System block diagram of an emulator that can be used as PV source or load or storage depending on the control signal. 77

A.1 A typical normalized insolation data recorded at the University of Witwatersrand, Johannesburg, South Africa. iii

A.2 Insolation data spectral analysis for a typical day in Johannesburg. iv

A.3 Heat map for 5 minute ramp rates of the insolation data recorded. The heat map also shows change in colour vertically which is an indication of under-sampling. vi

A.4 Heat map for 3 minute ramp rates of the insolation data recorded. vii

A.5 Heat map for 1 minute ramp rates of the insolation data recorded. The colour does not change vertically which is an indication that the data is being sampled at an appropriate ramp rate. viii

Acronyms

ESS	-	Energy Storage System
PV	-	Photovoltaic
DG	-	Distributed Generation
DC	-	Direct Current
AC	-	Alternating Current
LED	-	Light Emitting Diode
SoC	-	State of Charge
PHS		Pumped Hydro-Storage

Symbols

I_{pv+inv}	-	Norton equivalent current for the PV system.
R_{pv+inv}	-	Norton equivalent resistance for the PV system
V_{E+inv}	-	Thevenin equivalent voltage for the ESS.
R_{E+inv}	-	Thevenin equivalent resistance for the ESS
pu	-	per unit.
sec	-	seconds.
kWp	-	kiloWatt peak.
Ah	-	Amp-hour.
kWh	-	kiloWatt hour.
$P_{G(i,j,k)}$	-	Technical constraint that ensures power balance of the system.
W/m^2	-	Watt per square meter.
$\mathrm{R_{ave}}$	-	average ramp rate.
$\mathrm{R_{max}}$	-	peak ramp rate.
δ	-	power angle
V_{grid}	-	grid voltage
V_{grid}	-	grid voltage
f_0	-	Frequency setpoint

Important Definitions

PV system	-	A combination of the PV panels and a three-phase inverter.
ESS	-	A combination of the energy storage technology and a three-phase inverter.
Delay time	-	The amount of time the energy storage system requires to respond to a change in power demand.
Ramp rate	-	The rate at which the power flow can change. The ramp rate is also known as the slew rate.
Smoothen	-	Reduction of fluctuations on a power network.

Chapter 1

Introduction

1.1 Introduction

Studies have shown that more than 33% of the world's population has no access to electricity. The International Energy Agency (IEA) published a report that put the number of people without electricity at 1.2 billion [1]. The breakdown of this number is shown in figure 1.1.This figure shows that the highest number of people with no access to electricity are in Sub-Saharan Africa. The IEA report further pointed out that most of the affected communities are in remote areas where rural electrification was at 17% in 2014 [1]. The reason behind low rural electrification is mainly high transmission line costs and low power generation capacity. While most of the utility companies battle to keep up with the growing electricity demand in urban areas, remote communities are often the least serviced.

In Southern Africa particularly in Zimbabwe and South Africa, reports have suggested, that lack of maintenance of generators and transmission lines has led to decrease in power generation. At present in South Africa, power generation capacity has become lower than the growing power demand. This resulted in implementation of loadshedding across the

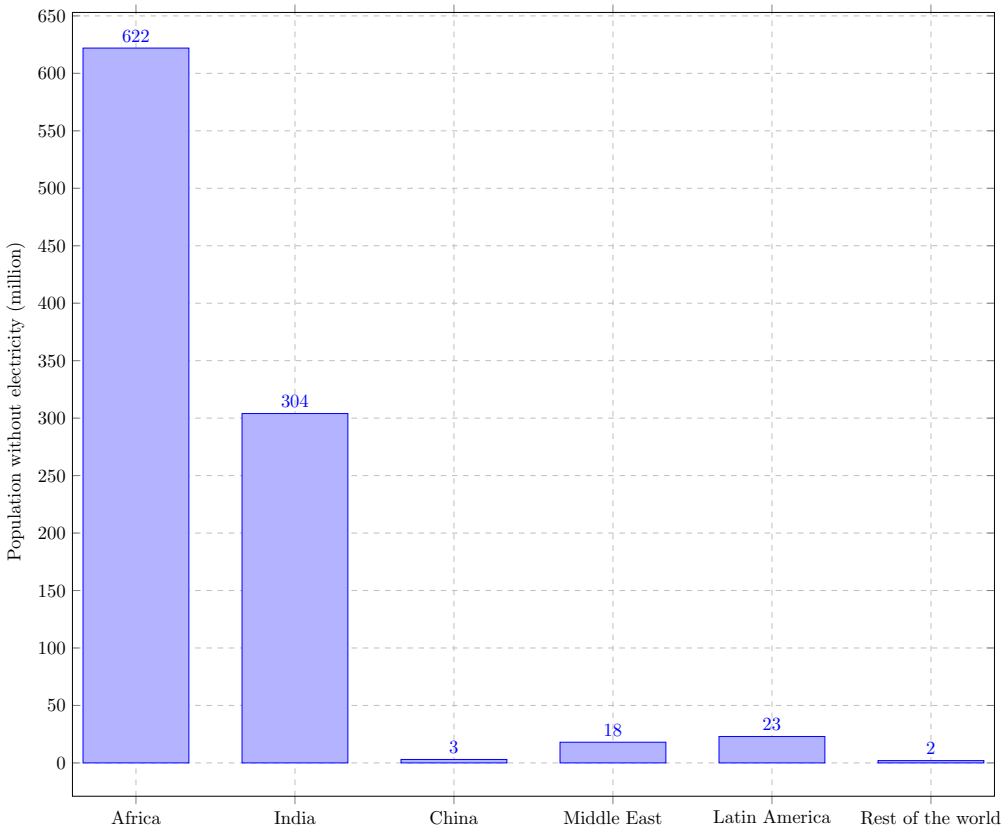


Figure 1.1. Electricity access regional aggregates [1].

country which negatively impacted on economic development. Global warming is beginning to affect electricity generation. In Zimbabwe for example, hydropower is the main source of electricity and it has been reported that the water levels at the main dams have become low due to high temperatures and low rainfall recorded over the past year [4]. It is becoming increasingly difficult for the utility companies to ramp-up rural electrification programs in the midst of this electricity crisis.

Microgrids are considered to be one of the promising technologies which can be used to the supply of electricity to remote communities. A microgrid is a low voltage power network that consists of Distributed Generation (DG), energy storage and loads [5]. These

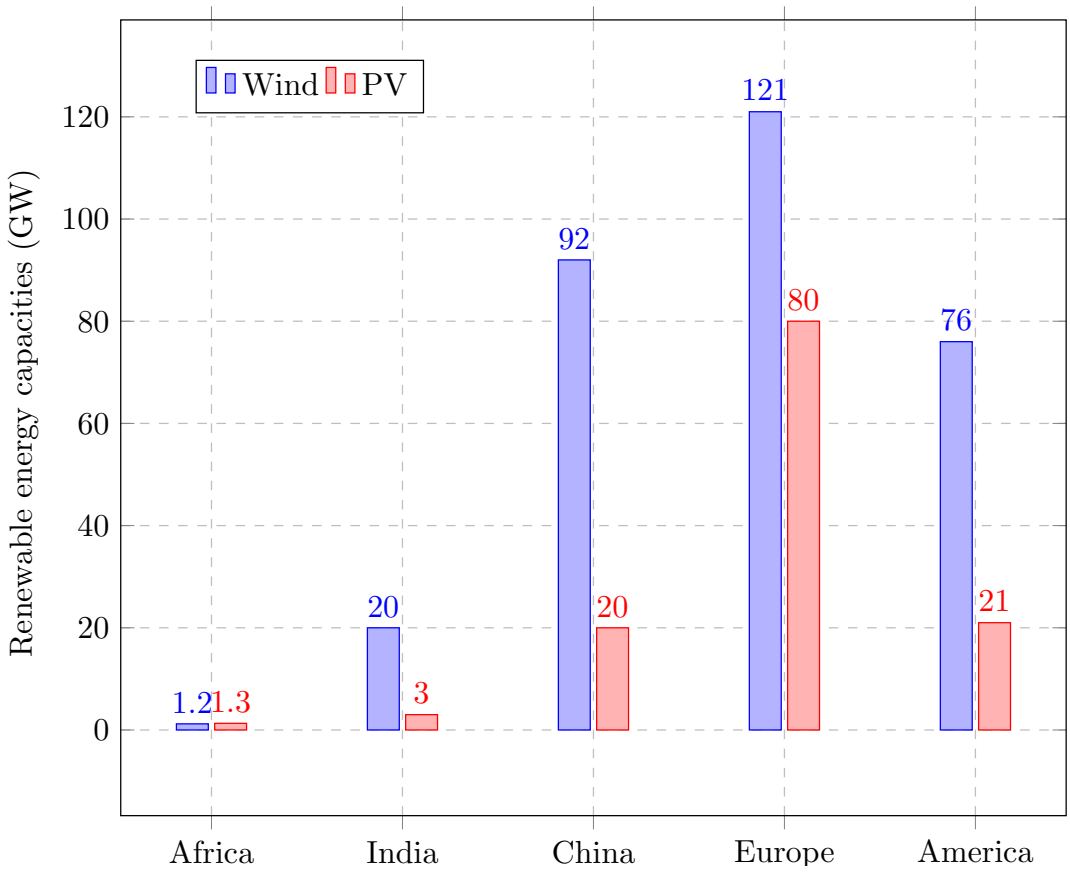


Figure 1.2. Globally installed capacities of Wind and PV as at December 2013 [2].

microgrids can operate in two modes, a grid-connect mode and a standalone mode.

In grid-connected mode, the microgrid is connected to the utility grid at a single point of connection. This mode reduces transmission line losses, increases local reliability, provides uninterrupted power supply during blackouts (i.e. it reduces over-reliance on the main utility grid). Grid-connect mode can also be used to reduce pressure on the utility grid during peak time. Currently, there are no reports in South Africa suggesting that the penetration of fluctuating renewable energy has reached significant levels to destabilize the operation of power systems at the point of connection. This is because the law does not allow households to feed power into the utility grid. The current grid-connected microgrids are small in capacity and any power fluctuations that may be produced are easily absorbed by the

utility grid without causing stability problems. However due to the increase in the use of renewable energy sources (i.e. increase in the capacity of grid-connected microgrids), the fluctuating power dynamics of the renewable sources may disturb the stability of the utility grid.

Standalone microgrids, on the other hand, are completely isolated from the main utility grid. These types of microgrids are mainly built in areas where utility grid cannot service. Standalone microgrids use mainly renewable sources and diesel generators as energy sources.

Renewable energy in particular has some advantages over the conventional methods of generating electricity (coal-fired stations). Some key advantages are:

1. The power is easily available and can be generated close to the consumers. This reduces the cost related to transmission of power from central stations.
2. Renewable energy sources have low carbon footprints.
3. A reduction in reliance on foreign energy sources.
4. They have the potential to create jobs.
5. They balance the use of fossils fuels.

The use of renewable energy sources has not been fully developed, particularly in Africa as shown in figure 1.2. Renewable energy sources provide a partial solution to electrification of rural areas, mainly because they do not provide continuous power generation to support the load [6]. This is due to the intermittent nature of renewable energy sources such as solar and wind energy [6]. For this reason, renewable energy sources have not been considered as a viable solution in Africa over the past years.

Power system equipment has also been reported damaged as a result of power fluctuations on a system. These power fluctuations are caused by the fluctuating nature of renewable sources and the nature of the load connected to standalone microgrids [7]. Power system

equipment is designed to operate within specific voltage and frequency bands and any deviation from these bands which may be caused by the grid power fluctuations can lead to power quality problems. These include [8]:

- Voltage sags and swells.
- Voltage transients.
- Over-voltage and under-voltages.
- Harmonic distortions.

Power fluctuations on a standalone microgrid can lead to voltage sags and voltages swells and the focus of this research is to detect these disturbances and how to respond before they result in brown-outs and black-outs. Other power quality issues are not part of the research.
Voltage sags and swells are variations in the voltage magnitude due to short circuit or overload or switching of large capacitors or removal of loads from a power network [8]. Connecting an energy source that can quickly ramp up or down to align the power generation with demand can minimize the occurrence of voltage swells and voltage sags on a power system[6]. Controllable energy storage can be used to address these issues as it can act as a buffer to either absorb excess power or supply power to meet the demand requirements [6].

When designing a microgrid, studies must be done to ensure that the power system components that are required, such as the distributed generation sources and energy storage are properly sized and chosen to supply sufficient power to the load while minimizing the cost of construction. Some of the energy storage technologies are very expensive and therefore a certain amount of optimization is necessary. This optimization requires that the size, ramp rate and delay time of the required energy storage system has to be specified. The

sizing of storage on the energy balance perspective has been addressed by many authors [9; 10] and this research therefore focuses on the ramp rate and delay time.

1.2 Research objectives

This research focuses on investigating the ramp rate and delay time requirements for controllable energy storage systems which are required to used to stabilize a three-phase low voltage PV microgrid. The research goal is to better understand the dynamics present in PV sources used to supply power to standalone microgrids with a fluctuating load. The main research question is:

How does the controllable energy storage technology ramp rate and delay time affect the grid stability of a standalone microgrid with a PV source and a fluctuating load?

A solution to the research question is determined by answering the following sub-questions

1. What is the required insolation data sampling time that can be used without losing any information in the PV source and load data?
2. What are the expected ramp rates from the insolation and the typical domestic appliances?
3. What must the energy storage system ramp rate and delay time values be for the energy storage system to keep the microgrid voltage within the band of 0.95pu to 1.05pu?

These energy storage ramp rate and delay time specifications are important in generating a framework that can be easily used when choosing appropriate energy storage systems.

1.3 Research assumptions

The following assumptions are made to contextualize the scope of the research.

- A single source, single energy storage and a single load is used in the study.
- The line impedance of the microgrid is resistive because the research is limited to a collocated system.
- The load connected to the microgrid is assumed to have a power factor of 1 i.e. purely resistive. There is no need for reactive power control. For most appliances, the power angle, θ is normally less than 45°. This means that real power ramp rate is higher than the reactive power ramp rate. Hence real power ramp rate requirements better approximate the system ramp rate requirements. For this reason, reactive power ramp rates are not considered in this research.
- The system frequency is assumed to remain constant at 50Hz because the research is limited to voltage control only.
- Three phase microgrid is assumed to be balanced and only one phase can be used in the analysis.
- The study was done for three-phase standalone microgrids. Normally, sources, energy storage and loads are connected to a DC bus on a microgrid. This may pose some problems if the microgrid size is increased. The current circulating in the system may be a danger to the community especially those in remote communities. For AC microgrids the power is shared between the three phases which makes it

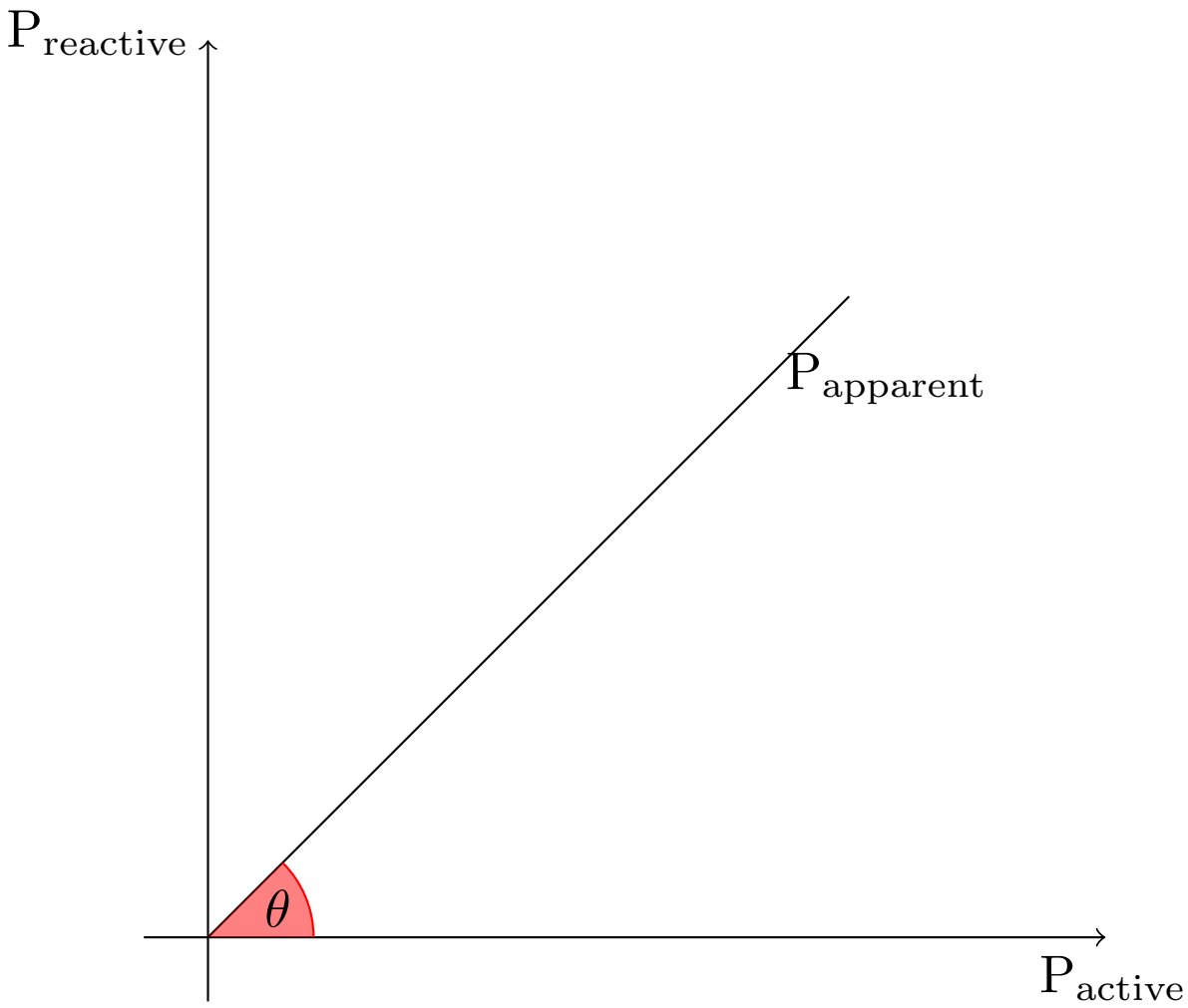


Figure 1.3. Power triangle showing power angle θ. Most appliances have a power angle less than 45°.

significantly safe. Furthermore, because DC does not have a zero crossing, protection required may be expensive as compared to the AC microgrid. A three phase microgrid is preferred because there is maximum power extraction from the PV panels and also it produces a rotating magnetic field that is required when three phase induction machines are connected to the system. These machines are mainly used for agricultural activities. Because AC systems offer these advantages over DC, it is preferred.

1.4 Research Methodology

There are several steps that need to be followed when determining the ramp rate and delay time requirements for energy storage on PV microgrids.

1. Energy resource and load demand data measurements. A pyranometer and Agilent data acquisition system [11] are used to measure insolation data. A power meter is also used to measured the power for typical domestic loads and also to measure the output power of a grid-tied inverter. The computer software Perl, is used to separate the data into a 24hr period and this data is used to identify days with severe fluctuations.

2. PV source and load demand ramp rate analysis. In this analysis, MATLAB® is used to compare these daily ramp rates to determine the average and highest ramp rates that can be expected from a PV source. A power meter is used to measure typical load inrush power.

3. Simulation to determine the effects of ramp rate and delay time on the microgrid voltage. Simulink® is used in this section. This involves importing the recorded daily insolation data and using the information to determine the effects of power fluctuations on the grid voltage.

4. Determining the range of ramp rate and delay time that ensures microgrid stability.

1.5 Dissertation Overview

The dissertation has been divided into chapters. The contents of each chapter are briefly summarized in this section.

Chapter 2:

The chapter discusses the importance of microgrids and the examples of the microgrids that have been built and are fully functional in Africa. The chapter also discusses existing literature on the variability of PV sources and the methods that have been used to reduce the effects of this variability on microgrids. The chapter also discusses different energy storage technologies that can be used to reduce power fluctuations.

Chapter 3:

In this chapter, recorded PV source and load data is used to analyze the ramp rates present on a microgrid with a fluctuating PV source and fluctuating load. The chapter also discusses ramp rates for typical loads that are normally used in a household, with an aim to determine the ramp rates required from the energy storage system to balance the power fluctuations.

Chapter 4:

The chapter links the theory and data analysis in Chapter 3 to determine the effects of ramp rate and delay time. The chapter includes simulation of a standalone microgrid with and without energy storage system. The graphs showing the effects of ramp rates and delay are presented in this chapter.

Chapter 5:

This chapter draws conclusions on the research with a discussion and evaluation of the work that was done and the benefits of the knowledge gained in this field. The chapter also discusses the future work that can be done to extend the findings of the research.

Chapter 2

Literature Review

2.1 Introduction

This chapter aims to give a detailed background on standalone microgrids. It discusses the current situation on microgrids, examples of standalone microgrids that have been built in the past and also presents the gaps in knowledge that have not been fully addressed. The research focuses mainly on energy storage systems as these have been identified as subsystems that play an important role in the proper functionality of a renewable energy based power system. The energy storage subsystem stores harnessed energy and provides power when the generated power does not meet demand. Choosing the correct energy storage involves identifying and optimizing on different characteristics of these systems. This chapter will also briefly discuss some essential energy storage subsystem characteristics.

2.2 Highlights on the importance of standalone microgrids

In 2011, Japan experienced an earthquake and a Tsunami thereafter. The disaster inflicted major damage on the nuclear plant in Fukushima [12]. The plant had to be closed down and efforts were made to stabilize the nuclear reactors. This led to drastic reduction in the country's generation capacity and they initiated loadshedding and voluntary power consumption reduction [12]. Since the incident, there was an introduction of distributed generation systems to support the weak grid. Other countries that have been affected by earthquakes and tsunamis include Chile in 2010 and the series of earthquakes in New Zealand [12] in 2010 and 2011. These disasters affected the electricity transmission and distribution systems. In Chile, the earthquake occurred on the island of Robinson Crusoe, where half of the grid was buried underwater. They had problems transporting diesel for their backup generators. The only feasible solution was to look for avenues of integrating local resources to supply critical loads [13]. Earthquakes in Christchurch, New Zealand also had similar consequences. Overhead power lines were buried mostly because of the soil liquefaction and ground shaking also affected buried power line cables [12]. These examples of disasters that have occurred in the past show that electricity distribution lines and power stations are the most affected.

Grid-tied microgrids have also been found to have similar effects and in many cases, failure on the main grid would also lead to blackouts. Queensland, Australia was affected by floods from December 2010 to January 2011 [13]. The flood covered three-quarters of the state and electrical power was cut-off due to safety concerns [13]. Some of the residents had grid-tied rooftop PV microgrids and unfortunately when the authorities switched off the power, they were also affected [13].

Most of these incidents show that relying entirely on the utility grid can be disastrous. Damages on either the power lines or the power station can result in severe blackouts. There is no technical barrier in having a standalone microgrid that would work in cases where the main grid is affected [13]. In some cases, disasters may be severe that, it will also damage the microgrid infrastructure. However, having many distributed microgrids

may reduce blackouts as the outage will only occur on the affected area. This is because if one of the standalone microgrids is affected, it may not necessarily affect other areas using different standalone microgrid.

2.3 Current situation in microgrids

The International Energy Agency estimated that universal energy access can only be achieved if 45% of the new connections are in the form of standalone microgrids by 2030 [14]. Because most African communities are affected by electricity shortage problem, stakeholders must do more in installing these standalone microgrids in Africa.
There are several PV microgrids in Africa that have been built and this section discusses how these microgrids are performing. The following examples show that standalone microgrids are a feasible solution. It also shows that in some cases, it leads to economic development.

2.3.1 Diakha Madina standalone microgrid in Senegal

The microgrid was installed in Diakha Madina, Senegal in 2007 and it has a maximum PV capacity of 3.15kWp [15] . The rated output of this microgrid is 4.803kWh. Batteries with a total capacity of 672Ah are connected. A backup diesel generator with a capacity of 4.2kW is also installed [16]. The microgrid is basically used to power public lights, water pump and a health care facility in the area. From the report released on this microgrid, no water interruptions have been experienced since installation[15]. The microgrid has also been found to have a good average state of charge for the battery [15].

2.3.2 Olosho-Oibor standalone microgrid in Kenya

The microgrid was installed in June 2009 by the United Nations Industrial Development Organisation (UNIDO) [15]. The system consists of 3kWp of PV panels, battery bank, 3kW wind turbine and a 10kW diesel generator [16]. The United Nations Development Programme (UNDP) later sponsored the installation of another 4kWp of PV panels as the power was not enough to support the basic loads [15]. The microgrid connects to a dispensary, a school, a church, a shop and it is also used to charge cell phones and LED lanterns[16].

The microgrid is run by the community and there is a certain amount of households and businesses that have to pay monthly fees to maintain the microgrid.

2.3.3 Akkan standalone microgrid in Morocco

Another example of a microgrid that has yielded positive results was built in Akkan, Morocco. The microgrid has a maximum PV installed capacity of 5.76kWp [15]. Batteries with a capacity of 1.5kAh are connected to the system together with a backup diesel generation rated at 8.2kVA [15]. These power sources coordinate to supply 23 households with 275Wh/day, three households with 550Wh/day, a school and a mosque with 550Wh/day and also 13 street lights with a combined rated power of 910W [15].

A survey done on this microgrid showed that the village does not experience frequent blackouts and the community members are satisfied with the presently contracted energy. Although the project has been a success, [17] acknowledged that lack of expertise to design, install and maintain the microgrid has been a challenge. This indicates that the solution may not be an optimum solution for a rural community.

2.3.4 Discussion on the microgrid examples

What is also clear in the examples of the microgrids presented in this section is the fact that battery storage appears to be a viable solution. The technical details on the ramp rate requirements were not fully addressed in the currently available literature [16]. It is suspected that for the Olosho-Oibor standalone microgrid, the sizing was not fully done during the design stage and this may have led to a shortage of power.
The standalone microgrids discussed in previous sections also shows that battery technology has been a preferred energy storage solution for most of the microgrids. This research aims to determine a framework that must be used when determining ramp time required by a standalone microgrid. The ramp time is then used to select an appropriate energy storage system that will make a standalone microgrid stable.

2.4 Current studies on variability of PV sources

Studies on the PV power fluctuations have been previously addressed by many authors. Some of the existing studies are discussed in this section. The section also aims to show that high penetration of fluctuating power can cause grid stability problems. It also discusses the factors that affect the PV system ramp rates.
A study was done at Oklahoma State University by Jewell *et al* [18] on the effects of moving clouds on the utility grid with dispersed PV generation. The study was conducted to determine the relationship between the size of the area which the small PV system are dispersed and the PV power ramp rate. The research proposed that the power from the utility be varied to balance the PV power fluctuations. The study found that power flow reversals would occur on the distribution system when there are PV power fluctuations. This is because sources can be connected at any point on the grid. Depending on the available power at each node, the power can flow in either direction [19]. These reversals

occurred when the penetration of PV power reached 15% of the total load. The reversals were found to have detrimental effects on the operation of the protection equipment. This is because existing protection equipment is unidirectional. It was also concluded that if the protection issues can be solved in any way, the utility grid would operate with high penetration of PV generation. This research is not possible if the only source of power is from a PV system. However it acknowledges that there is a need to connect a system that will cancel out the power fluctuations.

In a paper written by J.W. Smith *et al* on distribution modeling and analysis of high penetration PV, several points were made [20]. The paper highlighted the components that are essential in investigating the impact caused by high penetration of renewable energy sources. One of the components was the time varying nature of renewable energy sources and the unpredictability of loads as they interact with the feeders. In their research, they used distribution system analysis software (OPENDSS) to analyze issues with DG. The research also pointed out the factors that determine the ramp rate of the PV system. These were[20]:

- Size of the PV array.
- Centralized PV vs distributed PV system.
- Local weather patterns.

2.4.1 Size of the PV array

Several authors have acknowledged that large PV plants play an important role in reducing the amplitude of power fluctuations on microgrids that are caused by cloud movement [20; 21; 22; 23]. Kankiewic *et al* also found that the 6.4MW rooftop PV plant on EPRI's facility in Palo Alto had power fluctuations of up to ±10% of the plant capacity but the 0.8MW subsystem produced fluctuations of up to ± 25% for the same cloud movement. Research conducted by Van Haaren *et al* [24] also supports that there is a significant

decline in the ramp rate as the PV plant increase in size. These lower power fluctuations are based on the fact that the clouds will take longer to cover the entire PV plant.

2.4.2 Centralized vs distributed

The ramp rate of a PV system can also be influenced by the geographical dispersion. Studies done by Wiemken *et al* has shown that a single PV system with a size between 1kW - 5kW has a 5-minute ramp rate of 52% of the system capacity, whereas 100 PV systems with a combined capacity of 243kW showed 5-minute ramp rate of 5% of the total capacity [25]. This method of reducing power fluctuations is known as the smoothing effect [26]. Yanagawa *et al* also did some studies on estimating the spinning reserve capacity required to balanced off the disturbances caused by fluctuation of many photovoltaic plants located several kilometers apart [26].

2.4.3 Local cloud pattern

Different types of clouds have different effects on PV systems. There are five characteristics that describe the cloud pattern and these are [18]:

- Size and shape of the cloud.
- Percentage cloud cover.
- Speed and direction of the moving cloud.
- Optical transmission of the clouds.
- Variations in the optical properties within the cloud.

Considering these characteristics, a study done by Jewell *et al* has shown that cumulonimbus clouds will cause greatest power variations. This is mainly because they are thick and hence limited insolation manages to reach PV systems [18]. Cumulonimbus clouds have been found to have a very low cloud transmittance coefficient compared to other clouds such as cirrus, nimbostratus, altostratus, cirrostratus and altocumulus [18]. This contributes significantly to the insolation variation with cloud movement [18].

2.5 Methods for reductions of power fluctuations on micro-grid

As stated in previous sections, power fluctuations pose a threat to the stability of the grid. Omran *et al* [27] did a study on ways of reducing power fluctuations on grid-connected PV systems. The power fluctuations were found to change by 70% of the PV system capacity in a 5 to 10 minute time interval. In the study, energy storage systems were identified as one of the methods to reduce power fluctuations. This is because when there is excess power generation, they can store the energy and discharge when there is insufficient power from the PV generation. It was also highlighted in the study that, the response time of the storage must match the speed of the fluctuations. Batteries were identified as the suitable energy storage device. Omran *et al* formulated a revenue equation shown in equation 2.1 [27].

$$R = \max\left\{\sum_{k=1}^{T}\left[\left(\sum_{j=1}^{N}\sum_{i=1}^{M}\alpha \times \frac{\Delta t}{60} \times P_G(i,j,k)\right) \times \frac{1}{(1+d)^k}\right] - \beta\frac{1}{\eta_{PB}}P_{\text{B max}} - \gamma\frac{1}{\eta_{ch}}E_{\text{B max}}\right\} \tag{2.1}$$

where

$P_{G(i,j,k)}$ *is a technical constraint that ensures power balance of the system*
P_{Bmax} *and* E_{Bmax} *ensures that the battery power during discharge does not exceed the rating of the battery.*

From the equation, β and γ account for the costs related to the installation of energy storage. The studies concluded that installing an energy storage (battery in this case) would lead to a loss off revenue. This is evident from the equation above that an increase in the second and third term value would result in reduced revenue. It also concluded that increasing the energy storage ramp rate specifications would lead to a significant loss in revenue of between 18.5% to 34.5% for ramp rates of 400kW/10min to 0kW/10min (no fluctuations) respectively.

Ye *et al* [28] acknowledged that an integrated power management strategy of hybrid energy storage systems is required to meet the energy and power demand. The study further points out that the use of one type of the energy storage could mean oversizing one aspect to take care of other weakness, e.g. oversizing battery storage in the energy aspect could balance off the high power demand while capacitors can be over-sized to meet the energy demand. However in Ye *et al*'s studies, there is little emphasis on the ramp rate requirements of the energy storage.

The study done by Omran *et al* used a single energy storage technology. This may not be the optimum way of improving the ramp rate as states by Ye *et al*.

There have been ongoing studies on reducing power fluctuations on a microgrid. However assumes that the utility grid will have enough power to balance the load demand fluctuations. In the case of a standalone microgrid, the energy storage must balance both the PV and load fluctuations.

2.6 Potential energy storage systems for a microgrid

Depending on the requirements of the microgrid, different types of energy storage systems can be considered. These energy storage systems can be classified into short-term (high power density storage) and long-term storage (high energy density storage). Short-term

storage is mainly applied to maintain the voltage stability during transients/disturbances [29]. Long-term storage is deployed to contribute towards the energy management, frequency regulation and grid congestion management [29]. Figure 2.1 shows the energy storage technologies and their respective energy and power capabilities. This figure can be used to select the suitable storage once the energy and power rating of the standalone microgrid is known.

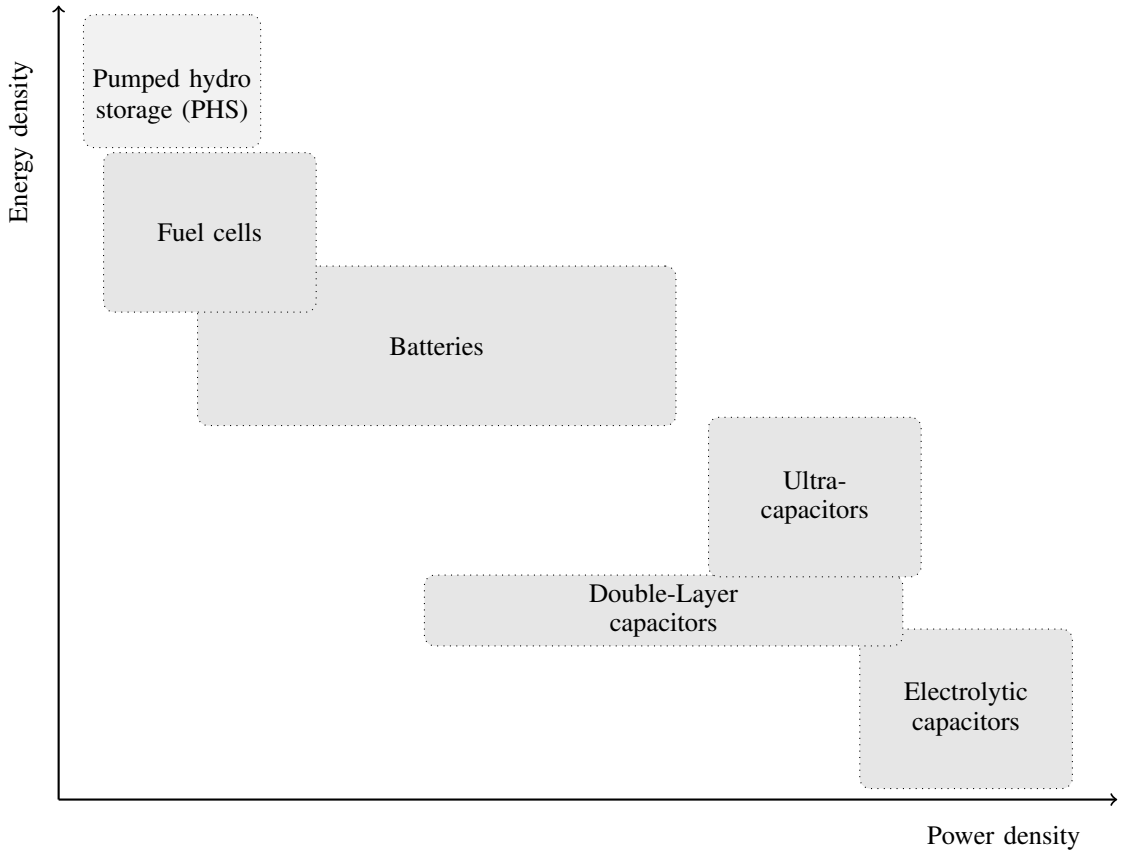


Figure 2.1. A diagram showing different energy storage technologies together with their power and energy capabilities [3].

Choosing the appropriate energy storage system to stabilize a microgrid requires an understanding of the characteristics of existing energy storage systems. These characteristics

include ramp rate, charge rate, discharge rate, efficiency, energy and power density and response time and are explained in below [14]:

- **Response time:** The amount of time the storage system requires to respond to a change in power demand. t_1 in figure 2.2 shows the response time.

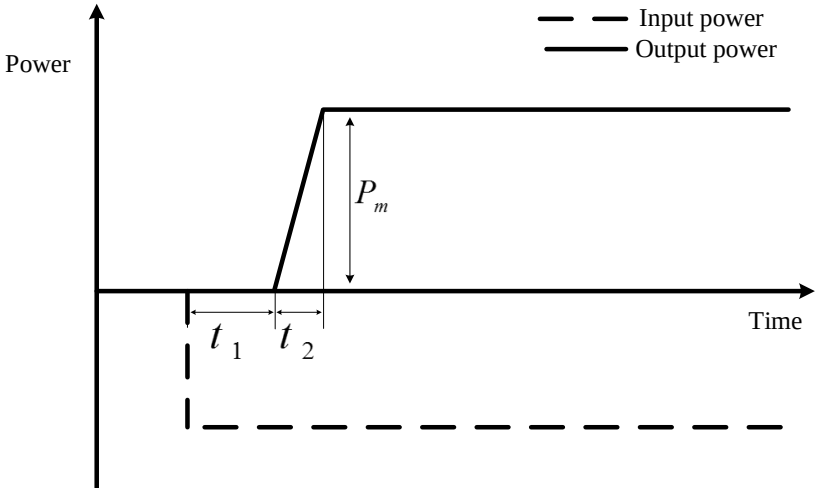


Figure 2.2. The dynamic characteristic the study will focus on. t_1 is the response time while P_m/t_2 is the ramp rate.

- **Ramp rate:** The rate at which the power flow can change and is sometimes known as the slew rate. P_m/t_2 in figure 2.2 is the ramp rate (slew rate).
- **Efficiency:** This is the amount of energy retained relative to the amount of the energy stored.
- **Energy retention time:** This is the amount of time required for the energy to retain its charge.
- **Energy and power density:** Energy density is stored energy divided by the volume of the energy storage. Power density is the rated output power divided by the volume.
- **Charge rate:** the rate at which the energy storage can be charged.

- **Discharge duration:** This is the amount of time at which the energy storage can be discharged at its rated output power without being charged.

For the current research, the most applicable dynamic characteristics are the ramp rate and the delay time.

2.7 Gap in knowledge

Existing literature has shown that more effort is being made on ramp rate analysis. Currently, there is limited literature on how to minimize power fluctuations as a result of both sources and loads on standalone microgrids. Papers reviewed in this report show that most authors are providing partial solutions which would only work if the microgrid is grid-connected. This is because an assumption of no load power fluctuations is made. In standalone mode, load fluctuations cause the biggest disturbances and hence need to include these fluctuations in the analysis.

2.8 Summary

In this chapter, examples of existing microgrids have been discussed. These examples help in identifying the challenges and advantages of building small islanded microgrids. As stated by the IEA, more effort is required to support the construction of standalone microgrids if total electrification is to be achieved. The chapter also included the current studies being done on the variability of PV sources. These studies alone can not be used to minimize power fluctuations on standalone microgrids because they do not incorporate load power fluctuations. This research aims to find solutions on how to minimize the combined load and source power fluctuations using energy storage systems.
This chapter showed that power fluctuations on microgrids are a major concern and efforts

are being made to find solutions. Available solutions do not fully address ramp rate problems on standalone microgrids hence the reason for pursuing the studies.

Chapter 3

Energy Resource and Load Data Analysis

3.1 Introduction

One of the initial steps in sizing storage required for stabilization of the standalone microgrids is analyzing the available energy resources and the demand requirements. Some of the fundamental specifications for energy storage include energy and power capacity and the response of the storage to changing power (ramp rate and delay time). These specifications can be estimated by analyzing the existing insolation and power demand data for that specific area. The dissertation will analyze data recorded in Johannesburg in March 2014. The data was recorded during cloudy days to provide the worst PV power fluctuations.

The chapter aims to discuss the steps that need to be followed when determining the ramp rate requirements for controllable energy storage that can be used to stabilize a PV microgrid. This microgrid is connected to different loads with different dynamic characteristics.

This chapter is an expansion of the papers that were published in the IEEE AFRICON 2015 which was held in Addis Ababa, Ethiopia and SAUPEC 2015, Johannesburg, South Africa. Further information on the contents of the reports are in Appendix C [30]. Prof W.A Cronje and Prof I. Hofsajer supervised the work. The work presented in the paper is part of Mr. Nyasha Horonga's M.Sc research.

3.2 PV source and load data analysis

A typical standalone microgrid is shown in figure 3.1 and this microgrid is powered from Distributed Generation (DG). These DGs include renewable energy sources and diesel generators. The research focuses on microgrids that receive power from renewable energy sources. This is because in Southern Africa there are abundant renewable sources that are currently being underutilized [31]. These sources are can be constructed close to where there are required and can provide power to remote areas which currently do not have

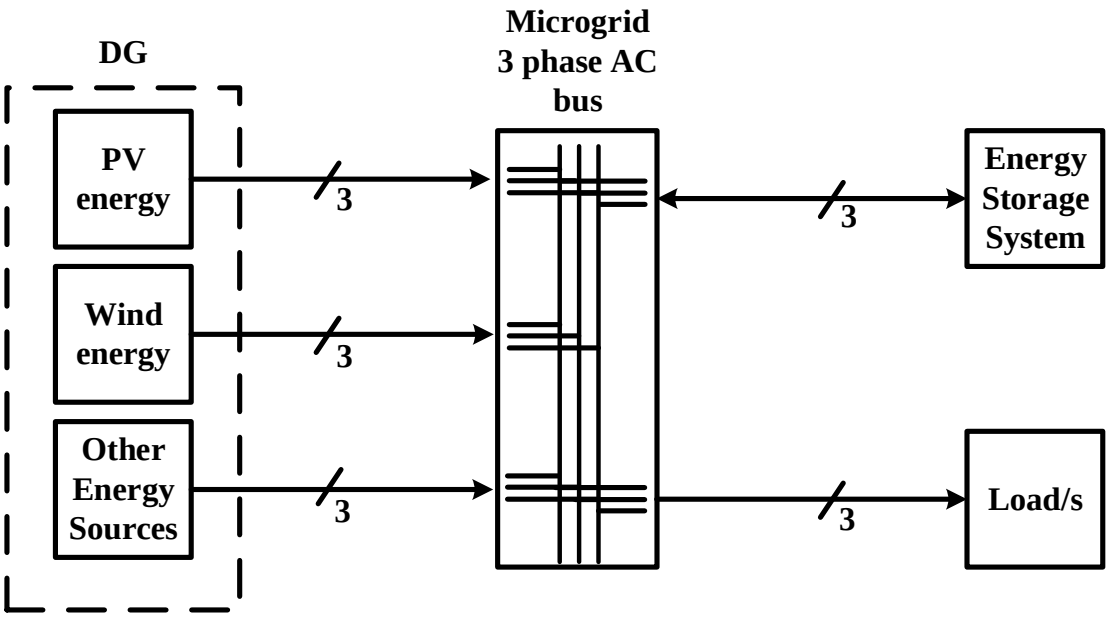


Figure 3.1. A single line schematic example of a three-phase low voltage standalone microgrid system.

access to electricity or can be used to supplement the stressed utility grids. Figure 3.2 shows typical insolation data of cloudy days in Johannesburg, South Africa. The insolation data was recorded at the roof of the Chamber of Mines building at the University of Witwatersrand. From the data in figure 3.2, a few conclusions can be made and these are:

- Renewable energy sources produce fluctuating power as mentioned in previous chapters.
- During the night or cloudy days, alternative source of energy must be used and these can be energy storage systems or utility grid.

Because the insolation data recorded is being used for a hypothetical scenario of varying generation for the purpose of the study, it has been normalised to the peak of 1536.5 W/m^2 for the 2 day period. Appendix A gives a detailed discussion on how the data was recorded.

A standalone microgrid must be self-sustaining and must be able to supply power to the load. Apart from the source fluctuations, another problem faced by standalone microgrids is the uncontrollable nature of the load. The microgrid control systems have very little knowledge of the time at which consumers will switch on appliances and how much power will be required.
The Genmin building load data shown in figure 3.3 is used to model a hypothetical microgrid load. The data was recorded for the Genmin building at the University of the Witwatersrand. This data represents a fairly bad day because there are abrupt changes in load which in many cases will draw more power from the microgrid which can result in voltage fluctuations. Because the size of the PV source is not the same as the size of the load used for measurements, the load data was also normalized to the peak of 3kW for the 2 days recorded. By normalizing the PV source and load, the data can be used to address the power fluctuations on PV microgrids.
Successful operation of any microgrid is determined by how well the sources meet the load

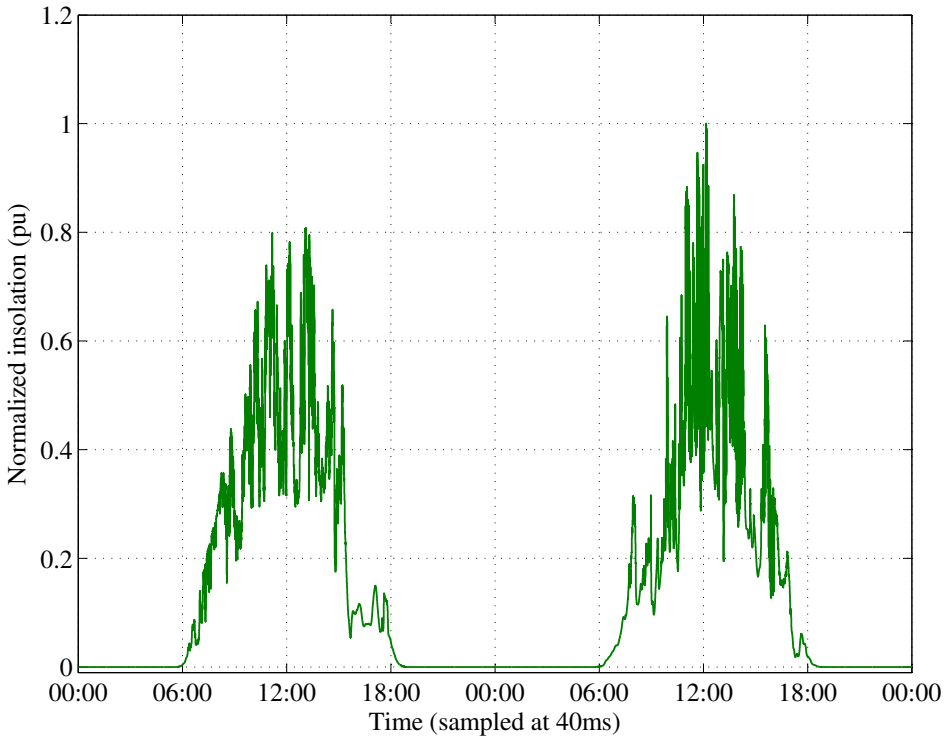


Figure 3.2. Normalized measured insolation (W/m^2) obtained at the Chamber of mines building (Wits University). The insolation values were normalized to the insolation peak for the 2 days shown in this figure. The data was sampled at 40ms intervals.

power demand. Ideally, the microgrid must have enough power circulation between power generation sources and loads.

3.3 Data set validation

Previous research on PV power variations has concluded that the size of the PV plant largely contributes to the system ramp rate [20; 21]. The PV plant used in this study is a small 2kW system. As such, the normalized inverter output ramp rates have been found to be the same as the normalized insolation data ramp rates obtained from the pyranometer.

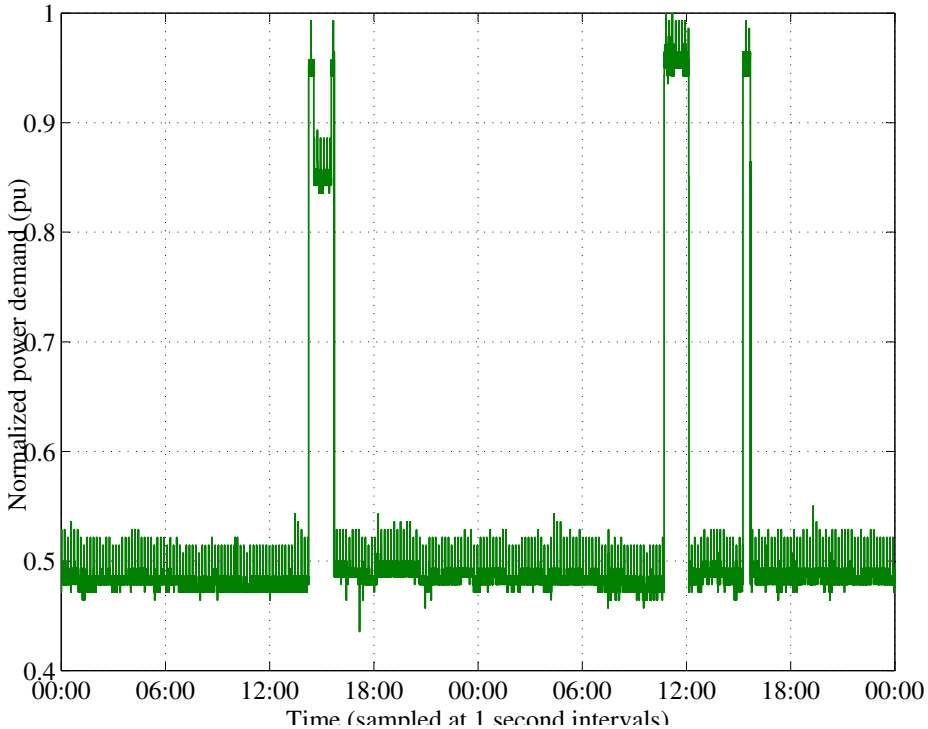


Figure 3.3. Normalized measured power demand for the Genmin building (Wits University). The power demand values were normalized to the Genmin building load peak for the 2 days shown in this figure. The original data was sampled at 100ms intervals and re-sampled at 1 second intervals.

Although Figure 3.4 shows lower inverter efficiency in region A when there insolation is low, The pyranometer and the inverter output data in figure 3.4 have relatively the same profiles and hence the same ramp rates. In Figure 3.5, a detailed look into a portion of plots in figure 3.4 shows the two profiles following each other closely. The figure also shows that the grid-tie inverter used to obtain these results regularly switched off. Although the cause for switching is not yet known, it is suspected that the inverter switches off to assess the state of the grid. Inverters have built-in intelligence to prevent them from supplying power to a faulty grid [32].

3.4 Analysis of PV data variations

When designing a standalone microgrid, one must have some knowledge on how fast the resources are changing and also the capacity of the installed PV system. As mentioned in Chapter 2, one of the standalone microgrids examples had to be re-designed as it was unable to support the load.

There are some loads that are sensitive to power fluctuations and there are some loads with higher surge current and these issues must be fully addressed during the design stage. This section is aimed at identifying the average and the highest power ramp rate of a PV source. Figure 3.6 is a plot of insolation data ramp rates for a 2 day period. Figure 3.6 shows that the average ramp rate (R_{ave})is generally low (approximately 0.011pu/sec)

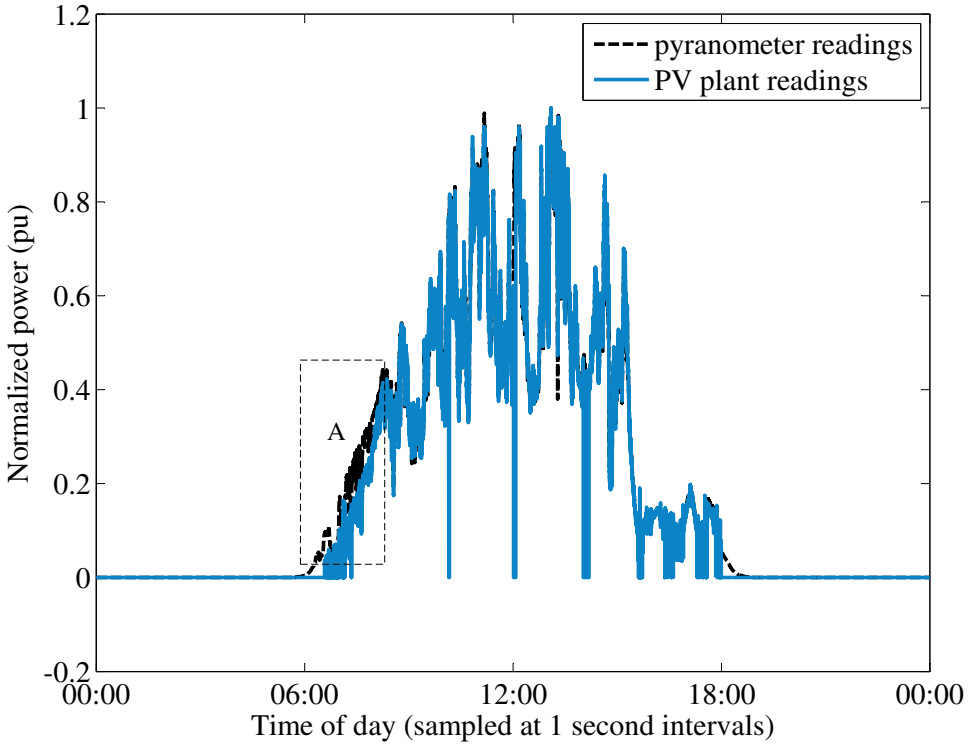


Figure 3.4. PV inverter output overlaid on the insolation data.

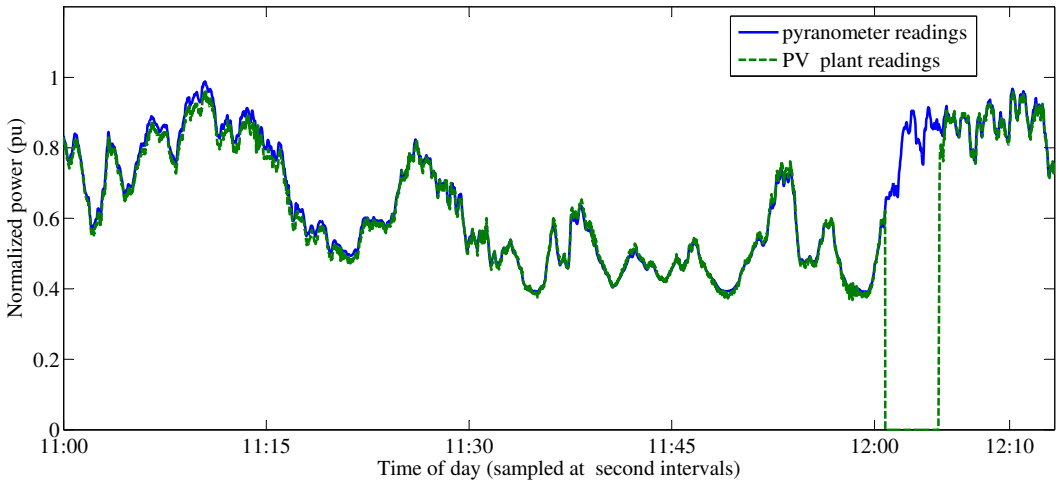


Figure 3.5. An extract of the data in figure 3.4.

compared to the peak ramp rate (R_{max}) of 0.12pu/sec. R_{ave} was calculated by adding all the non-zero 1 second averaged ramp rates and divide by the number of these non-zero 1 second averaged ramp rates. The variation in the ramp rates as seen in figure 3.6 indicates potential power fluctuations and the standalone microgrid must be designed to smoothen the power flow.

Figure 3.7 shows that most of the insolation fluctuations are as a result of cloud movements. It shows that when the sky is clear (i.e. smooth insolation curve), no fluctuations are experienced. This finding further points out that when designing a microgrid, a partly cloudy day must be used. Complete cloud cover will not result in power fluctuations. However, the storage must have enough storage capacity to supply power.

The ramp rates obtained from the pyranometer/small PV plant is significantly higher compared to that of a large PV system. This is because a pyranometer/small PV plant is small in size and can be covered by the clouds instantaneously. Large/dispersed PV have large surface area and hence can not be covered by the clouds instantaneously and these factors further smoothen the system power fluctuations as discussed in Chapter 2. Measurements obtained from the pyranometer/ small PV plant represent the worst case scenario. All the PV plants will have fluctuations which are less severe compared to this

worst case scenario.

The pyranometer readings will be used throughout the rest of the document.

3.5 Analysis of load demand variations

The load demand data in Figure 3.3 shows that the load can switch on or off very fast. This is because typical microgrid loads are mainly controlled by switches. PV source fluctuations are slow and the ramp rate required by the load must come from the installed energy storage device. Sizing the energy storage devices requires knowledge on how often

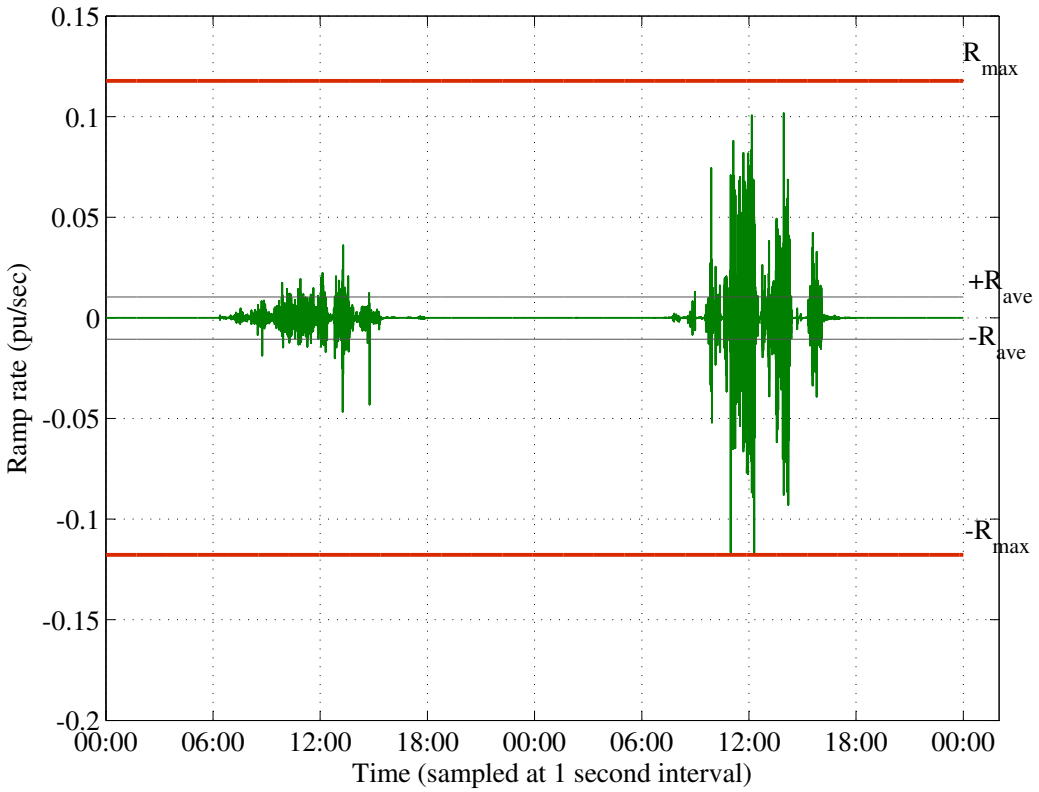


Figure 3.6. Ramp rates for the insolation data recorded on the roof of Chamber of mines building at the University of the Witwatersrand.

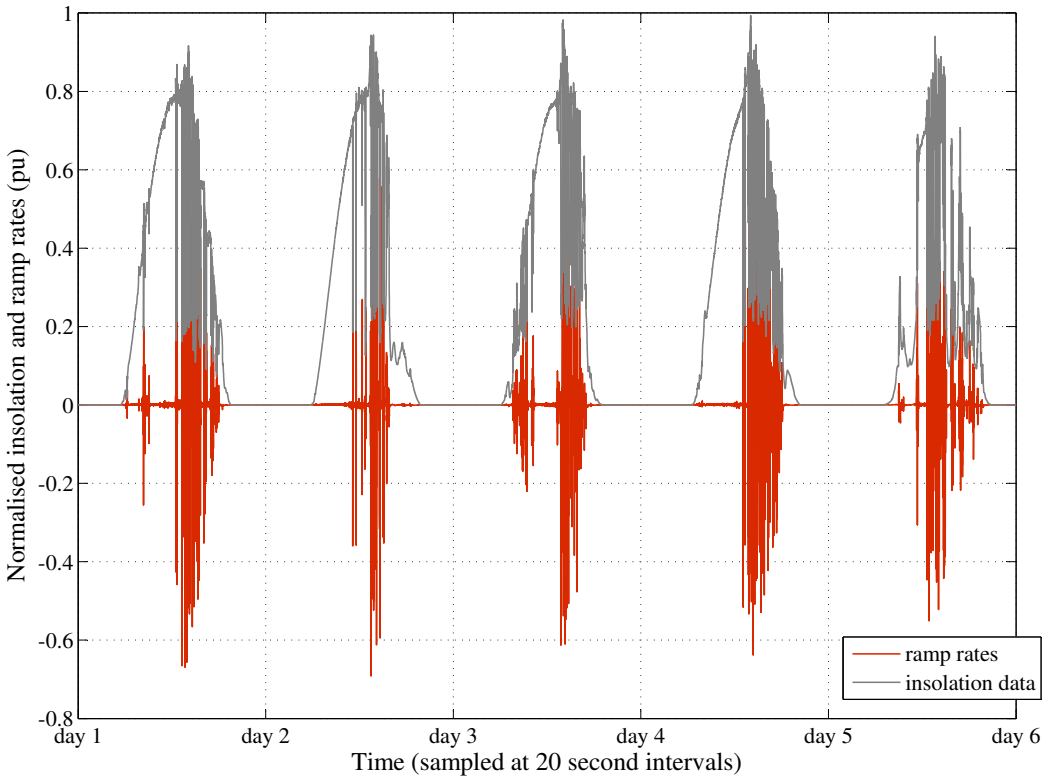


Figure 3.7. Insolation data overlaid on the ramp rate data.

the loads are being switched on and off. From the load demand data provided in Figure 3.3, it is seen that step changes in the load do not occur often and therefore a smaller high power density storage is required to avoid blackouts.

The unpredictable nature of the load is one of the major concerns. There is little knowledge on times at which appliances will be switched on or off and the state of the energy source (i.e. in this case PV source). In some cases, an appliance may be switched on while there is cloud cover and the energy storage must supply the required power at an appropriate rate.

The available insolation and the Genmin building load data was re-sampled at 1 second. This means that for a period of one day, there are 86400 data points. As such, the calculated ramp rates obtained by sliding the load data over the insolation curve resulted in an 86400 by 86400 matrix. Sliding the load data on the PV source data was done to determine the maximum possible ramp rates assuming that the load switching events can

occur at any time during the day. This amount of data is too large to analyze individual data points and it was decided to group the ramp rates in the following ranges in Table 3.1. The probability of occurrence of the resulting ramp rates was obtained by scanning through the 86400 by 86400 matrix and counting the number of occurrences in each range. The number of occurrences is then divided by the total number of data points (86400 $\times$ 86400). By comparing the insolation ramp rates to the ramp rates obtained by sliding the Genmin building load demand data, it can be seen that higher ramp rates are a result of load dynamics in most cases. The probability of occurrence of ramp rates above 0.1pu/sec is low because the load demand data does not have too many switching events. The results

Table 3.1: The probability of occurrences of the calculated ramp rates in the ranges in the table.

Ramp rate range (pu/sec)	Probability of occurrence of the calculated ramp rates
$\leq$0.1	0.83
0.1 - 0.2	0.13
0.2 - 0.3	0.0320
$\geq$ 0.3	0.005

in Table 3.1 further affirms that for this case, ramp rates above 0.1pu/sec do not occur often. A smaller high power density energy storage is therefore required to provide power during the switching time and a high energy density storage to provide power during other times.

The data in Figure 3.3 is for a big load and these type loads take a long time to ramp up to the maximum power. In many cases, standalone microgrids are designed for smaller loads that have high ramp rates. Some of the typical loads that can be connected to a standalone microgrid include laptops, heaters, fans, fridge, stove and microwave. The loads used in this study may not be relevant to rural communities at the moment. It is suspected that the reason for not using these appliances may be due to limited access to electricity. Any solution to the electricity problem must not limit these communities. The

study must be done to take into account most of the typical loads that can be expected to be present in a typical urban household. The study must also include some loads that may not necessarily be used in urban areas such as water pumps. This will represent the worst case on the load demand side.

The circuit diagram and the experimental setup for measuring the power of typical domestic loads during the initial transients are shown in Figure 3.8 and 3.9 respectively. DUT represent appliance being tested and MB is the measurement box. A power meter is used to measure the power every 20ms. From the results shown in figs. 3.10 to 3.14, it can be seen that these devices have different initial transients. The figure 3.10 shows that a laptop charger rated at 65W uses 5 times the normal power during the first 40ms. The results also show that the ramp rate that would be required if these appliances are connected to a standalone microgrid will be relatively higher than the ramp rate from a PV system. This is because most of the appliances will draw more current within the first 20ms. An energy storage system is required to supply the power at this rate. The ramp rates required for the appliances tested are shown in Table 3.2. The ramp rates

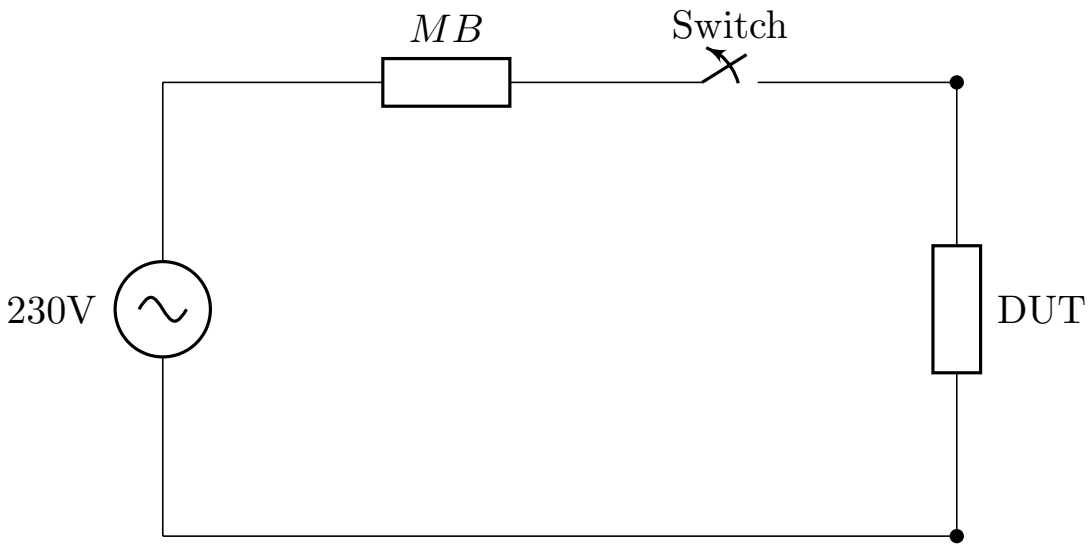


Figure 3.8. Circuit diagram used to measure the ramp rate of typical house appliances that can be connected to a microgrid.

were calculated by dividing the measured initial transient change in power by the ramp time. These ramp rate requirements represent the worst case if there are no other sources supplying power apart from the energy storage. If the PV system is also supplying the power, the energy storage ramp rate requirements may be lower depending on the available insolation at that time.

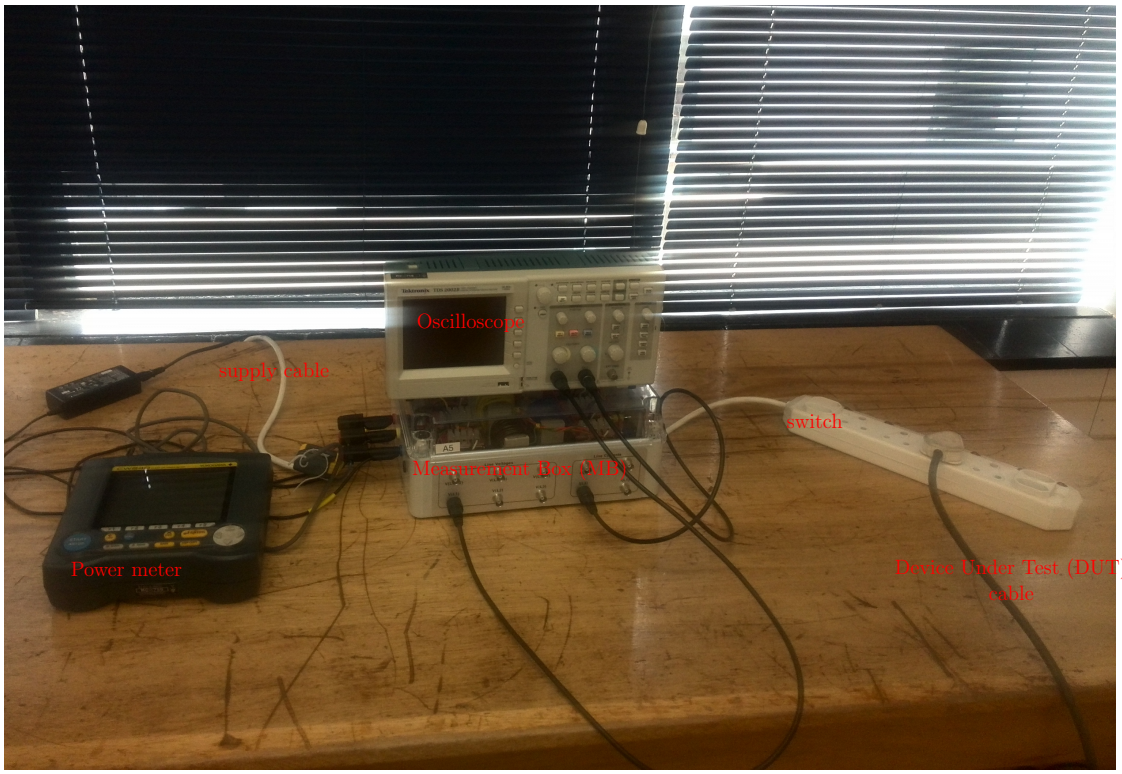


Figure 3.9. The experimental setup used to measure the ramp rate for household appliances

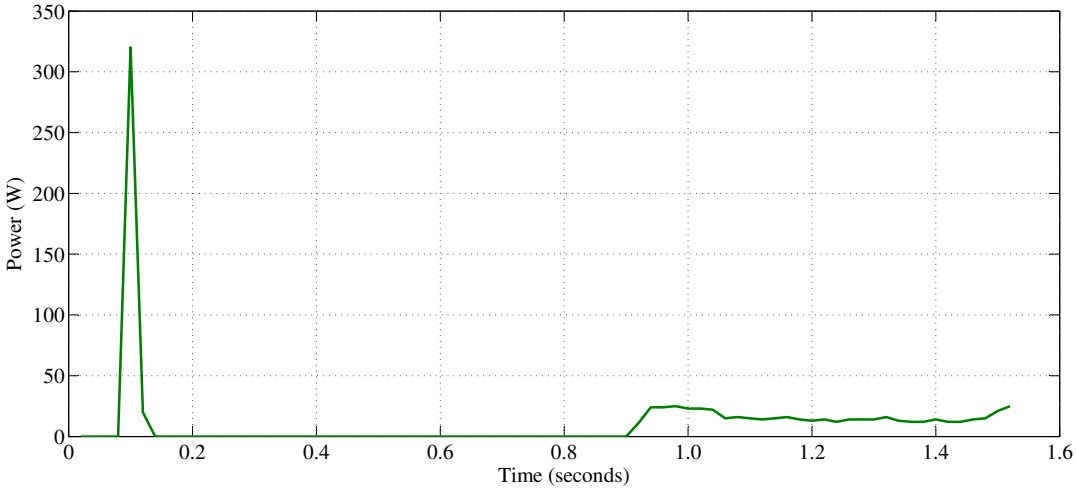


Figure 3.10. Measured power required by a laptop charger few seconds after closing the switch.

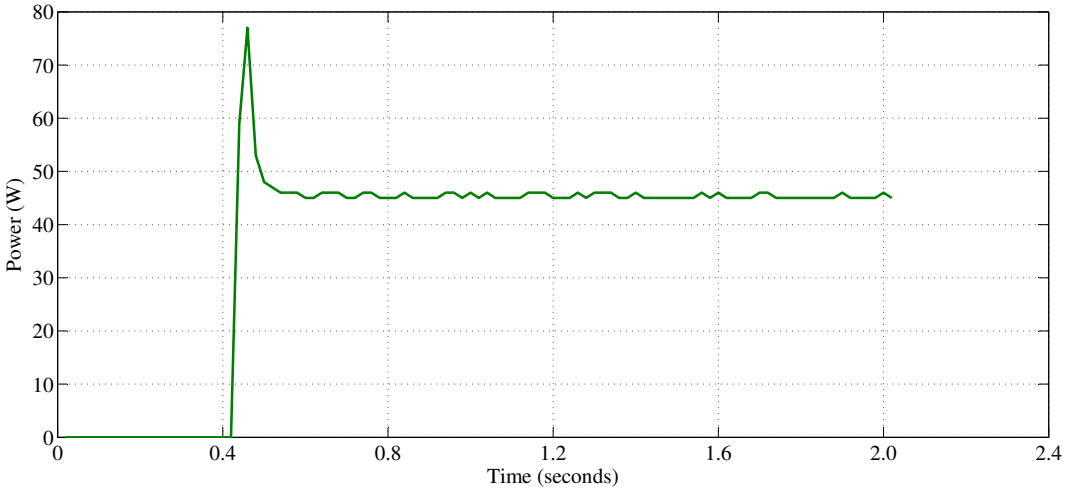


Figure 3.11. Measured power consumed by a light bulb during the first 2 seconds.

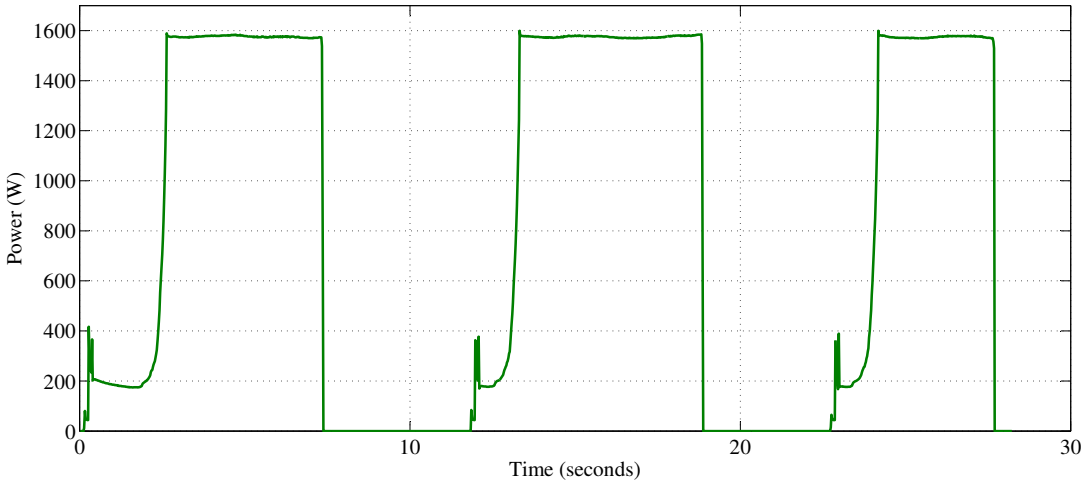


Figure 3.12. Measured power consumed by a 1.5kW rated microwave during the first 30 seconds.

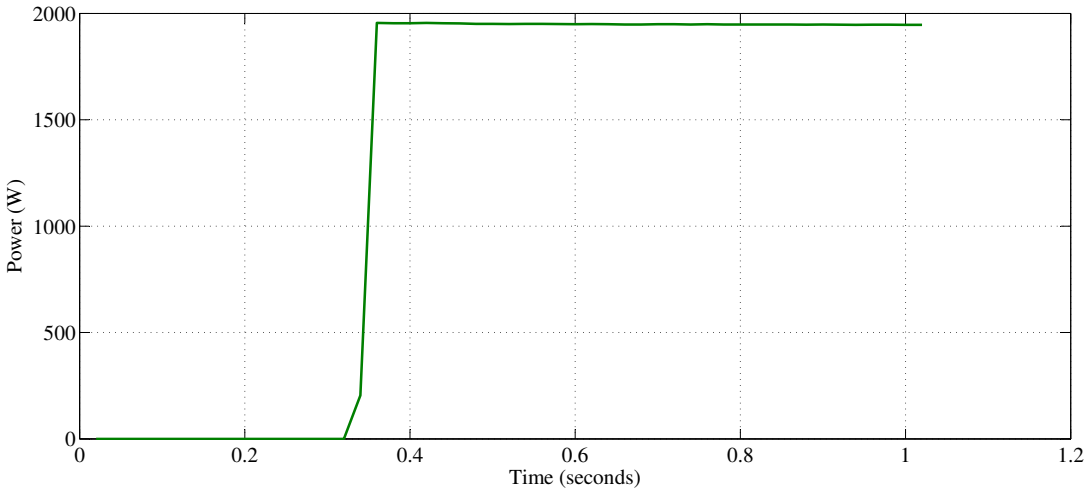


Figure 3.13. Measured power consumed by a 2kW rated heater during the first 1 second.

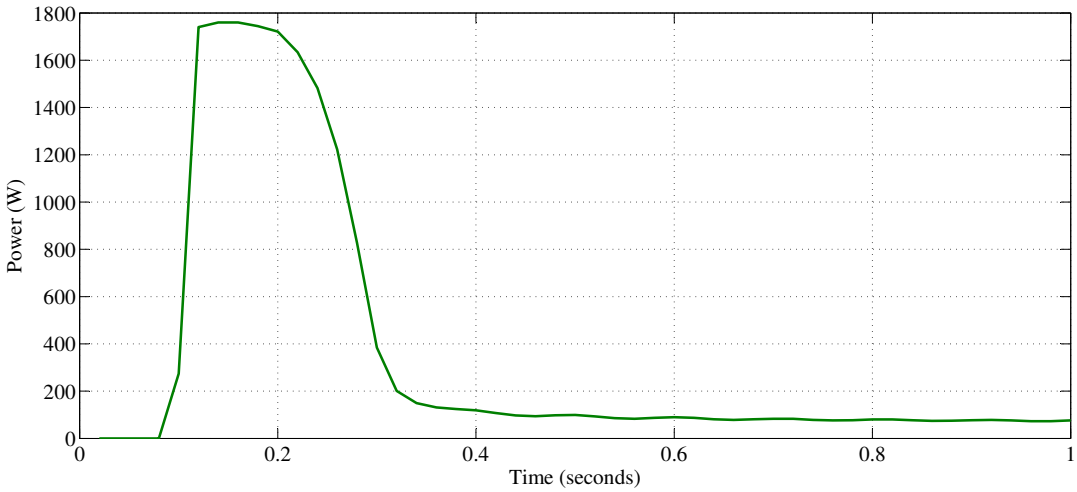


Figure 3.14. Measured power consumed by a 68W rated fridge during the first 1 second.

Table 3.2: Measured ramp rates for selected household appliances.

Household appliances	Appliance rating (W)	Peak/Rated power ratio
Laptop	65	5
Light bulbs	45	1.5
Microwave	1500	1
Heater	2000	1
Fridge	68	25.7

These typical microgrid loads are normally rated using the steady state power. It is clear from the recorded data that in microgrids, the transient power is one of the major problems. A lamp for example requires 1.5 times the rated power during the initial transients and a laptop charger consumes approximately 5 times the rated power. A fridge also consumes 25 times the rated power when a compressor switches on. If these three appliances are connected to a standalone microgrid, the combined power required during the initial transient (first 30ms) is approximately 12 times their combined rated power. This means that to avoid overloading during these transients, the inverter power rating must be approximately 12 times bigger. If resistive loads are also connected to the microgrid, the ratio of the required inverter rated power to the combined rated load demand power was found to decrease. Adding a 2kW electric heater and a 1.5kW microwave to the three loads discussed earlier (i.e. laptop charger, light bulb and fridge) was found to reduce the ratio from 12 to 1.5. This means that increasing load diversity on a PV microgrid can also lead to reduced fluctuations. Increasing load diversity in this context means increasing the number of load with different dynamics and different initial transients. This will result in reduced overall load dynamics. This can increase the size of the microgrid.

The total energy required during the initial transient for the light bulb, laptop charger and fridge is obtained by calculating the area under the power curve for the duration of the first transient. This energy is found to be 2Whr, 6.5Whr and 192Whr for a light bulb, laptop charger and fridge respectively. It is clear from these calculated values that the energy storage required for these transients is very small. However the energy storage must deliver the power over a very short time (i.e. 60ms for a laptop charger, 40ms for and

light bulb and 180ms for a fridge). Adding resistive loads basically means a high energy density storage must be used because once the resistive load is turned on, they will draw a constant power.

3.6 Summary

This chapter explained that for the proper sizing of the energy storage system used on a standalone microgrid, resource and load data must be analyzed. Because the PV system used in this study is small, the output power from the panels can be assumed to have the same profile as the output from the pyranometer. This was verified by plotting the data measured from the pyranometer and that measured from the PV panels. The data was found to have the similar dynamics. For large/dispersed PV plants, point measurements from a single pyranometer are not necessarily the same as the measurements from the PV plant.

The average ramp rate for a PV source is very low (0.011pu/sec) compared to the peak ramp rate of 0.12pu/sec. The Genmin load data used does not fully represent all the load transients experienced on microgrids. This is because it does not have high ramp rates compared to the typical domestic loads. Further studies on the loads that can be connected to standalone microgrids were done. These studies show that the load ramp rate requirements are relatively high (at least 2.95kW/s for a 45W light bulb) compared to the 1 second averaged ramp rates measured from the PV source data.

The chapter was aimed at discussing a framework that can be used when determining the ramp rate requirements for controllable energy storage. Using the framework, it has been found that sizing of energy storage systems using the rated load demand power is inadequate. This is because some loads draw more power during initial transients which can exceed the energy storage and the inverter ratings. The framework proposes that energy storage sizing must be done using the peak power.

The power required during initial transients can be reduced by load diversity on microgrids.

It can also be seen from the load data analysis that more efficient appliances with a lower inrush current can significantly improve the operation of the PV microgrid.

Chapter 4

Microgrid Simulations

4.1 Introduction

The chapter aims to illustrate the effects of power fluctuations on PV microgrids. The chapter also aims to find the range of ramp rate and delay time for the controllable energy storage system that ensure grid stability. The simulations are performed in Simulink®, using idealized models to better understand the ramp rate and delay time requirements for the controlled energy storage. The three-phase system is reduced to a single phase equivalent because of the assumption made of balanced conditions. In these simulations, PV system is modeled using Norton equivalent circuit with a controlled current source while energy storage system is modeled using Thevenin equivalent.

The basic inverter controllers in this chapter are only used to determine the ideal controllable energy storage power response that ensures that the microgrid voltage is within the standardized range between 0.95pu and 1.05pu. The ideal power response is then used for further ramp rate and delay time studies.

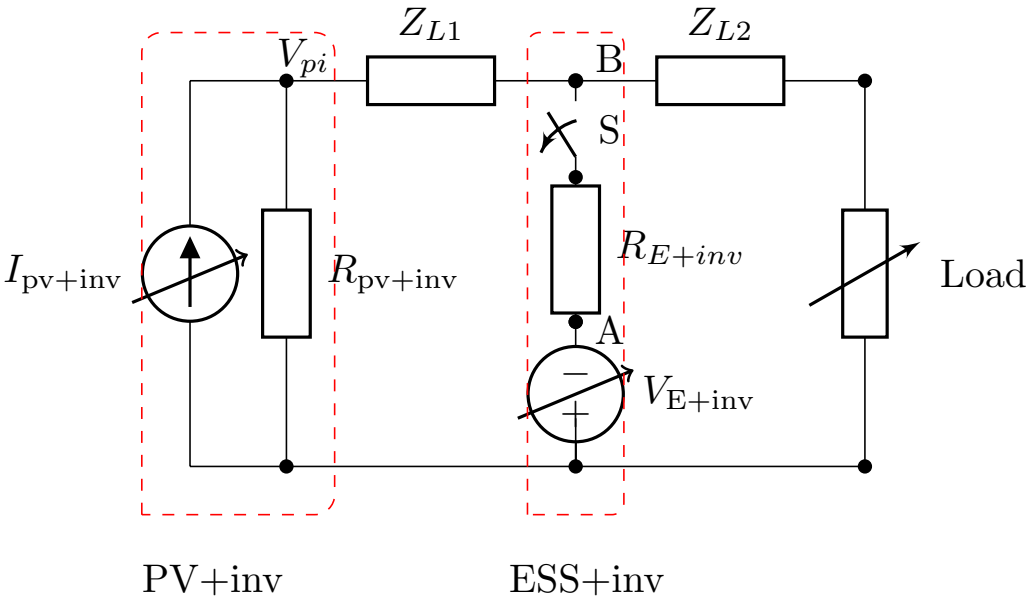


Figure 4.1. Simulation circuit for a standalone microgrid with a current and a voltage source modeling a PV source + inverter and an energy storage+ inverter respectively.

4.2 Microgrid model

Figure 4.1 shows a simulation model used to determine the behavior of a standalone microgrid. In the circuit shown in figure 4.1, a current source is used to model a PV system while a voltage source is used to model an energy storage system respectively. When the switch (S) is open, the microgrid operates without the controllable energy storage. The output voltage of the PV source + inverter model is as would be seen at the output of a three-phase PV inverter. Z_{L1} and Z_{L2} are the line impedances. For the simulations to follow in this chapter, The line impedances are assumed to be resistive and very small because an assumption of a collocated system was made. $R_{\text{pv+inv}}$ is assumed to be very large (1 MΩ) compared to the load resistance (between 50Ω and 200Ω) and this means that almost all the power from the output of the inverter is transferred to the load.

A load can sometimes draw more power which the sources may not be able to supply

and this can lead to a decrease in the microgrid voltage. This decrease in voltage can fall below the grid recommended boundary value of 0.95pu which can result in unwanted blackouts. In some cases, users can choose to disconnect non-essential loads when the PV power is low. An increase in PV power can also lead to a rise in microgrid voltage. The PV inverter model is designed to curtail the power from the PV panels to minimize the increase in microgrid voltage. However, the inverter will eventually disconnect if the voltage continues to rise beyond the upper boundary value of 1.05pu.

4.3 Microgrid model validation

A mathematical equation is used to validate the microgrid model. Superposition is used to determine the voltage at B (microgrid voltage). To determine the contribution of the voltage source ($V_{\mathrm{E+inv}}$) on the microgrid voltage, the current source $\mathrm{I_{pv+inv}}$ open circuited. To determine the contribution of the current source ($\mathrm{I_{pv+inv}}$) on the voltage at B, the voltage source ($V_{\mathrm{E+inv}}$) is short-circuited. The resulting circuit diagrams are used to derive the mathematical equations in 4.1 and 4.2.

$$V_{BE} = \frac{Z_{L1} + Z_{L2} + R_p + R_L}{R_E(Z_{L1} + R_p)(Z_{L2} + R_L) + Z_{L1} + Z_{L2} + R_L + R_p} \times V_{E+inv} \tag{4.1}$$

$$V_{BP} = \frac{R_p R_E R_t}{(R_p + R_t)(R_t + R_E)} \times I_{pv+inv} \tag{4.2}$$

where $R_t = \frac{R_E(Z_{L2}+R_L)}{R_E+Z_{L2}+R_L}$, V_{BE} is the voltage at B as a result of connecting $V_{\mathrm{E\ +inv}}$ and V_{BP} is the voltage at B as a result of connecting current source ($I_{\mathrm{pv\ +\ inv}}$)
The microgrid voltage is then given by:

$$V_{grid} = V_{BE} + V_{BP} \tag{4.3}$$

For utility grid R_E is very small and equations 4.1 and 4.2 reduces to:

$$V_{BE} = V_{\mathrm{E\ +\ inv}} \tag{4.4}$$

$$V_{BP} = 0 \tag{4.5}$$

Equations 4.4 and 4.5 shows that, for a grid with a very low resistance value R_E (i.e. stiff grid), addition of PV sources will not affect the grid voltage. However if the resistance value R_E is increased, the addition of other sources will affect the grid voltage (i.e. weak grids). This research is aimed at standalone microgrids (weak grids) and the resistance value R_E is chosen such that an increase or decrease in insolation can lead to voltage swells and voltage sags if the energy storage does not respond accordingly to reduce its internal voltage ($V_{\mathrm{E+inv}}$).

4.4 Simplified PV source inverter model

Droop control method was traditionally used to emulate the behavior of synchronous generators under both normal load and overload conditions [33]. A stable power system requires a good control of the real power (P) and the reactive power (Q). This control technique can be used to avoid overloading inverters without any communication between the power sources and load [34].

The active and reactive power flow in a line in figure 4.2 is given by equation 4.6, 4.7 [35].

$$P = \frac{U_1^2}{Z}\cos\theta - \frac{U_1 U_2}{Z}\cos(\theta + \delta) \tag{4.6}$$

$$Q = \frac{U_1^2}{Z}\sin\theta - \frac{U_1 U_2}{Z}\sin(\theta + \delta) \tag{4.7}$$

Given that $Ze^{j\theta} = R + jX$, equation 4.6 and 4.7 can be reduced to equation 4.8 and 4.9.

$$U_2 \sin\delta = \frac{XP - RQ}{U_1} \tag{4.8}$$

$$U_1 - U_2 \cos\delta = \frac{RP + XQ}{U_1} \tag{4.9}$$

Assuming that the power angle δ is small, $\sin\delta \approx \delta$ and $\cos\delta \approx 1$ and also assuming a resistive line impedance, equation 4.8 and 4.9 can be further reduced to equation 4.10 and 4.11 [36].

$$\delta \cong \frac{-RQ}{U_1 U_2} \tag{4.10}$$

$$U_1 - U_2 \cong \frac{RP}{U_1} \tag{4.11}$$

Therefore, it can be seen that the voltage largely depends on the active power whereas the frequency is affected by injecting reactive power. From the equation 4.10 and 4.11,

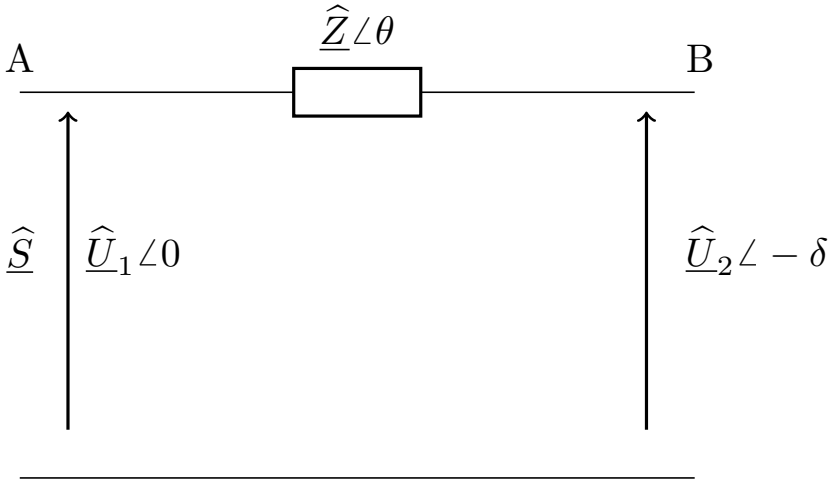


Figure 4.2. Power flow through a power line.

the droop control expressions for resistive networks can be written as [36]:

$$V - V_0 = -k_p(P - P_0) \tag{4.12}$$

$$f - f_0 = k_q(Q - Q_0) \tag{4.13}$$

Because an assumption was made of a resistive load on the microgrid, the reactive power is zero and hence the frequency remains constant at f_0 which is set at 50Hz. This means that instead two control loops (i.e. voltage and frequency control loops), only the voltage loop can be used to regulate real power on the network. The simulation studies that follow will use the simplified droop control and assumes a constant frequency of 50 Hz.

Figure 4.3 demonstrates the operation of the simplified PV inverter. The inverter consists of two loops; One that regulates the panel power and the one that regulates the voltage when the controllable energy storage node is not connected. The inverter will only start to inject current when there is enough insolation to blackstart the grid (i.e. insolation available is greater than i_{min}). The inverter will also maintain a current of I_{imax} when the insolation available is higher than i_{max}. The injected current I_{inv} is then compared to the grid current requirements. If I_{inv} is less than I_{min}, it means that the available insolation cannot sustain the grid voltage and hence the inverter must disconnect. If the injected current I_{inv} is above I_{max}, this means that the available PV power is higher than the power required by the load. In this case, there are risks of voltage swells and hence the system must also trip. The inverter is allowed to operate only if the injected current I_{inv} is between I_{min} and I_{max} because this range keeps the grid voltage within the range of 0.95pu -1.05pu as required by the standard.
If the controllable energy storage is connected, the PV inverter must switch to grid-tie mode. In this mode, the PV inverter must inject current and must not control the grid voltage. However if the grid voltage is above 1.05pu or below 0.95pu, the PV inverter must disconnect. A flow diagram for PV inverter in grid-forming mode is shown in figure 4.4.

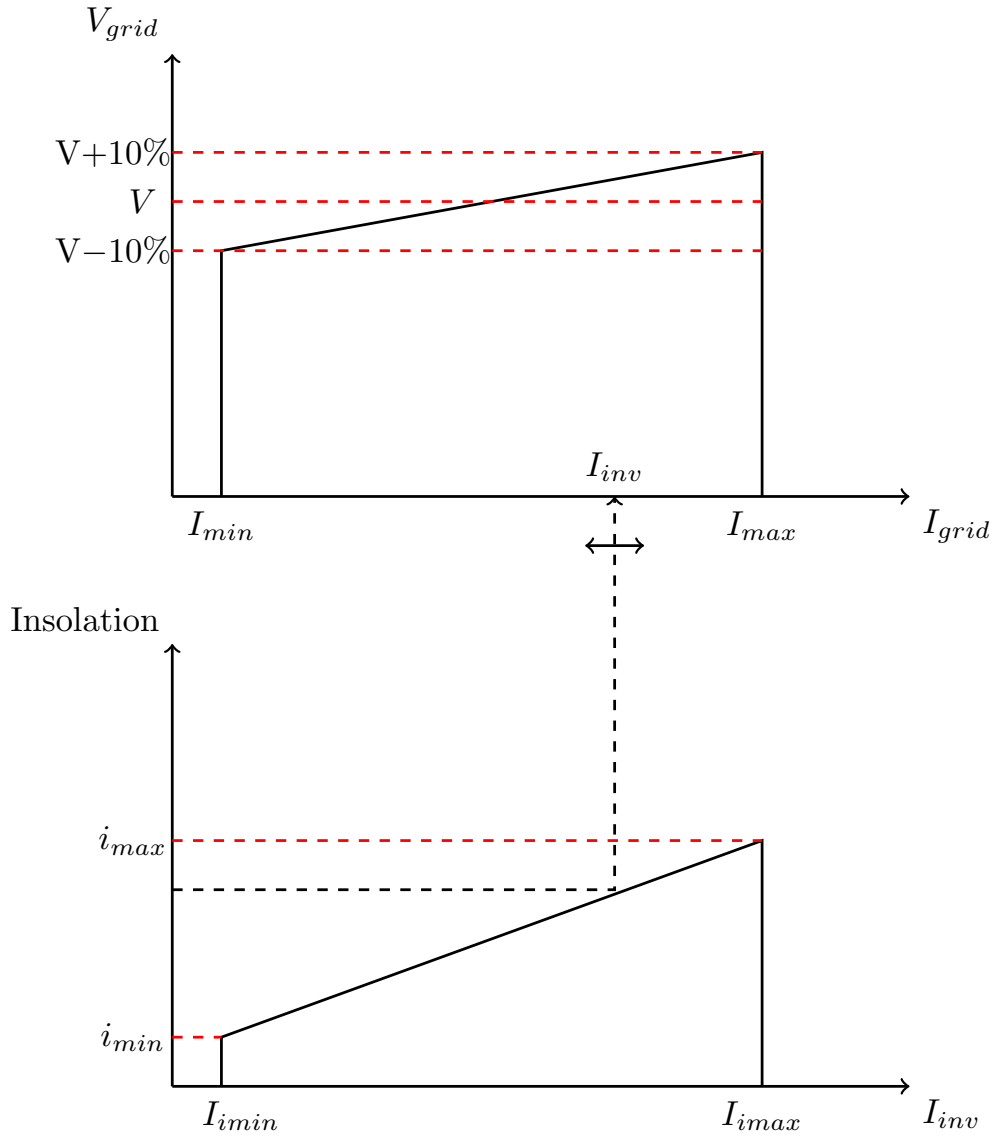


Figure 4.3. V-I curve illustrating the operation of a simplified grid-forming PV inverter used.

4.5 Energy storage model

The energy storage system (i.e. combination of the energy storage and inverter) is modeled using a controlled voltage source to regulate the microgrid voltage so that it remains within the range at all time. By increasing or decreasing the internal voltage V_{E+inv} of the energy storage system, the direction of power flow can be changed as required. The internal voltage of the energy storage depends on the state of the charge and the power

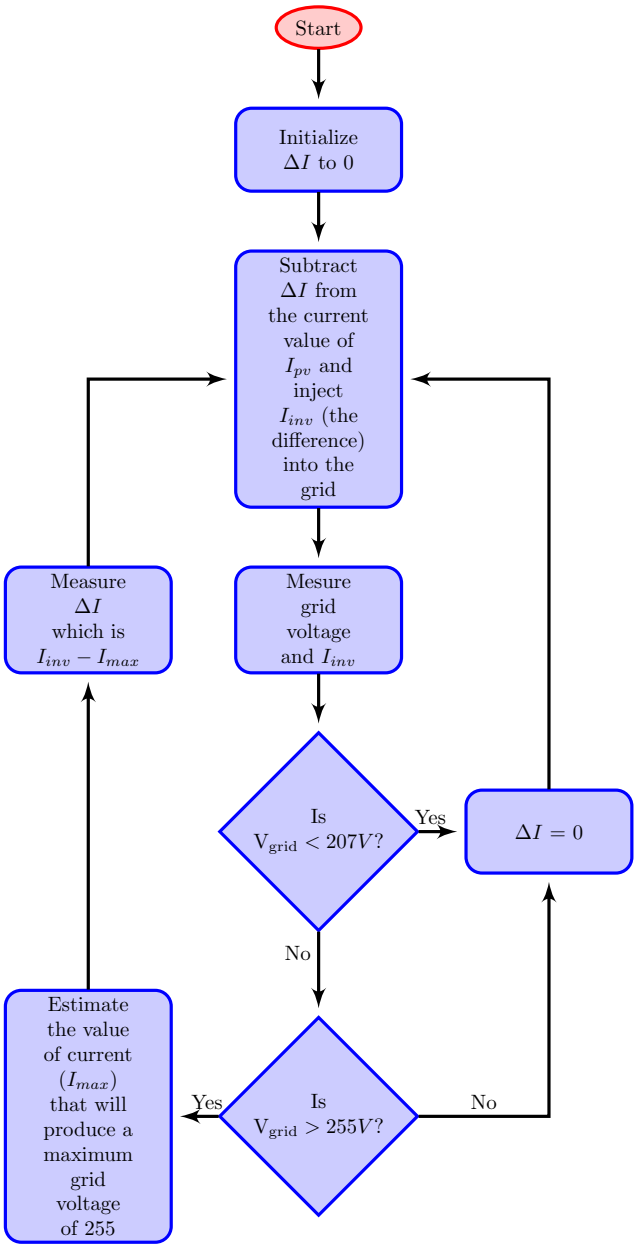


Figure 4.4. A block diagram showing the operation of the grid-forming PV inverter.

required by the load. If the energy storage is not fully charged and the grid voltage is above 1.02pu, the energy storage inverter controller decreases its internal voltage. The current drawn by the energy storage increases and this will result in a decrease in the microgrid voltage (V at B). If the grid voltage is below 0.98pu and above 0.95pu, the

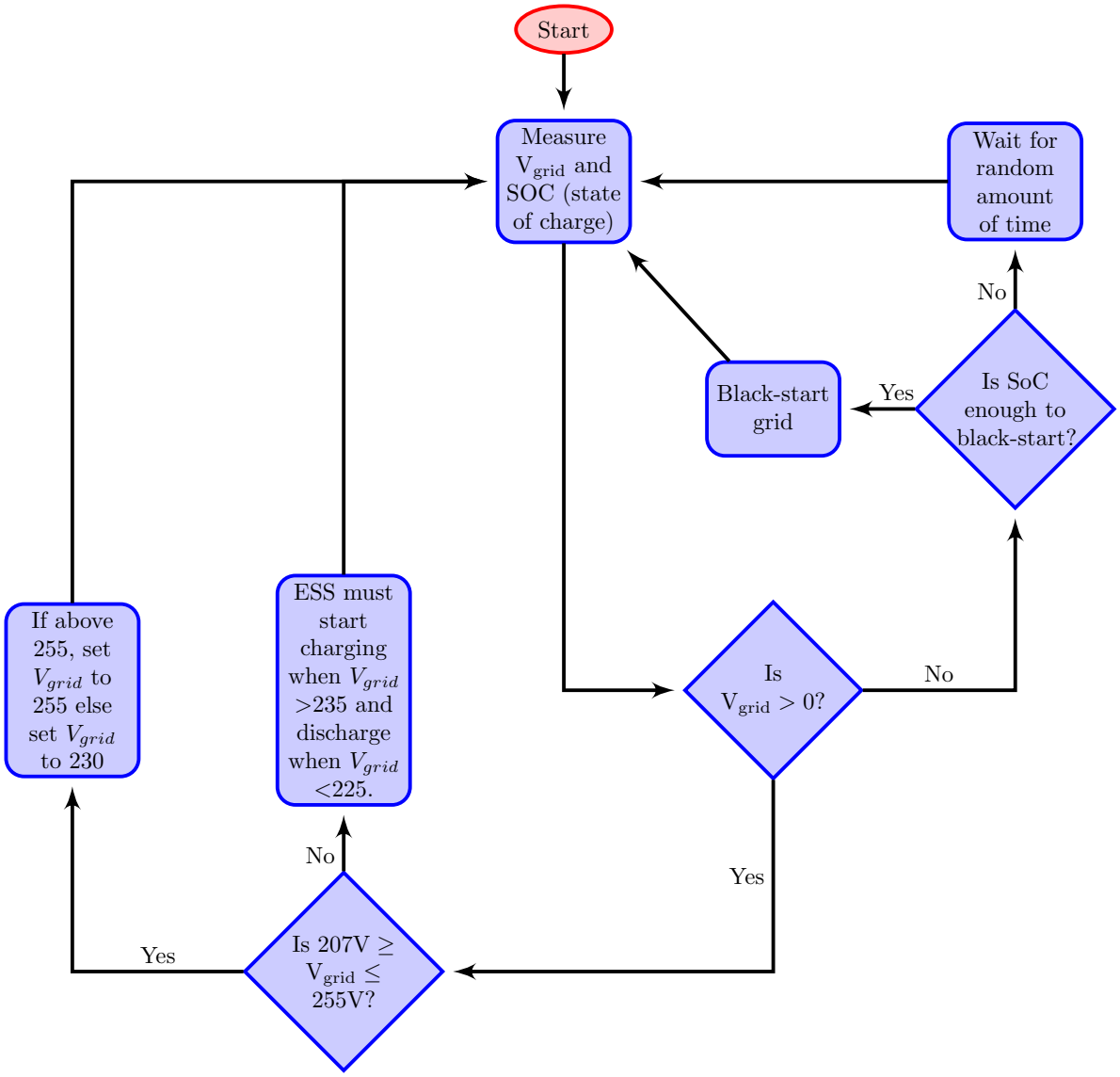


Figure 4.5. A flow diagram for the basic energy storage controller used in the simulations.

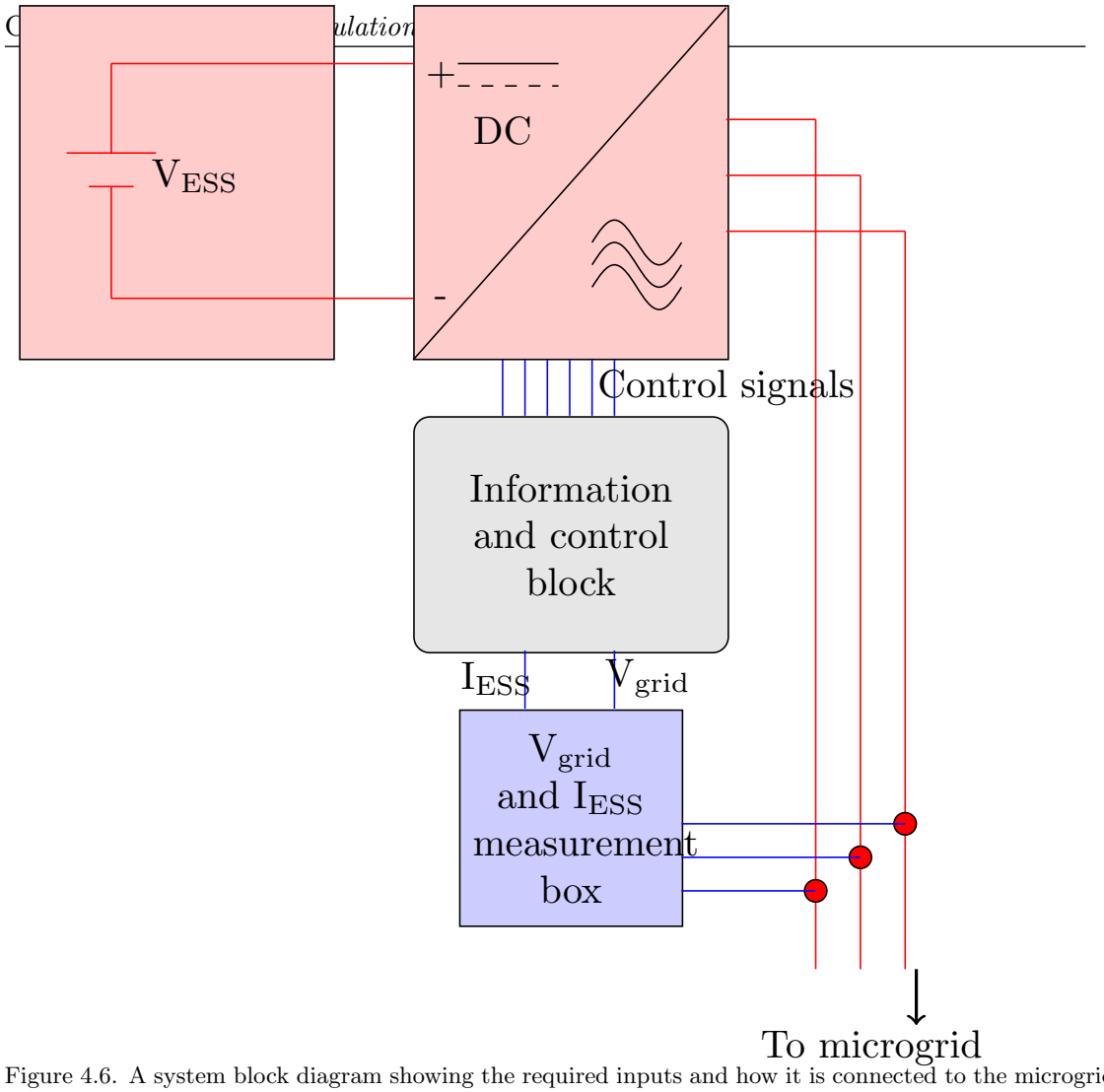


Figure 4.6. A system block diagram showing the required inputs and how it is connected to the microgrid.

controllable energy storage must raise its internal voltage to supply power to the microgrid. A flow diagram for the controllable energy storage algorithm is shown in figure 4.5. For a real system, the energy storage system must be connected as shown in figure 4.6.

4.6 Requirements for reliable operation of a collocated standalone microgrid

Some important requirements for optimum operation of the standalone microgrid in this study are listed below:

- The inverter based sources must jointly coordinate to regulate the bus voltage.
- The sources must share the power according to the source size to avoid overloading.
- Addition of a source/energy storage/load node should not affect the operation of the microgrid i.e. must be able to operate in a plug and play mode.
- Voltage control must be achieved by using the point of connection measured signals only. Communication of inverters must be done using the node voltage and current signals and no direct connection between inverters is allowed.

4.7 Simulations of a standalone microgrid without a controllable energy storage system

The Simulink® model used of a standalone microgrid without a controllable energy storage system is shown in figure 4.7. The PV inverter controller used in this case has both the grid-forming and grid-tie algorithms. It is designed to check if there is a voltage on the grid and adjust its mode of operation accordingly. If the energy storage system is not connected, the PV inverter must switch to grid-forming mode. The Simulink® controller block diagram is shown in figure 4.8. The line impedance has been assumed to be very small (0.1Ω). The grid voltage in figure 4.9 shows that during the night, the voltage is 0V and during the day PV power fluctuations which are experienced can also lead to an unstable microgrid.

It has also been observed that connecting more appliances on a standalone microgrid without an energy storage device can result in severe blackouts. Figure 4.10 shows that, as the load is increased (i.e reducing the load resistance), the blackouts become more severe. Severe blackouts generally mean that the size of a high power density energy storage system to supply power during the regular switching must be increased. This is very expensive and hence for an optimum solution, a balance between the size of the load connected and the size of the high power density energy storage is required.

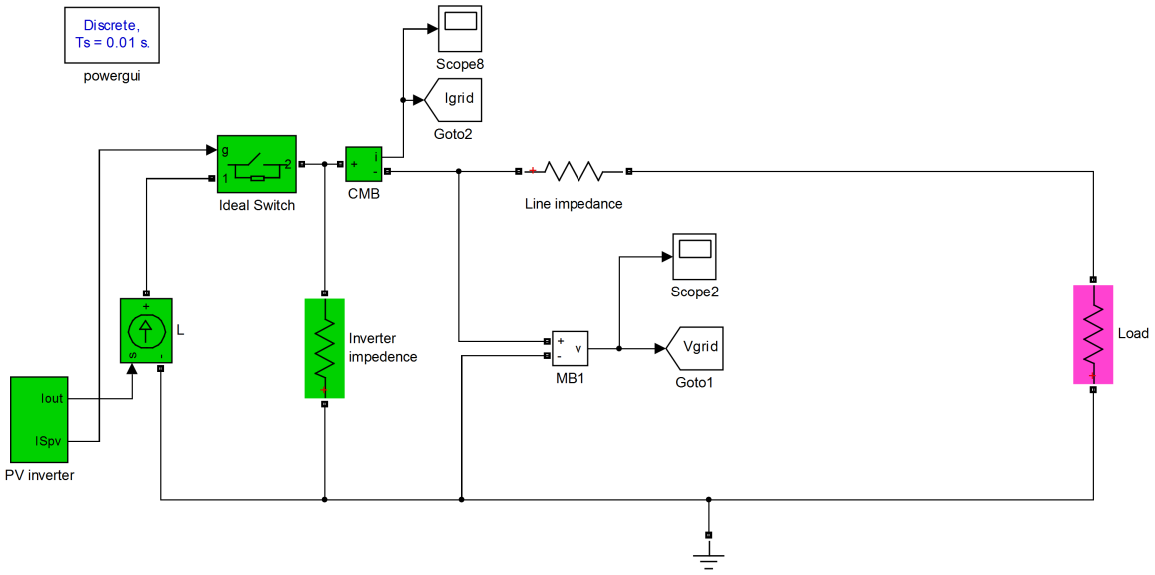


Figure 4.7. A Simulink® model of a standalone microgrid without a controllable energy storage.

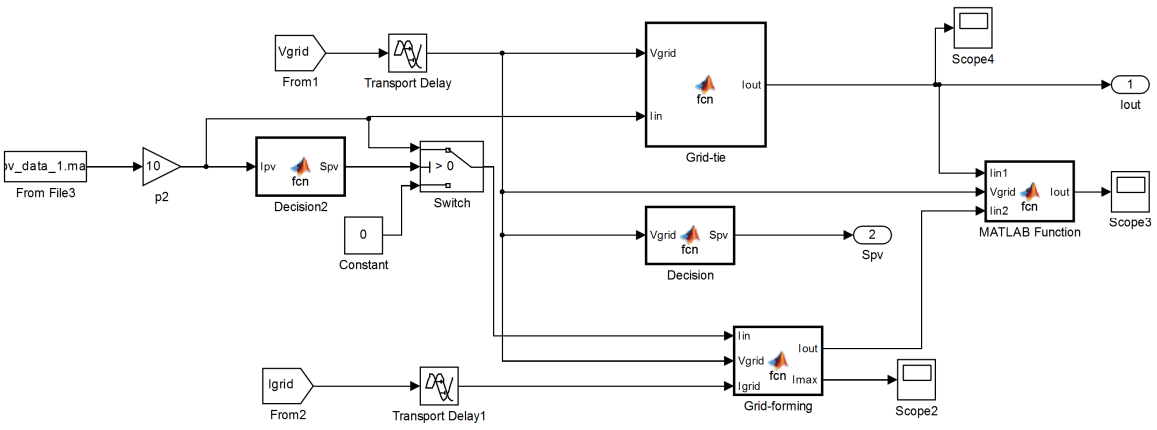


Figure 4.8. A Simulink® block diagram showing the simplified PV inverter controller used in the simulation.

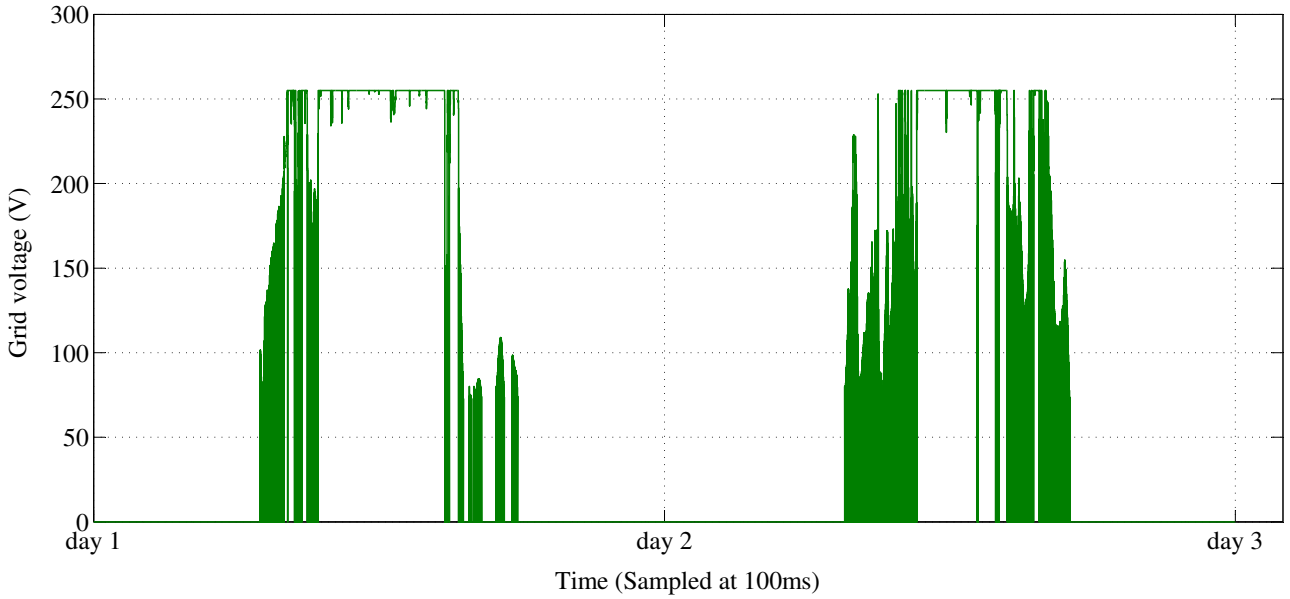


Figure 4.9. The simulated voltage of a standalone microgrid without a controllable energy storage.

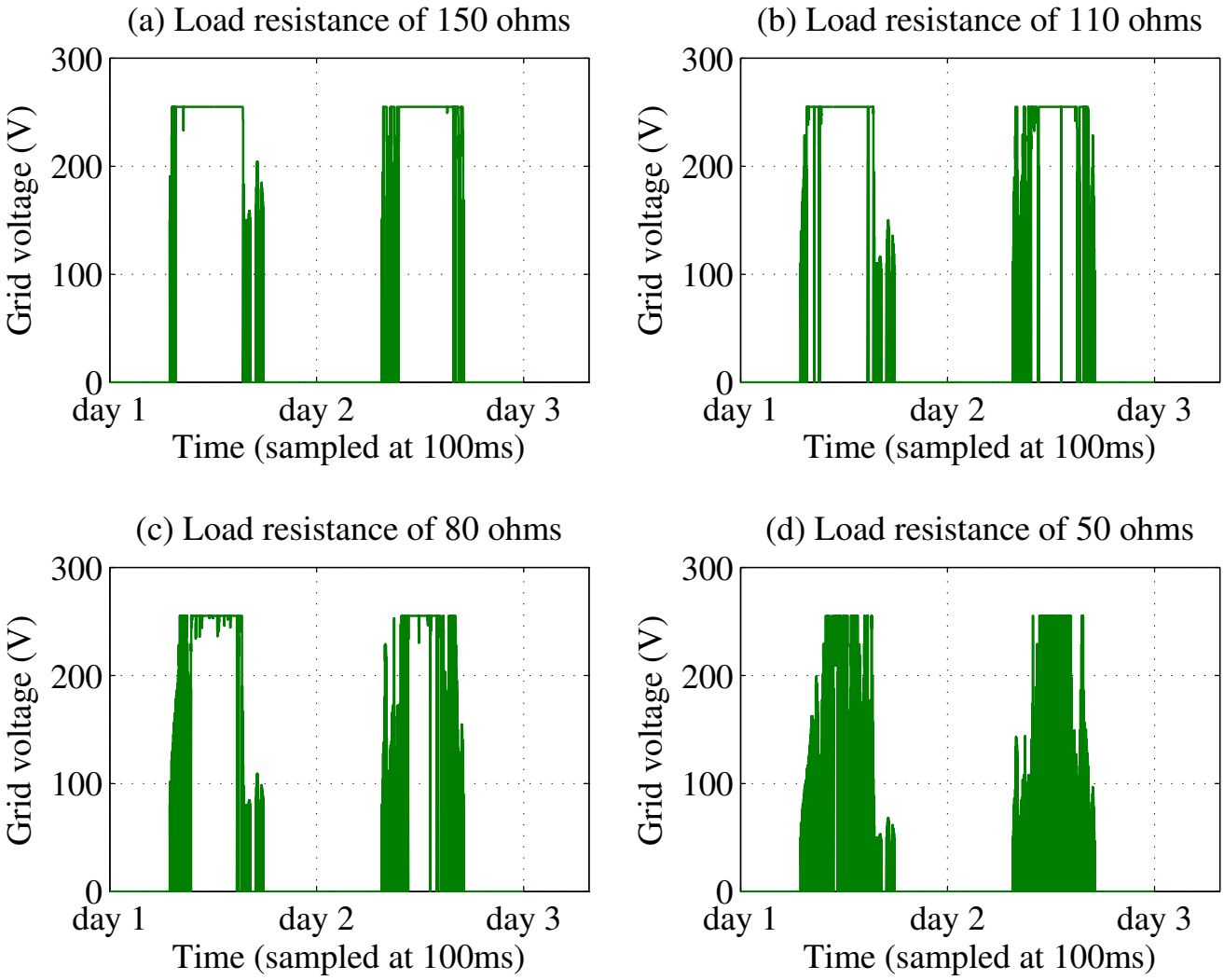


Figure 4.10. The simulated voltages showing the effects of adding load on a standalone microgrid without controllable energy storage .

4.8 Simulations of a standalone microgrid with a controllable energy storage present

A standalone microgrid operates with a controllable energy storage device when the switch (S) in figure 4.1 is closed. The energy storage system has a control block that monitors the grid voltage (V_{grid}), the output current (I_{ESS}) and the State of Charge (SoC). The

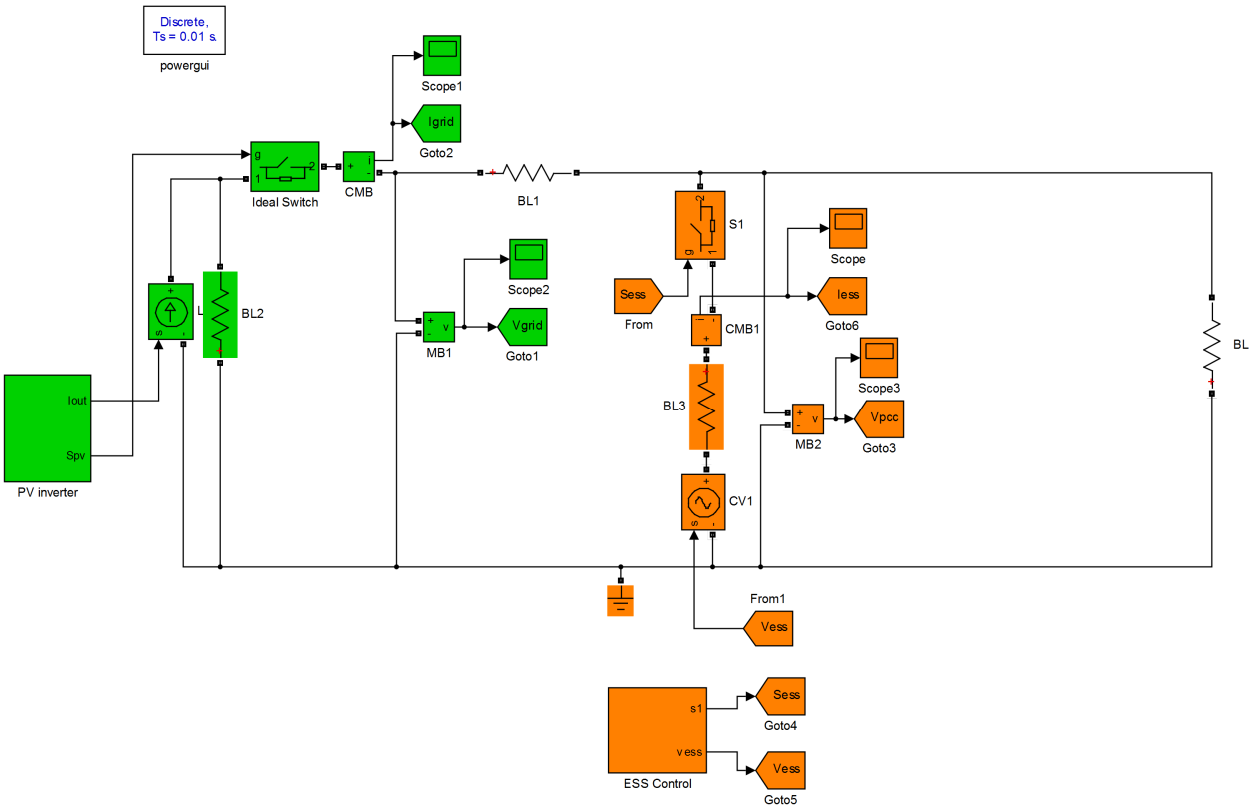


Figure 4.11. A standalone microgrid Simulink® model used to determine the controllable energy storage ideal response.

energy storage system basic controller in figure 4.12 uses the RMS voltage to predict the state of the grid. The voltage and current signals are also used to keep track of the energy storage State of Charge.

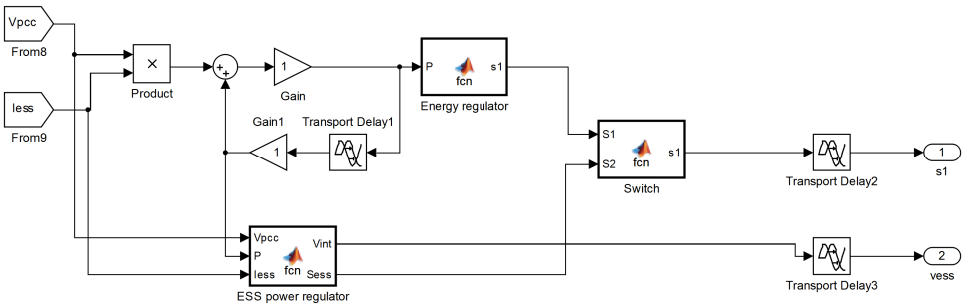


Figure 4.12. A Simulink® block diagram of the energy storage controller.

4.8.1 Simulation with constant load

A simulation was done for a single PV source and a constant load. With no delay and infinite ramp rate, the power response of the energy storage is as shown in figure 4.13. This is the ideal power response which is expected from the energy storage system. However

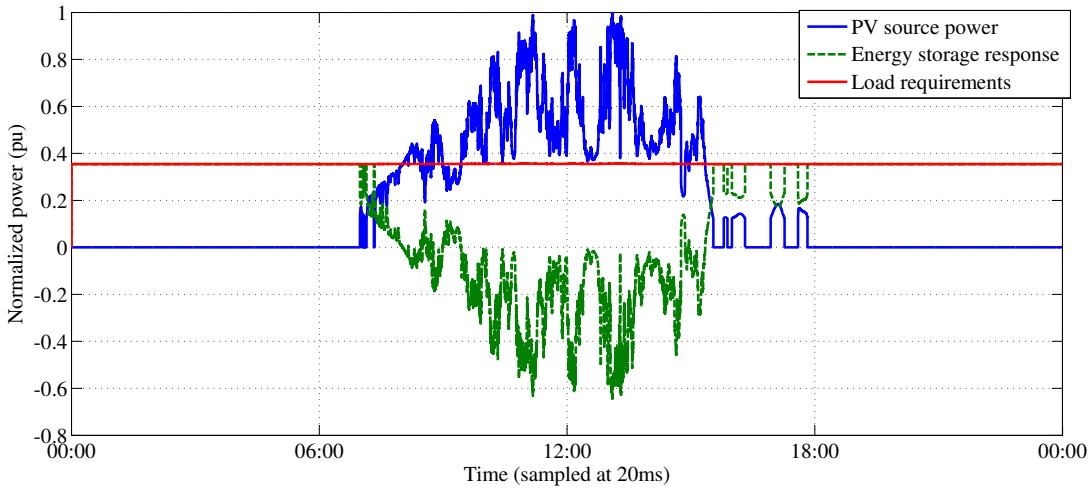


Figure 4.13. Response of an ideal energy storage to a standalone microgrid with a fluctuating source and a constant resistive load.

existing energy storage technologies have ramp rate limits and delay time. High power density energy storage system have high ramp rate limit and a very small delay time, which enables them to respond faster to changing power.

The simulation was done to determine the effects of insolation fluctuations on the microgrid voltage. Only source fluctuations were considered.

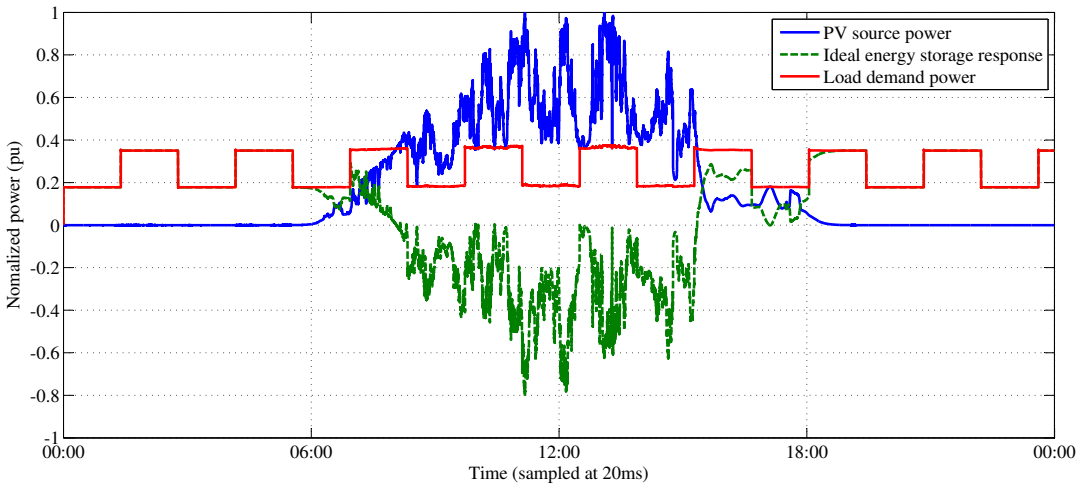


Figure 4.14. Response of an energy storage system to a standalone microgrid with a fluctuating source and a varying resistive load.

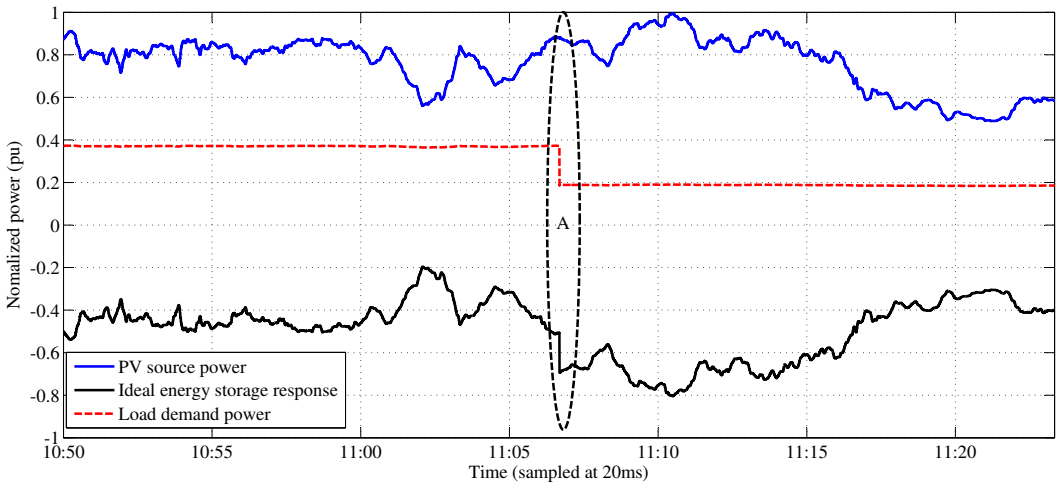


Figure 4.15. An extract of the data in figure 4.14 clearly showing that the energy storage must match that of a load with faster dynamics.

4.8.2 Simulation with a varying load

Subsequent to the simulations of a microgrid with a constant load, an additional resistive load controlled by a PWM signal is connected. The load draws current instantaneously when switched on. This section aims to determine the ramp rate requirements for such loads. Figure 4.14 shows the ideal energy storage system response to the fluctuating load. An extract of the data in figure 4.15 shows that for a load with ramp time 50 times smaller than the PV source ramp time, the energy storage system must match the rate required by the load and this is shown in region A in figure 4.15. The ramp time measurements for typical microgrid loads were found to be in the range of 20 - 60ms as compared to the PV source ramp time of 1s. This means that these PV source ramp rates do not contribute much during the load switching events.

4.9 Summary

This chapter described the microgrid components used in the research. These components include the PV source + inverter single phase equivalent which was modeled using a controlled current source. The other component discussed was the basic operation of the energy storage system. The energy storage system(i.e. energy storage + inverter) was modeled using a controlled voltage source. Because load transients mainly occur at the moment when the switch is closed/opened, a resistive load in series with a switch was used to model fluctuating load. Results of the simulations are discussed in next chapter.

Chapter 5

Discussion of Simulation Results

5.1 Introduction

This chapter discusses results of the simulations done in Chapter 4. Simulations were done for a microgrid with and without a controllable energy storage system. These simulations are performed to determine the effects of energy storage on a standalone microgrid for a specific case and although the final ramp rate requirements may vary from one standalone microgrid to another, the procedure used in this research will be the same for any other standalone microgrid.

5.2 Discussion of Simulation Results

Figure 5.1 shows the effects of delay time on the grid voltage. As the delay time increases, the power fluctuations become more severe which results in an unstable grid. There are two types of fluctuations that need to be considered; switching fluctuations which occur

when big loads are turned on or off and the insolation fluctuations that occur as a result of changes in insolation. The switching fluctuations are more severe and have shorter ramp time (i.e. in the range of 20ms - 60ms) while insolation fluctuations have been found to have to be much slower (1 second ramp time).
It must be noted that the energy storage ramp rate requirements when a big load is turned on or off is the same as the ramp rate required when there is a sudden loss in PV source. Figure 5.3 also shows a gradual increase in voltage swell amplitudes as the energy storage delay time is increased. The magnitude of voltage sags on the microgrid also decreases as the energy storage system delay time is increased. Operating a standalone microgrid with a voltage outside the standardized range from 207V to 255V is not recommended because most appliances are designed to operate in this range. The maximum allowable energy storage system delay time when considering only the insolation fluctuations has been found to be 0.53s as shown in figure 5.3. Operating with an energy storage system delay time below 0.53s when a constant power load is connected ensures that the voltage is always within the standardized range stated above.

The simulation results in figure 5.4 shows the effects of energy storage ramp rate on the grid voltage. Limiting the energy storage system ramp rate will result in slow response which can lead to large voltage swells or voltage sags. This figure also shows that the energy storage system ramp rate required when a standalone microgrid with fast load transients (i.e. ramp time of 20ms) must be above 8.5pu/sec to keep the voltage within the standardized range. This ramp rate is required to smooth out initial load transients. For smoothening PV power, the minimum energy storage system ramp rate required has been found to be 0.3pu/sec as shown in figure 5.5. This value is approximately 28 times lower than the minimum ramp rate required to smoothen power fluctuations during load transients. This shows that if the energy storage system is designed to meet the load ramp rate requirements, voltage fluctuations resulting from PV power can be easily smoothened without an additional energy storage.

Although energy balance is not the main focus of the research, adding more load can

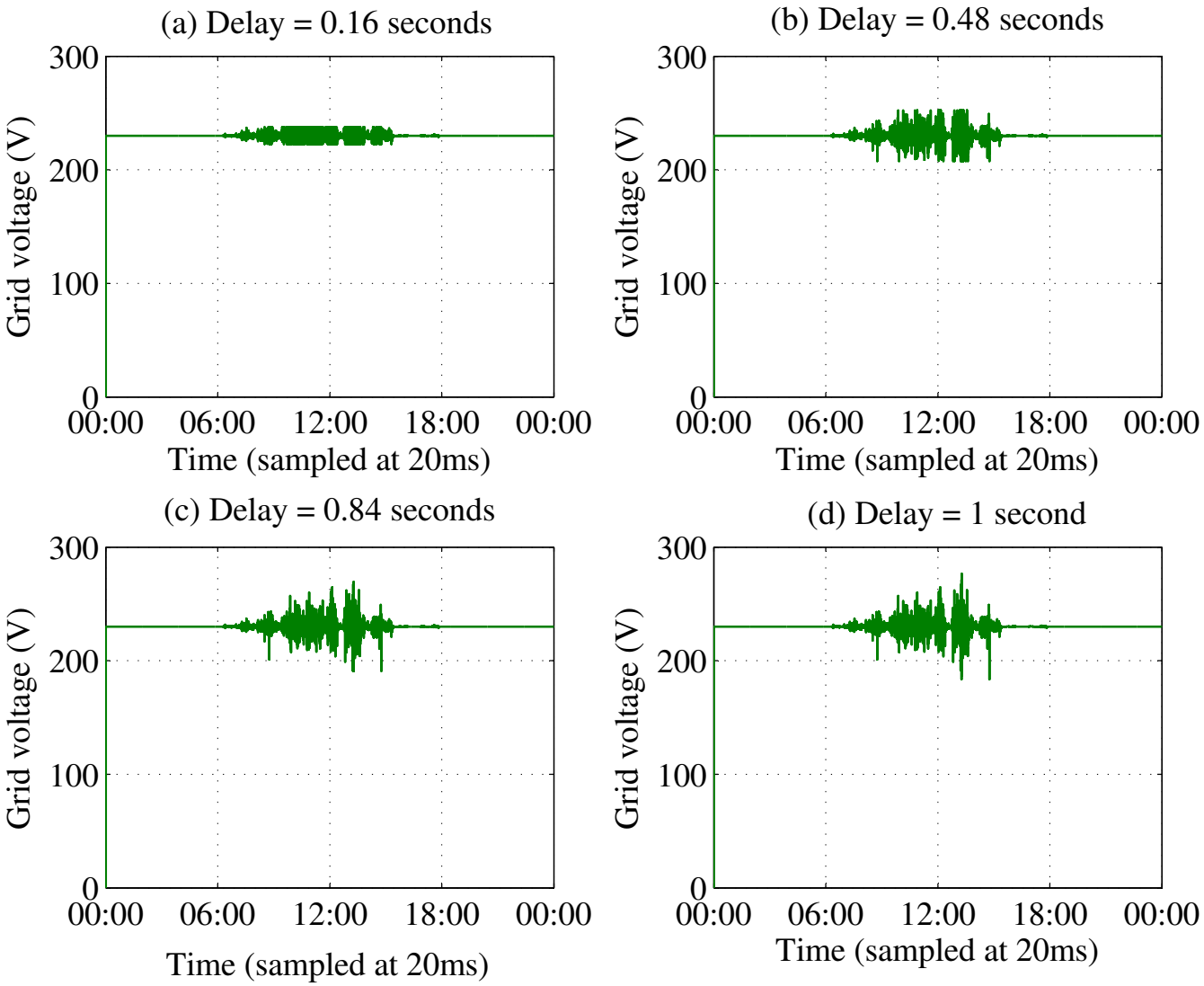


Figure 5.1. Effects of energy storage delay time on the microgrid voltage.

also lead to energy imbalance. One of the requirements for a stable operation of the microgrid is the energy balance. The storage must have sufficient power to charge during the day. Increasing the load can result in limited charging time for the energy storage. Figure 5.6 shows the effects of connecting more load on the microgrid. Normal operation would require the State of Charge to be 50% at the beginning of each day. Figure 5.6c is the ideal State of Charge (SoC) curve required for the normal operation of a standalone microgrid. Figure 5.6a shows that the energy storage will be empty at the beginning of

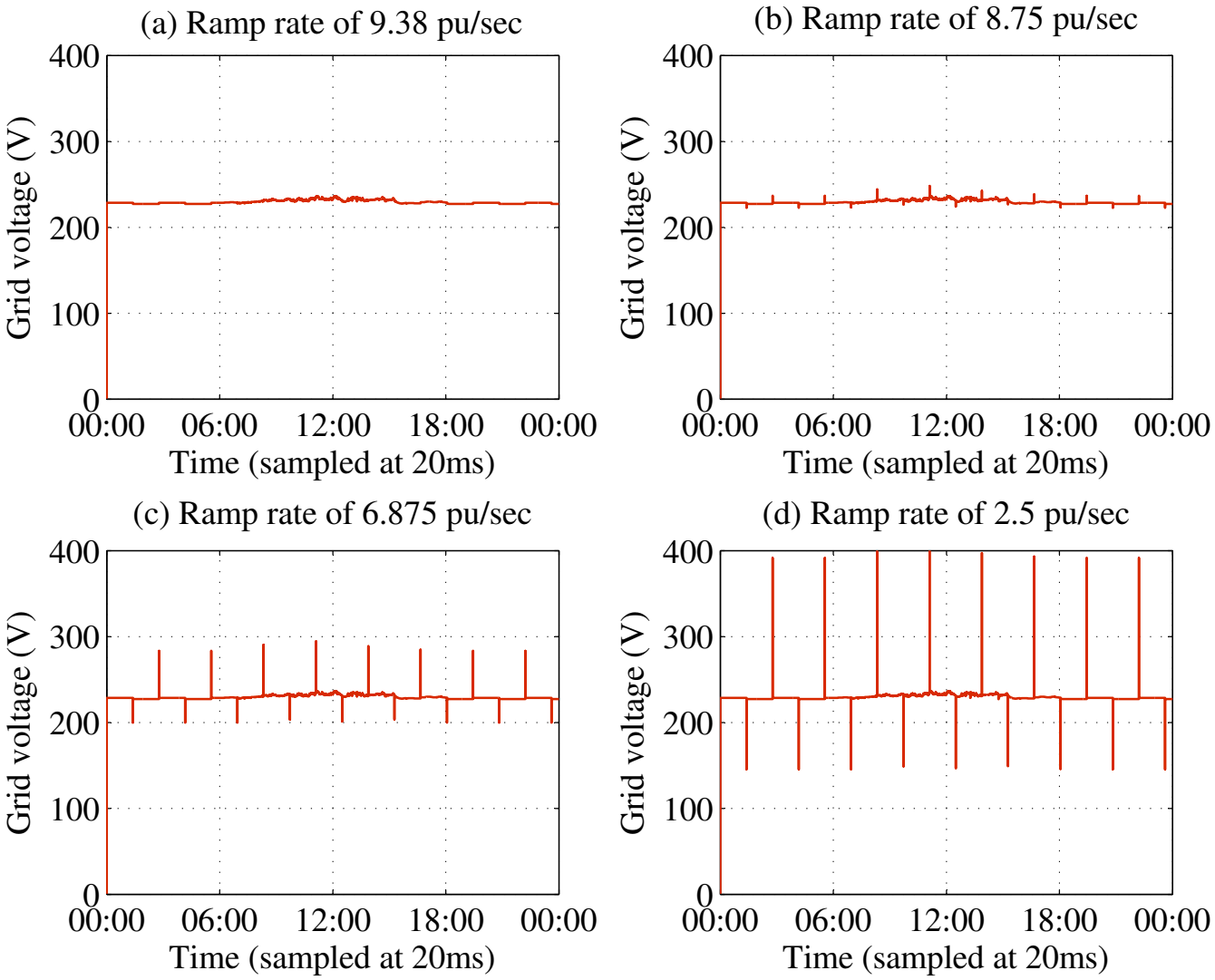


Figure 5.2. Effects of ramp rate on the microgrid voltage. Increasing the ramp rate of the energy storage would result in a stable microgrid.

the next day and this will lead to blackouts from 00:00 till dawn. This is because, from the time the sun sets until dawn, the energy storage must be able to supply the power.

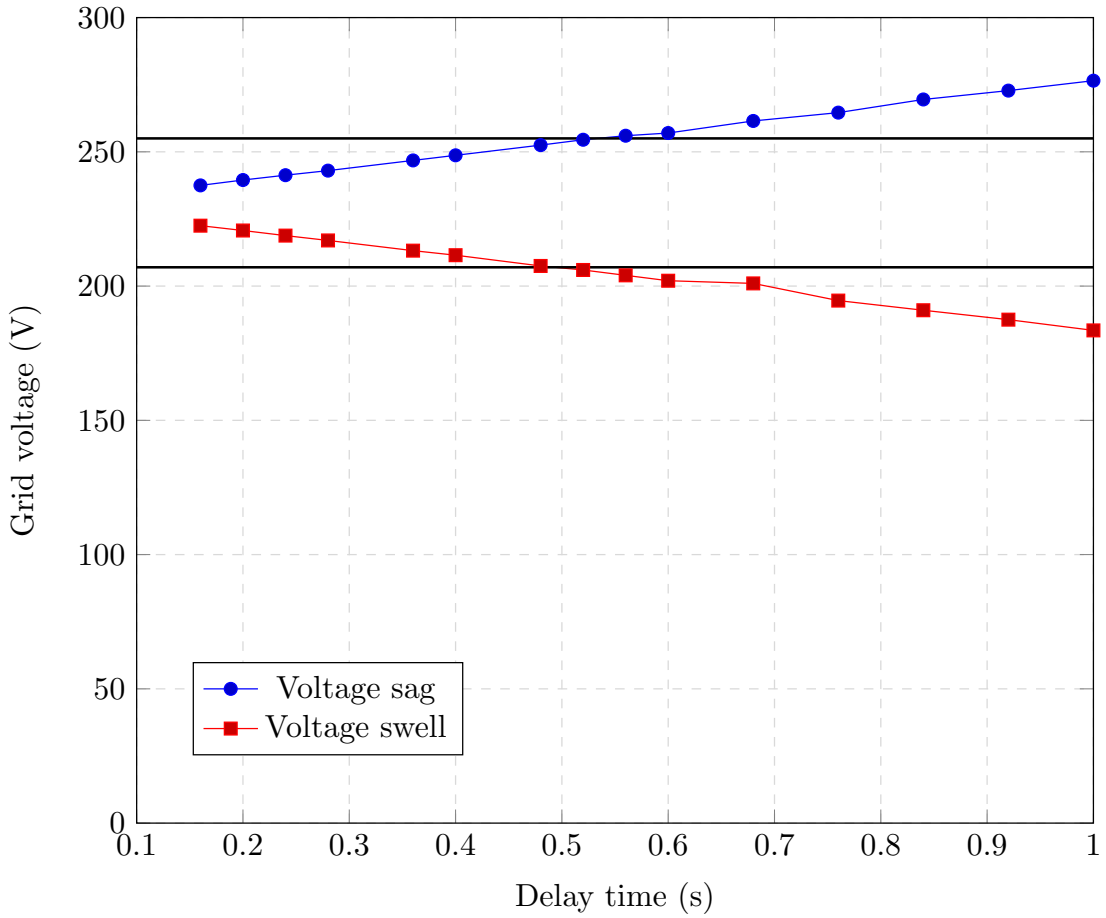


Figure 5.3. Effects of delay time on the magnitude of voltage swells and voltage sags caused by PV panel power fluctuations

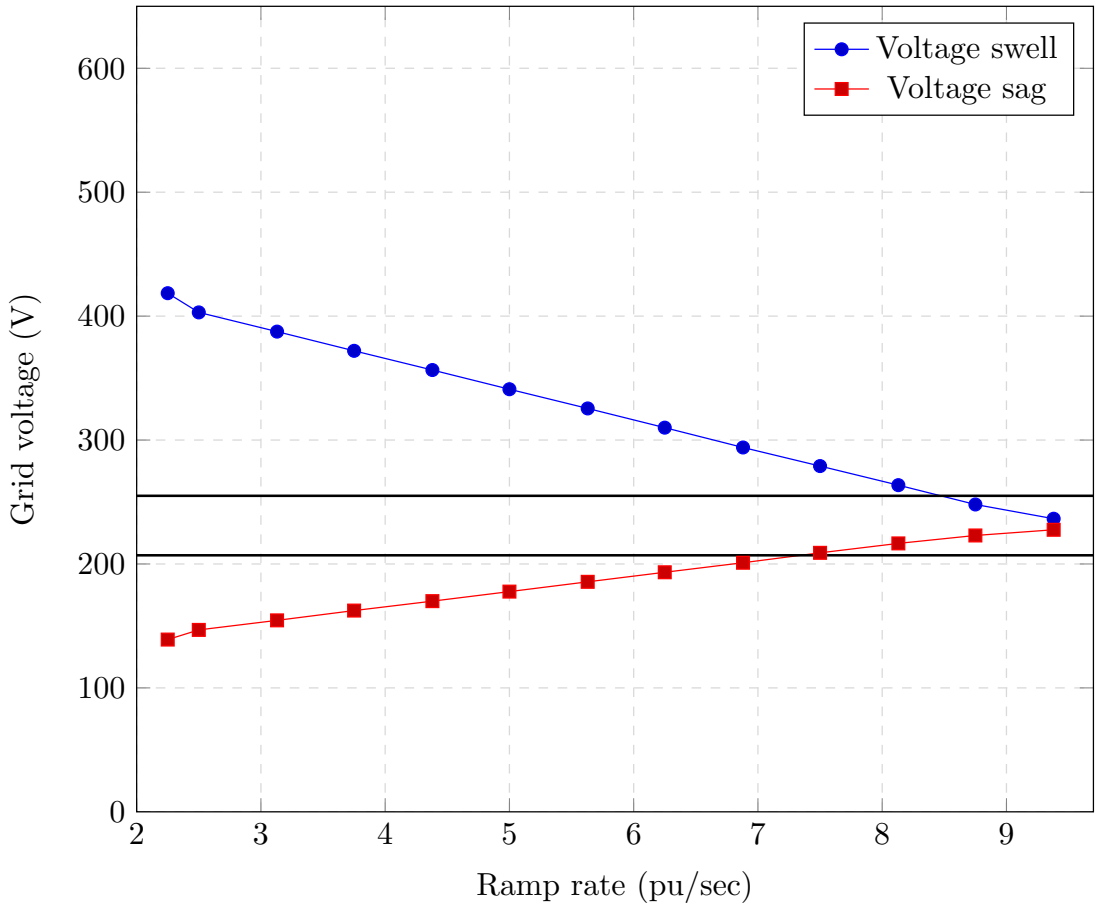


Figure 5.4. The effects of energy storage system ramp rate on the voltage of a standalone microgrid with loads with a ramp time of 20ms and above.

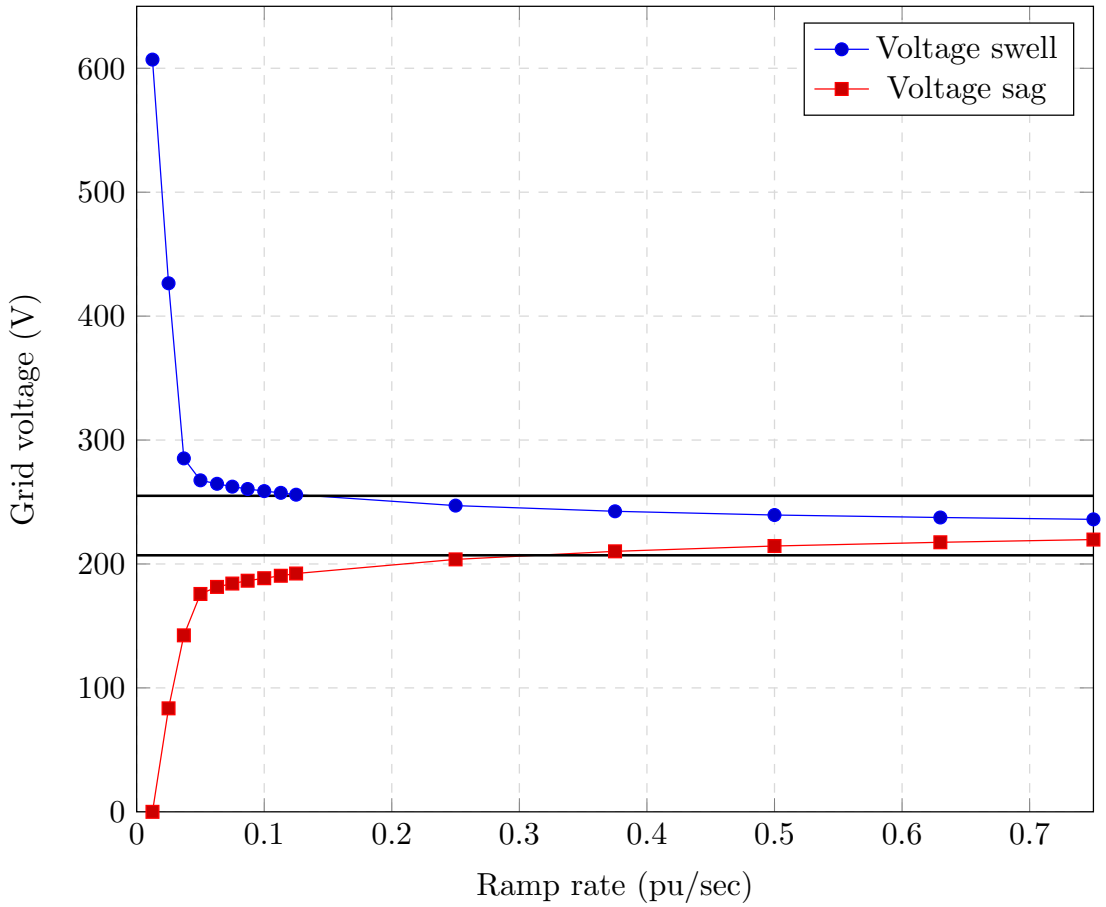


Figure 5.5. The effects of energy storage system ramp rate on a standalone microgrid with a PV source and a constant load.

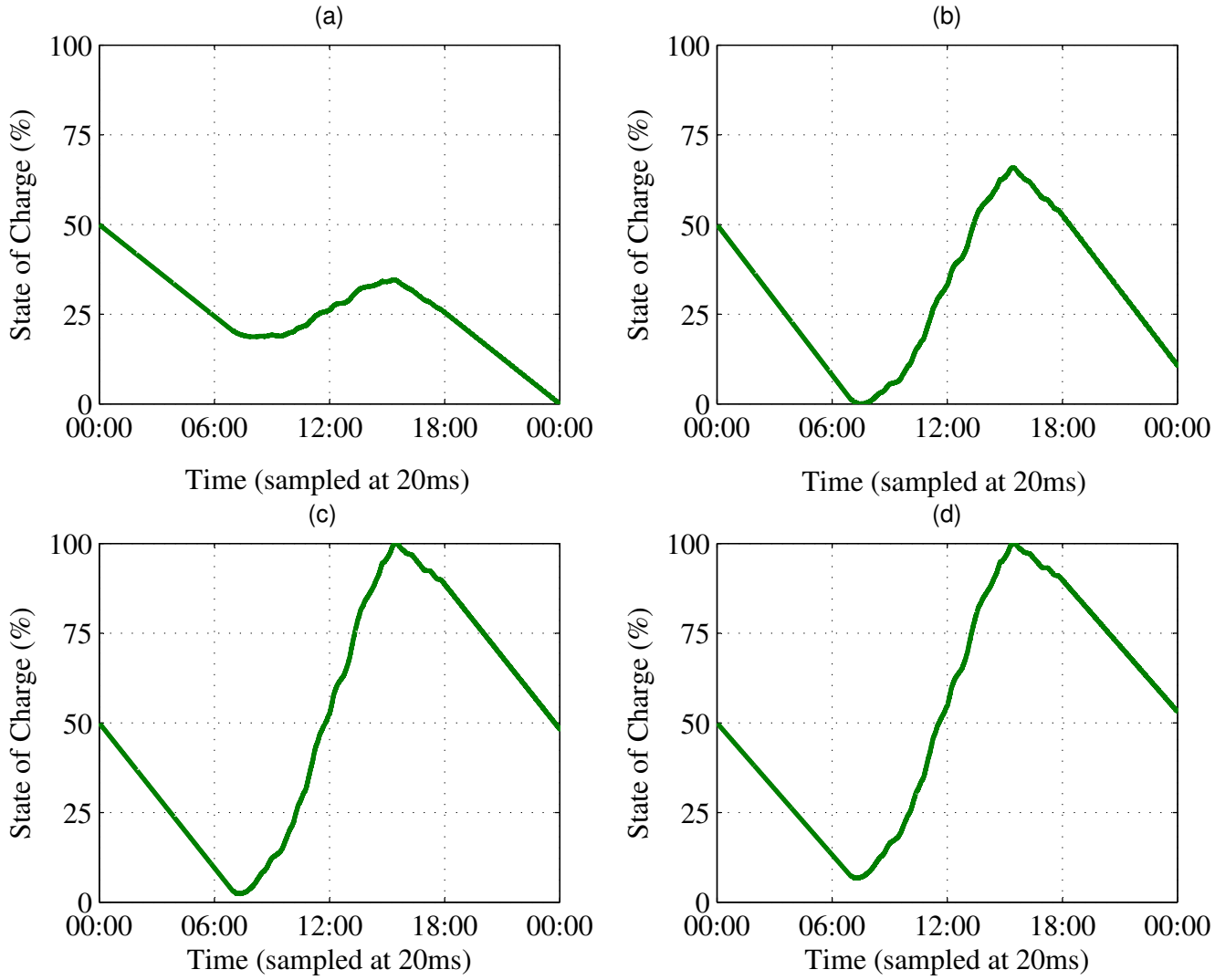


Figure 5.6. The graphs show that an increase in the energy required by the load can result in insufficient charging time for the energy storage system to fully charge at least once in a 24hr period. Normal operation requires the state of charge of the energy storage 50% at the beginning of each day.

5.3 Summary

One of the immediate findings obtained was the need for energy storage on standalone microgrids. It has also been shown that adding more load can result in an expensive microgrid because of the high power density energy storage required to respond to frequent switching on the grid. Connecting many appliances has also been found to cause energy imbalance.

The ramp rate and delay time of energy storage technologies play an important role on the stability of the standalone microgrids. When frequent switching occurs on the grid an energy storage system with a shorter delay time and higher ramp rate is required. It has also been found that the energy storage system ramp rate required during load switching transient must be as high 8.15pu/sec to keep the microgrid stable. This load ramp rate requirement was found to be 28 times the maximum insolation ramp rate obtained. This means that the energy storage system dynamic specifications must be calculated using the load data.

The maximum allowed delay time has also been found to be 0.53s to balance insolation fluctuations. For load power fluctuations, even a delay as small as 10ms can result in voltage swells and sags. This is mainly because of the tight allowed voltage band of $1\pm5\%$.

Chapter 6

Conclusions and Recommendations

6.1 Conclusions

The analyses into the dynamic power requirements for controllable energy storage used on photovoltaic microgrids has been presented. These dynamics requirements were identified as; ramp rate and delay time. The background into the importance of the understanding these dynamic power requirements were also presented.
The main objective of the research was to generate a framework which can be used when choosing appropriate energy storage systems for standalone microgrids. To achieve this objective the following steps had to be done:

- PV source and load demand data measurements. At this stage, A computer software Perl was used to separate the data. The resulting data was used to identify days with severe fluctuations.

- Using insolation data measured for the day with severe fluctuations and load demand data for typical domestic appliances, PV source and load demand ramp rate analysis was done.
- Simulation to determine the effects of the energy storage system ramp rate and delay time on the microgrid voltage.
- Determining the range of energy storage system ramp rate and the delay time that ensures microgrid stability.

Measurements were done for the PV source and load data at the University of the Witwatersrand. Pyranometer readings were used because they represent the worst case scenario for the insolation fluctuations. The Genmin building load demand used was found to not represent the load power fluctuations that occur on standalone microgrids. Further measurements were done on typical domestic appliances that have different dynamic behavior. These appliances include; a 65W laptop charger, a 68W refrigerator, 1.5kW microwave, 2kW electric heater and a 45W light bulb. The appliance power measurements were recorded very 20ms because an assumption was made that the controllers would use RMS values of voltage and current.

6.1.1 Findings from PV source and load demand ramp rate analysis

An analysis of the insolation ramp rate revealed that the average ramp rate and peak ramp rate for the 2 day period were found to be 0.011pu/sec and 0.12pu/sec respectively. These insolation ramp rate values have been found to be very low compared to the load ramp rates, especially for a small standalone microgrid. This is because most loads draw peak power in the first 20ms - 60ms as compared to the 1 second insolation fluctuations. It has also been found that sizing of energy storage must be done using load data.
Load transients have also been found to cause grid stability problems. Traditionally, the standalone microgrid size was mainly determined using the load rated power. In

many cases, the load rated power is lower than the load peak power required by the load as demonstrated from measured power for typical domestic appliances. More efficient appliances with a low peak power to rated power must be used.

6.1.2 Findings from the microgrid simulations

The simulations have shown that standalone microgrids are more susceptible to voltage fluctuations because of the varying nature of PV sources. Energy storage systems must be designed to detect these power fluctuations and respond before the standalone microgrid becomes unstable.

It was also found that adding more load on a microgrid without an energy storage system can lead to frequent blackouts. These blackouts can be minimized by installing an energy storage system. However, a large high power density storage is required to respond to these fluctuations which normally result in an expensive solution.

The energy storage system ramp rate and delay time have been found to affect the microgrid voltage. Low ramp rate can result in a slow response to power fluctuations and this can lead to voltage swells and voltage sags. It has been found that the energy storage system ramp rate required to cancel out insolation fluctuations was 0.3pu/sec compared to the energy storage ramp rate of 8.5pu/sec required for a systems with load fluctuations. The maximum allowable delay time has also be found to be 0.53s to avoid blackouts that result from insolation fluctuations. For loads with ramp time of 20ms, the energy storage delay time must be very small (less than 5ms).

If the standalone microgrid is powering a load with power that does not does change all the time, only the insolation data can be used when sizing the energy storage system. This will relax the energy storage system ramp rate and delay time requirements.

6.2 Recommendations

Recommendations for future work are listed below.

- Analysis of inverter response during transients must be done to determine if inverters have some additional limitations can result in slow response to fluctuating PV sources and fluctuating loads.
- The microgrid simulation and control was done for loads with a power factor of 1, in a real system, any load can be connected and the energy storage inverters must be able to also control reactive power in the system. The simplified droop control implemented must be further expanded to include frequency control which is useful in regulating the reactive power component in the system.
- The research was mainly on data analysis prior installation of standalone microgrids. Results obtained have been verified in simulation but there are other problems can only be seen when a real system has been built which may not necessarily be identified in simulation and hence the need for an experiment.
  Several studies have been done on how a standalone microgrid can be emulated. A microgrid testbed in figure 6.1 is being developed to better understand the interaction of PV sources, energy storage system and loads.
  Sets of induction machines and variable speed drives will be used to emulate various DGs or energy storage systems as shown in figure 6.2 depending on the control signal used. Each emulator will receive a control signal that is used to generate a power profile resembling DGs or loads or energy storage system response.
  Currently, efforts were made to validate the method of carrying out experiments and details can be found in the following papers.

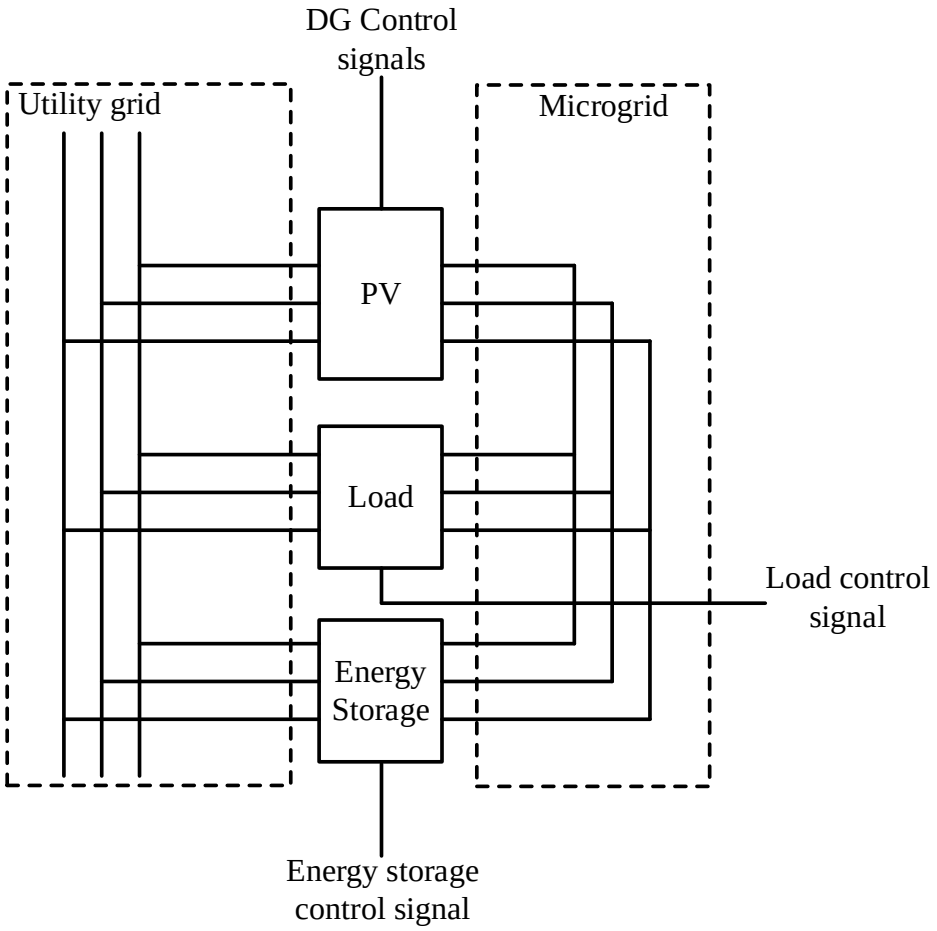


Figure 6.1. System block diagram of the microgrid testbed that will be used in this study.

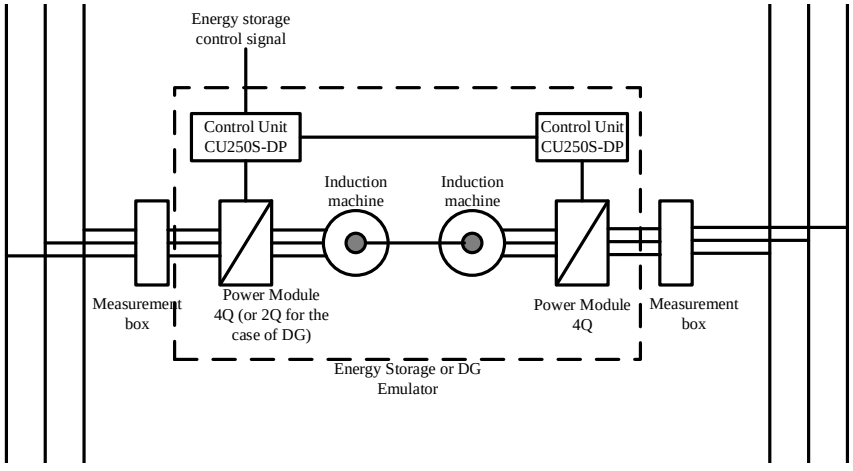


Figure 6.2. System block diagram of an emulator that can be used as PV source or load or storage depending on the control signal.

References

[1] International Energy Agency. "World Energy Outlook 2015.", 2015. URL http://www.worldenergyoutlook.org/media/weowebsite/2015/WEO2015Electricitydatabase_forweb.xlsx. Last accessed: 10-01-2016. ix, 4, 5

[2] T. Bischof-Niemz. "Green Energy Technologies: Challenges and Opportunities for Africa." 2015. ix, 6

[3] SBC Energy Institute. "Leading the Energy Transition: Electricity Storage.", 2013. URL http://www.sbcenergyinstitute.com/Publications/ElectricityStorage.html. Last accessed: 15-01-2016. ix, 23

[4] M. Hill. "World's biggest dam has extremely dangerous low water levels." URL http://www.bloomberg.com/news/articles/2016-01-08/world-s-biggest-dam-has-extremely-dangerous-low-water-levels. Last accessed: 20-03-2016. 5

[5] J. W. Simpson-Porco, F. Dorfler, and F. Bullo. "Voltage stabilization in microgrids via quadratic droop control." In *2013 IEEE 52nd Annual Conference on Decision and Control (CDC)*, pp. 7582–7589. IEEE, 2013. 5

[6] S&C Electric Company. "The role of energy storage in smart microgrids.", 2013. URL

http://www.sandc.com/edocs_pdfs/edoc_076176.pdf. Last accessed: 15-02-2016. 7, 8

[7] A. De Almeida, L. Moreira, and J. Delgado. "Power quality problems and new solutions." *ISR–Department of Electrical and Computer Engineering University of Coimbra, Pólo II*, pp. 3030–290, 2003. 7

[8] S. Chowdhury and P. Crossley. *Microgrids and active distribution networks*. The Institution of Engineering and Technology, 2009. 8

[9] S. X. Chen, H. B. Gooi, and M. Q. Wang. "Sizing of Energy Storage for Microgrids." *IEEE Transactions on Smart Grid*, vol. 3, no. 1, pp. 142–151, March 2012. 9

[10] M. Korpaas, A. T. Holen, and R. Hildrum. "Operation and sizing of energy storage for wind power plants in a market system." *International Journal of Electrical Power & Energy Systems*, vol. 25, no. 8, pp. 599–606, 2003. 9

[11] Keysight Technologies. "Keysight 34970A/34972A Data Acquisition/Switch Unit." URL http://literature.cdn.keysight.com/litweb/pdf/34972-90010.pdf?id=1838006. Last accessed: 30-08-2016. 12

[12] A. Kwasinski. "Technology Planning for Electric Power Supply in Critical Events Considering a Bulk Grid, Backup Power Plants, and Micro-Grids." *IEEE Systems Journal*, vol. 4, no. 2, pp. 167–178, June 2010. 15

[13] C. Abbey, D. Cornforth, N. Hatziargyriou, K. Hirose, A. Kwasinski, E. Kyriakides, G. Platt, L. Reyes, and S. Suryanarayanan. "Powering Through the Storm: Microgrids Operation for More Efficient Disaster Recovery." *IEEE Power and Energy Magazine*, vol. 12, no. 3, pp. 67–76, 2014. 15

[14] B. Espinar and D. Mayer. "The role of energy storage for mini-grid stabilization." Tech. rep., Jul. 2011. URL https://hal-mines-paristech.archives-ouvertes.fr/hal-00802927. 48 pages. 16, 24

[15] X. Vallve, A. Graillot, S. Gual, and H. Colin. "Micro storage and demand side management in distributed PV grid-connected installations." In *Electrical Power Quality and Utilisation, 2007. EPQU 2007. 9th International Conference*, pp. 1–6. Oct 2007. 16, 17

[16] X. Vallve. "Rural PV micro grids in Africa." In *Jeju 2011 Symposium on Microgrid*. 2011. 16, 17, 18

[17] N. Thirumurthy, L. Harrington, D. Martin, L. Thomas, J. Takpa, and R. Gergan. "Opportunities and challenges for solar minigrid development in rural India." *National Renewable Energy Laboratory (NREL), NREL/TP-7A40-55562*, 2012. 17

[18] W. Jewell and R. Ramakumar. "The Effects of Moving Clouds on Electric Utilities with Dispersed Photovoltaic Generation." *IEEE Transactions on Energy Conversion*, vol. EC-2, no. 4, pp. 570–576, Dec 1987. 18, 20, 21

[19] S. Puladasu, M. Sushama, and B. Sarvesh. "Protection issues of power systems with PV systems based distributed generation." *IOSR Journal of Electrical and Electronics Engineering*, vol. 9, no. 3, pp. 18–27, 2014. URL http://www.iosrjournals.org/iosr-jeee/Papers/Vol9-issue3/Version-5/D09351827.pdf. 18

[20] J. Smith, R. Dugan, and W. Sunderman. "Distribution modeling and analysis of high penetration PV." In *2011 IEEE Power and Energy Society General Meeting*, pp. 1–7. July 2011. 19, 30

[21] A. Kankiewicz, M. Sengupta, and D. Moon. "Observed impacts of transient clouds on utility-scale PV fields." In *Proc. ASES National Solar Conference*. 2010. 19, 30

[22] J. Marcos, L. Marroyo, E. Lorenzo, and M. García. "Power output fluctuations in large PV plants." In *International Conf. on Renewable Energies and Power Quality*. 2012. 19

[23] J. Marcos, L. Marroyo, E. Lorenzo, and M. García. "Smoothing of PV power fluctuations by geographical dispersion." *Progress in Photovoltaics: Research and Appli-*

cations, vol. 20, no. 2, pp. 226–237, 2012. URL http://dx.doi.org/10.1002/pip.1127. 19

[24] R. Haaren, M. Morjaria, and V. Fthenakis. "Empirical assessment of short-term variability from utility-scale solar PV plants." *Progress in Photovoltaics: Research and Applications*, vol. 22, no. 5, pp. 548–559, 2014. 19

[25] E. Wiemken, H. Beyer, W. Heydenreich, and K. Kiefer. "Power characteristics of PV ensembles: experiences from the combined power production of 100 grid connected PV systems distributed over the area of Germany." *Solar Energy*, vol. 70, no. 6, pp. 513 – 518, 2001. URL http://www.sciencedirect.com/science/article/pii/S0038092X00001468. Grid-Connected PV. 20

[26] K. Otani, J. Minowa, and K. Kurokawa. "Study on areal solar irradiance for analyzing areally-totalized PV systems." *Solar Energy Materials and Solar Cells*, vol. 47, no. 14, pp. 281 – 288, 1997. URL http://www.sciencedirect.com/science/article/pii/S0927024897000500. 20

[27] W. Omran, M. Kazerani, and M. Salama. "Investigation of Methods for Reduction of Power Fluctuations Generated From Large Grid-Connected Photovoltaic Systems." *IEEE Transactions on Energy Conversion*, vol. 26, no. 1, pp. 318–327, March 2011. 21

[28] Y. Ye, R. Sharma, and P. Garg. "An integrated power management strategy of hybrid energy storage for renewable application." In *IECON 2014-40th Annual Conference of the IEEE Industrial Electronics Society*, pp. 3088–3093. IEEE, 2014. 22

[29] T. Masaud, K. Lee, and P. Sen. "An overview of energy storage technologies in electric power systems: What is the future?" In *North American Power Symposium (NAPS), 2010*, pp. 1–6. Sept 2010. 23

[30] N. Horonga, W. Cronje, and I. Hofsajer. "Estimating the dynamic power requirements for controllable energy storage on PV microgrid." In *AFRICON, 2015*, pp. 1–5. IEEE, 2015. 28

[31] Department of Energy South Africa. "Renewable: Solar power.", 2016. URL http://www.energy.gov.za/files/esources/renewables/r_solar.html. 28

[32] K. Remmers. "Inverter, Storage and PV System Technology-Industry Guide 2014.", 2014. 31

[33] J. Lopes, C. Moreira, and A. Madureira. "Defining control strategies for microgrids islanded operation." *IEEE Transactions on Power Systems*, vol. 21, no. 2, pp. 916–924, 2006. 48

[34] M. C. Chandorkar, D. M. Divan, and R. Adapa. "Control of parallel connected inverters in standalone ac supply systems." *IEEE Transactions on Industry Applications*, vol. 29, no. 1, pp. 136–143, 1993. 48

[35] K. De Brabandere, B. Bolsens, J. Van den Keybus, A. Woyte, J. Driesen, and R. Belmans. "A Voltage and Frequency Droop Control Method for Parallel Inverters." *IEEE Transactions on Power Electronics*, vol. 22, no. 4, pp. 1107–1115, July 2007. 48

[36] J. Rocabert, A. Luna, F. Blaabjerg, and P. Rodriguez. "Control of Power Converters in AC Microgrids." *IEEE Transactions on Power Electronics*, vol. 27, no. 11, pp. 4734–4749, Nov 2012. 49, 50

Appendix A

Data Measurements

A.1 Introduction

This appendix gives a detailed analysis on how the insolation data recorded at the University of the Witwatersrand was processed. A data acquisition system and a power meter are used to measure insolation and three-phase inverter output respectively. Two methods namely; Nyquist's sampling theorem and graphical methods are used to determine the highest ramp rate present in the measured insolation data.

A.2 PV Data Measurements

One of the requirements of the requirements of the research is to analyze the resource available. A pyranometer (SP110) was mounted at the roof of Chamber of mines, University of the Witwatersrand, Johannesburg, South Africa to record the insolation data. The reasons for mounting on this building is the fact that there are no tall buildings around

and it is a restricted access area which makes the equipments safe. The pyranometer was connected to the data acquisition unit (Agilent 34972). The Agilent was used because it can sample data faster and has a USB function to provide enough storage capacity.
Data is recorded to determine the dynamics present in insolation. Sampling time of 40ms was used and Initial findings showed that the data was oversampled. Figure A.1 shows an extract of the recorded data. The data was recorded in February 2015 on the roof of Chamber of mines at the University of the Witwatersrand. The building is situated away from tall buildings which makes it a good location for PV system installation because it receives direct sunshine over a large portion of the day. What is clear from this recorded data in figure A.1 is the fact that it is non constant and it depends on the available insolation power. What is not entirely clear on the figure is the rate at which the insolation power changes. The following subsections explains how the ramp rates in the data was extracted.

A.3 Determining The Sampling Rate

Two methods are used to determine the sampling time of insolation data. These methods are:

- Nyquist' sampling theorem.
- Graphical method using heat maps.

A.4 Using Nyquist' Sampling Theorem

A frequency spectral analysis in figure A.2 for the insolation data in figure A.1 shows that the signal can be re-sampled at 2.5 seconds (0.2 Hz) without losing any information. This

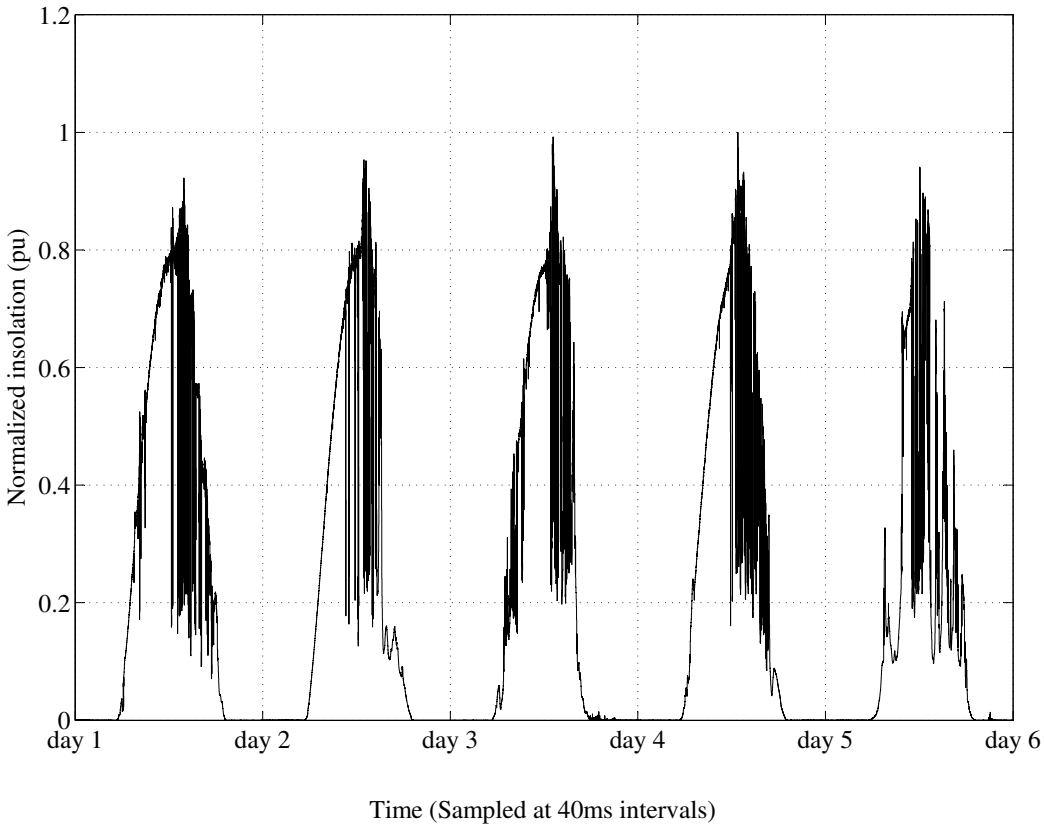


Figure A.1. A typical normalized insolation data recorded at the University of Witwatersrand, Johannesburg, South Africa.

result implies that the insolation does not necessarily change at a rate faster than 2.5 seconds.

A.5 Using Graphical Method

A heat map can be used to determine the required sampling time to capture the data. Basically recorded data which is initially a $N \times 1$ matrix (where N is the number of samples

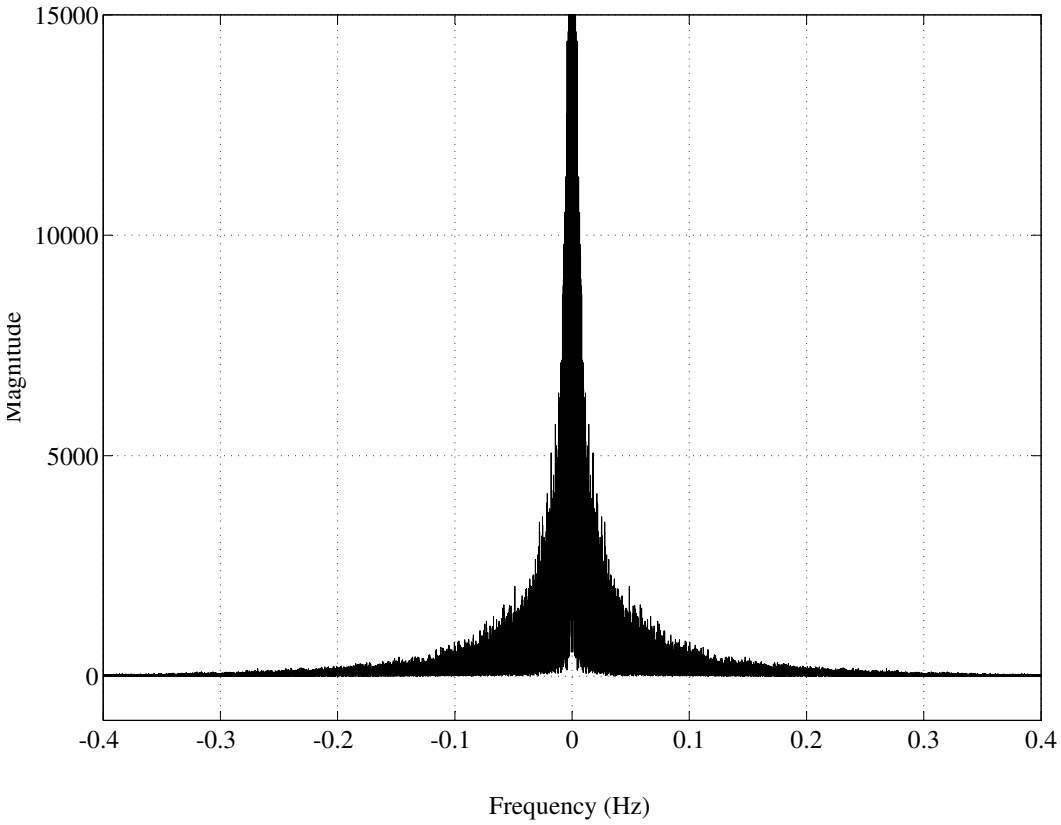


Figure A.2. Insolation data spectral analysis for a typical day in Johannesburg.

present in the data) is used to generate a $A \times B$ matrix where B is number of the samples in the original data that falls in one re-sampled time and A is the number of bins which contains arrays of data. Matrices below best illustrate the procedure for determine the sample time. Equation A.1 relates N to A and B. Any variation in the color in each row indicates that, the insolation variation. This means that the data is being under-sampled. The sample time must then be reduced until the color in reach row does not change.

$$D_{original} = \begin{Bmatrix} y_1 & y_2 & y_3 & \cdots & y_N \end{Bmatrix}$$

$$Heat = \begin{Bmatrix} a_{11} & a_{12} & a_{13} & \cdots & a_{1A} \\ a_{21} & a_{22} & a_{23} & \cdots & a_{2A} \\ . & . & . & \cdots & . \\ . & . & . & \cdots & . \\ . & . & . & \cdots & . \\ a_{B1} & a_{B2} & a_{B3} & \cdots & a_{BA} \end{Bmatrix}$$

$$N = A \times B \tag{A.1}$$

The data sampling time is decreased from 5 mins to 1 mins and the results are shown in figures A.3, A.4 and A.5. Sampling time of 5 minutes shows that most of the row at noon contains more than one colour which is an indication of under-sampling. As the sampling time is reduced to 1 minute, the colour does not change vertically but rather horizontally. This means that the sample time of 1 minute is enough to capture the insolation data recorded. This method however relies on visualization using eyes which is not accurate especially when expecting smaller insolation variations .

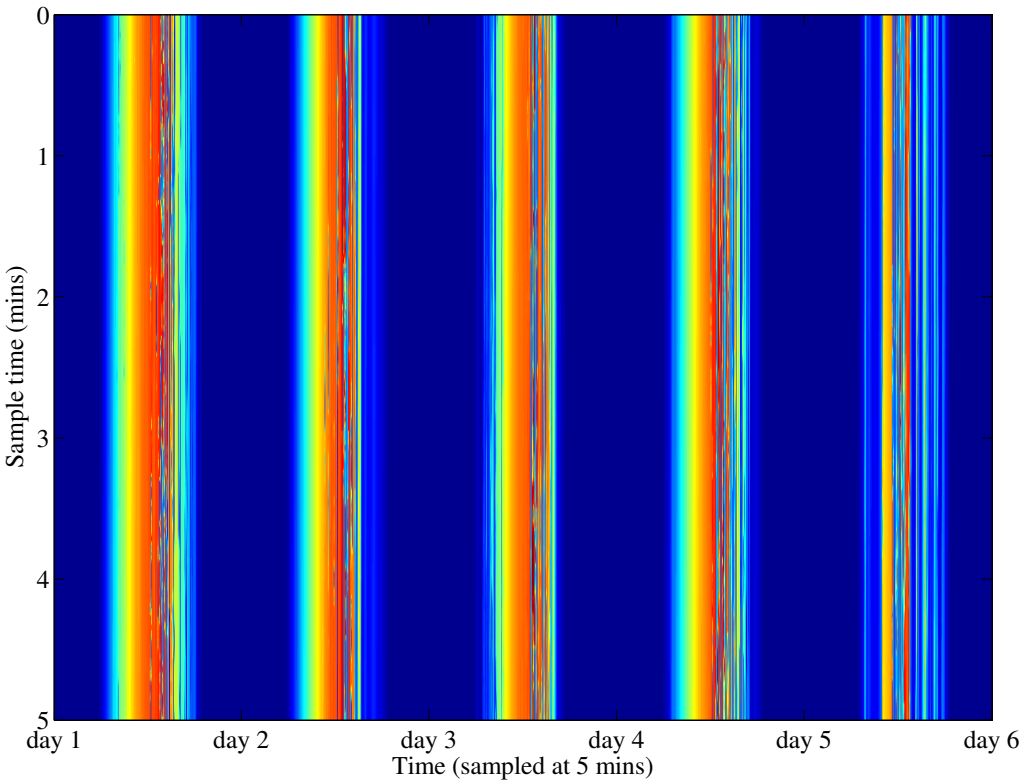


Figure A.3. Heat map for 5 minute ramp rates of the insolation data recorded. The heat map also shows change in colour vertically which is an indication of under-sampling.

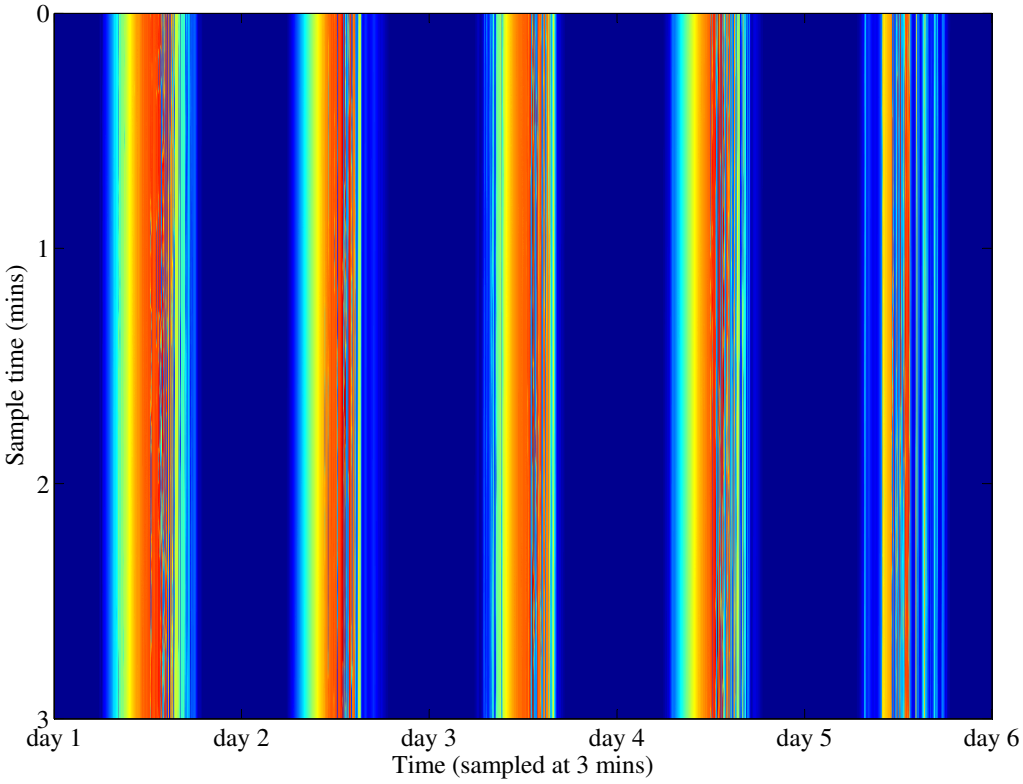


Figure A.4. Heat map for 3 minute ramp rates of the insolation data recorded.

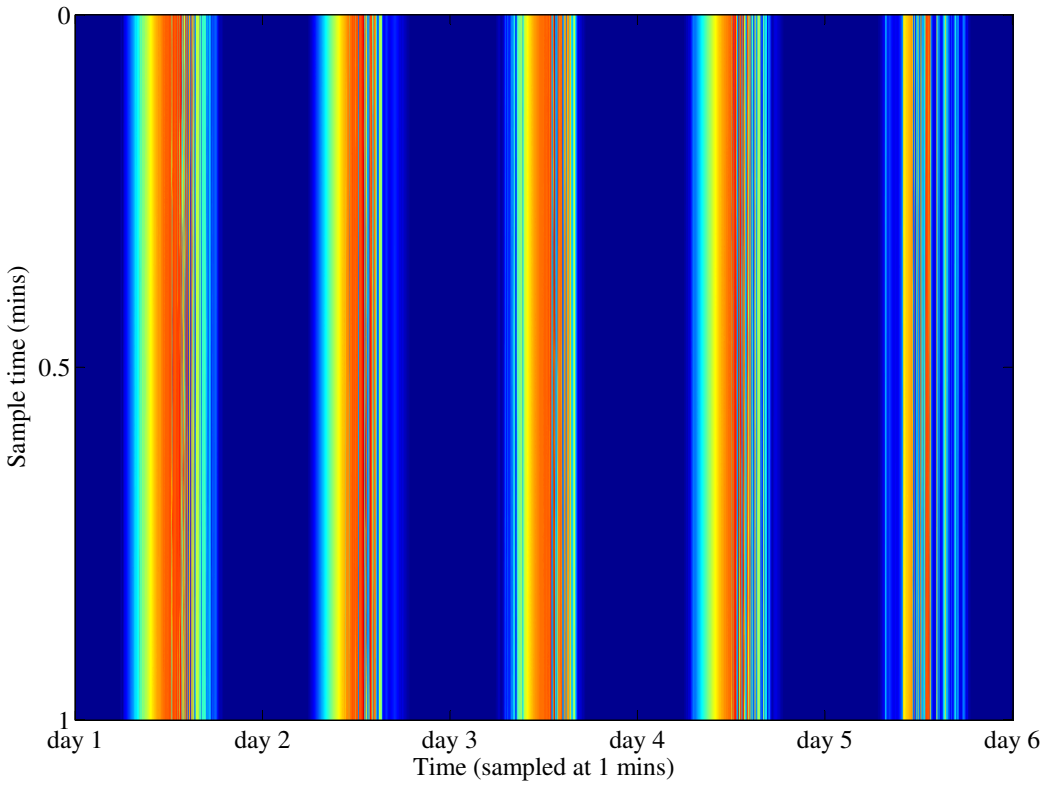


Figure A.5. Heat map for 1 minute ramp rates of the insolation data recorded. The colour does not change vertically which is an indication that the data is being sampled at an appropriate ramp rate.

A.6 Conclusion

The appendix is an extension of the Data analysis chapter. Two methods were used to analyze insolation ramp rate and these included, using Nyquist's Sampling Theorem and also using graphical analysis. Nyquist method gave more accurate ramp rate. The graphical method gave estimates because unlike the Nyquist method that gave exact values, graphical method relied mostly on identifying colour change which in many case depends on the human eye.

Appendix B

Ramp Rate Analysis MATLAB Code

B.1 Introduction

The appendix contains MATLAB® code used in the research. The code was used to determine the ramp rates present in the insolation data measured at the University of the Witwatersrand, Chamber of Mines Building.

B.2 MATLAB Code

```
1 clc;
2
3 clear all;
4
```

```
PV_in_data= csvread('PV_power_inveter_in_40ms_3days 20150123.csv'); ...
    %loading recorded data

PV_in_1s=transpose(PV_in_data./max(PV_in_data));


sec =60;

min =7; % sec and min determines the sampling time of the data

sum_power =0;

average_power =0;

s_time = 23*sec*min; %It is multiplied by 23 because the was 23 samples ...
    in 1 second

X = floor(length(PV_in_1s)/s_time);

S_PP =zeros(1,X);

S_PP(1) = PV_in_1s(1);

for a=1:X

for i=1:s_time

%wait for the next sample

end

S_PP(a)=PV_in_1s(a*s_time);

average_power =0;

end
```

```
39
40 figure1 = figure(1);
41
42 plot(S_PP); %plots the sampled insolation data
43
44
45 %Ramp rate analysis begins here
46
47 Ramp=zeros(1,X);
48
49 prev_value = 0;
50
51 pres_value =0;
52
53 for a =1:X
54
55 pres_value = S_PP(a);
56
57 Ramp(a) = pres_value - prev_value;
58
59 prev_value = pres_value; %calculates the change in insolation between ...
       two samples
60
61 end
62
63 figure2 = figure(2);
64
65 plot(Ramp);
66
67
68 Ramp_sum=0;
69
70 for i=1:X
71
72 Ramp_sum = Ramp_sum+ abs(Ramp(i));
73
```

```
74 end
75
76
77 %=========================================================================
78
79 rsec =1;
80
81 rmin =1;
82
83 sum_ramp =0;
84
85 average_ramp =0;
86
87 rs_time = rsec*(rmin);
88
89 X1 = floor(length(Ramp)/rs_time);
90
91 S_RR =zeros(1,X1);
92
93 count =0;
94
95 RR = 0.4.*ones(1,X1);
96
97 for a=1:X1
98
99 for i=1:rs_time
100
101 sum_ramp =sum_ramp + Ramp((a-1)*rs_time +i);
102
103 end
104
105 average_ramp = sum_ramp/rs_time; %calculate the avarage ramp rate
106
107 S_RR(a)=average_ramp;
108
109 if(average_ramp > 0.4)
```

```
110
111 count = count +1;
112
113 end
114
115 sum_ramp =0;
116
117 average_ramp =0;
118
119 end
120
121 figure3 = figure(3);
122
123 t_r = 0:1:X1-1;
124
125 plot(t_r,S_RR, t_r,RR);
126
127 count %count is used to count the change in insolation between two ...
        successive samples that exceed 0.4 pu
128
129 %================================================================================
130
131 Ramp_sum/5
132
133 %grouping of the ramp rate.
134
135 ramp_freq = zeros(1,41);
136
137 for a=1:length(S_RR)
138
139 if((abs(S_RR(a))>-0.0001)&&(abs(S_RR(a))≤0.0001)) %a bin which contains ...
        the number of occurence of ramp rate below abs(0.0001)
140
141 ramp_freq(21)=ramp_freq(21)+1;
142
```

```
143 elseif((abs(S_RR(a))>0.0001)&&(abs(S_RR(a))≤0.05)) %a bin which ...
        contains the number of occurence of ramp rate between abs(0.0001) ...
        and abs(0.05)
144
145 if(S_RR(a)<0)
146
147 ramp_freq(22)=ramp_freq(22)+1;
148
149 else
150
151 ramp_freq(20)=ramp_freq(20)+1;
152
153 end
154
155 elseif((abs(S_RR(a))>0.05)&&(abs(S_RR(a))≤0.1)) %a bin which contains ...
        the number of occurence of ramp rate between abs(0.05) and abs(0.1)
156
157 if(S_RR(a)<0)
158
159 ramp_freq(23)=ramp_freq(23)+1;
160
161 else
162
163 ramp_freq(19)=ramp_freq(19)+1;
164
165 end
166
167 elseif((abs(S_RR(a))>0.1)&&(abs(S_RR(a))≤0.15)) %a bin which contains ...
        the number of occurence of ramp rate between abs(0.1) and abs(0.15)
168
169 if(S_RR(a)<0)
170
171 ramp_freq(24)=ramp_freq(24)+1;
172
173 else
174
```

```
175 ramp_freq(18)=ramp_freq(18)+1;
176
177 end
178
179 elseif((abs(S_RR(a))>0.15)&&(abs(S_RR(a))≤0.2)) %a bin which contains ...
        the number of occurence of ramp rate between abs(0.15) and abs(0.2)
180
181 if(S_RR(a)<0)
182
183 ramp_freq(25)=ramp_freq(25)+1;
184
185 else
186
187 ramp_freq(17)=ramp_freq(17)+1;
188
189 end
190
191 elseif((abs(S_RR(a))>0.2)&&(abs(S_RR(a))≤0.25)) %a bin which contains ...
        the number of occurence of ramp rate between abs(0.2) and abs(0.25)
192
193 if(S_RR(a)<0)
194
195 ramp_freq(26)=ramp_freq(26)+1;
196
197 else
198
199 ramp_freq(16)=ramp_freq(16)+1;
200
201 end
202
203 %=================================================================
204
205 elseif((abs(S_RR(a))>0.25)&&(abs(S_RR(a))≤0.3)) %a bin which contains ...
        the number of occurence of ramp rate between abs(0.25) and abs(0.3)
206
207 if(S_RR(a)<0)
```

```
208
209  ramp_freq(27)=ramp_freq(27)+1;
210
211  else
212
213  ramp_freq(15)=ramp_freq(15)+1;
214
215  end
216
217  elseif((abs(S_RR(a))>0.3)&&(abs(S_RR(a))≤0.35)) %a bin which contains ...
         the number of occurence of ramp rate between abs(0.3) and abs(0.35)
218
219  if(S_RR(a)<0)
220
221  ramp_freq(28)=ramp_freq(28)+1;
222
223  else
224
225  ramp_freq(14)=ramp_freq(14)+1;
226
227  end
228
229  elseif((abs(S_RR(a))>0.35)&&(abs(S_RR(a))≤0.4)) %a bin which contains ...
         the number of occurence of ramp rate between abs(0.35) and abs(0.4)
230
231  if(S_RR(a)<0)
232
233  ramp_freq(29)=ramp_freq(29)+1;
234
235  else
236
237  ramp_freq(13)=ramp_freq(13)+1;
238
239  end
240
```

```
241 elseif((abs(S_RR(a))>0.4)&&(abs(S_RR(a))≤0.45)) %a bin which contains ...
        the number of occurence of ramp rate between abs(0.4) and abs(0.45)
242
243 if(S_RR(a)<0)
244
245 ramp_freq(30)=ramp_freq(30)+1;
246
247 else
248
249 ramp_freq(12)=ramp_freq(12)+1;
250
251 end
252
253 elseif((abs(S_RR(a))>0.45)&&(abs(S_RR(a))≤0.5)) %a bin which contains ...
        the number of occurence of ramp rate between abs(0.45) and abs(0.5)
254
255 if(S_RR(a)<0)
256
257 ramp_freq(31)=ramp_freq(31)+1;
258
259 else
260
261 ramp_freq(11)=ramp_freq(11)+1;
262
263 end
264
265 %=================================================================
266
267 %=================================================================
268
269 elseif((abs(S_RR(a))>0.5)&&(abs(S_RR(a))≤1)) %a bin which contains the ...
        number of occurence of ramp rate above abs(0.5)
270
271 if(S_RR(a)<0)
272
273 ramp_freq(32)=ramp_freq(32)+1;
```

```
274
275  else
276
277  ramp_freq(10)=ramp_freq(10)+1;
278
279  end
280
281  end
282
283  end
284
285  t = -100:5:100;
286
287  figure4 = figure(4);
288
289  ax =gca;
290
291  scatter(t,ramp_freq) %scatter plot of the probability that the ramp ...
         rate will fall in one of the bins
```

Appendix C

Publications

C.1 Introduction

The appendix contain publications that were submitted for review and accepted at conferences. The conference papers submitted were part of the on-going research presented in this dissertation. The papers are listed as follows:

1. Estimating the dynamic power requirements for controllable energy storage on PV microgrid.
2. Dynamic power requirements for controlled energy store used for stabilization of three-phase low-voltage standalone microgrid.

ESTIMATING THE DYNAMIC POWER REQUIREMENTS FOR CONTROLLABLE ENERGY STORAGE ON PV MICROGRID

Nyasha Horonga
School of Electrical and Information Engineering
University of the Witwatersrand
Johannesburg, South Africa
Email: nhoronga@gmail.com

Willie Cronje
School of Electrical and Information Engineering
University of the Witwatersrand
Johannesburg, South Africa
Email: willie.cronje@wits.ac.za

Ivan Hofsajer
School of Electrical and Information Engineering
University of the Witwatersrand
Johannesburg, South Africa
Email: ivan.hofsajer@wits.ac.za

***Abstract*—This paper investigates the dynamic power requirements for controllable energy storage systems used for stabilization of standalone three-phase low-voltage microgrids with high penetration of PV energy. It uses recorded data of fluctuating Photo-voltaic (PV) sources and fluctuating loads to determine how an ideal controllable energy storage can be used to stabilize a microgrid with 100% PV energy penetration. Using the data recorded for a typical bad day in Johannesburg, the sampling time required to capture the dynamics in PV sources was found to be 2 seconds. However this report uses sampling time of 1 second to calculate the ramp rate required for the energy storage to stabilize a PV microgrid. For the case considered in this paper, the ramp rate was found to be 0.4 pu/second.**

I. Introduction

Islanded microgrid studies are being done because the utility grids, mainly in African countries are under pressure from increasing power demand in urban communities and industries. Expansion of these grids to supply power to remote communities is increasingly becoming impossible. Islanded microgrids can be used as one of the solutions. Renewable energy sources with large fluctuations are frequently the source of power for these standalone microgrids. The fluctuating nature of these renewable sources often leads to frequent blackouts. This research is aimed at minimizing these power fluctuations using controllable energy storage systems.
The remaining sections in this paper will discuss the background and a brief discussion on results of this research.

II. Background

An example of a typical standalone microgrid is shown in figure 1. This microgrid receives power from Distributed Generation (DG) sources such as renewable energy sources or diesel generators. Figure 2a shows typical insolation data in Johannesburg, South Africa. This data was recorded at the roof of the Chamber of mines building at the University of Witwatersrand. The insolation ($P_{\text{PV}}(t)$) was normalized to the peak measured of 31.28W/m^2 for the 2 day period. This figure clearly shows how the PV power is influenced by varying weather as the case with most renewable energy sources.
The primary goal for any grid is to transfer enough power

978-1-4799-7498-6/15/$31.00 ©2015 IEEE

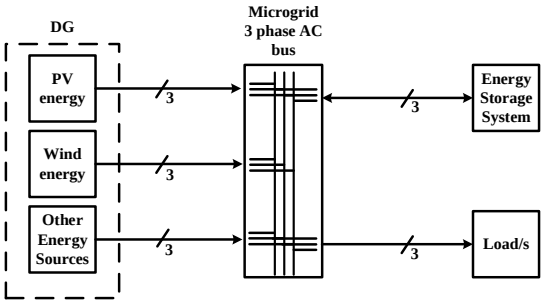


Fig. 1: A single line schematic example of a three-phase low voltage standalone microgrid system.

to the load and one of the challenges is the unpredictable nature of most of these loads. The normalized recorded data for the power demand ($P_{\text{load}}(t)$) of a representative load in figure 2b clearly shows power demand fluctuations. These load fluctuations cannot be controlled but the power sources can be adjusted to meet the load demand. Failure to meet the load demand will result in blackouts[1] [3]. In most cases the power generated from renewable sources does not meet the load demand and controllable energy storage system can be used to balance the power flow [4], [5], [6], [7], [8], [9]. The insolation and load demand data were not recorded on the same day but was hypothetically combined because it represents a fairly bad day due to abrupt changes in both the load and the source.
This study will focus on a simplified standalone microgrid that has a single source (in this case a PV source), a single load and a controllable energy storage to limit the complexity of the problem.
Energy storage system is chosen depending on the requirements of the microgrid. Preliminary data analysis has shown that PV power must be sampled at at-least at 2 second intervals. This sampling time was calculated using insolation data spectral analysis in figure 3. This paper will use sampling time of 1 second. The figure shows that to capture all the frequencies present in this insolation data, the sampling frequency must be 0.5Hz (2 seconds) using Nyquist's sampling

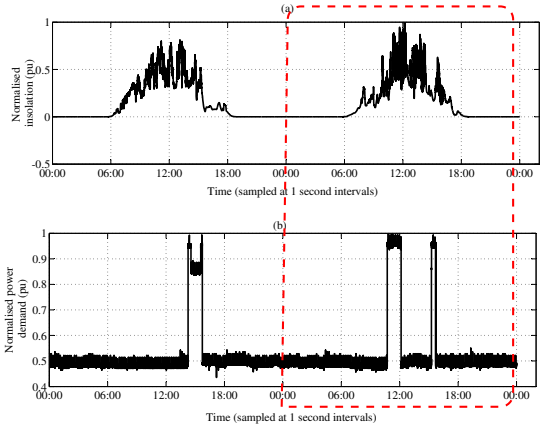


Fig. 2: A typical normalized insolation and load demand data recorded at the university of Witwatersrand, Johannesburg, South Africa.

theorem.

The insolation data also shows that during night, the power generation is zero and a storage must be installed. This energy storage must respond fast to cancel the PV power fluctuation and must be able to sustain the grid during the night.

Energy storage systems can be classified into short-term and long-term as shown in figure 4. Short-term storage is mainly applied to maintain the voltage stability during transients/disturbances[10]. Long-term storage is deployed to contribute towards the energy management, frequency regulation and grid congestion management [10].

This paper focuses on understanding the dynamics present in power networks that use fluctuating sources. Once an understanding has been established and documented future work will look at appropriate storage systems or combination

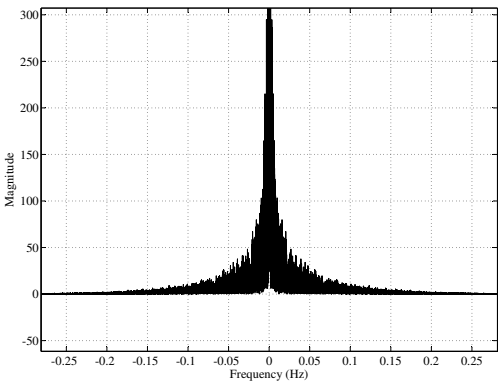


Fig. 3: Insolation data spectral analysis for a typical day in Johannesburg.

of storage systems from the list in figure 4 that meet the requirements.

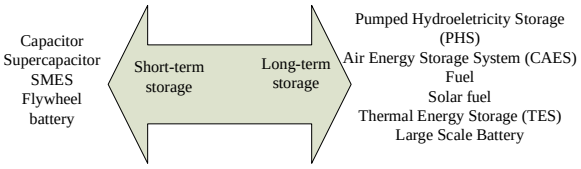


Fig. 4: Energy storage classification [11].

The paper will focus on the ramp rate, which is defined as the rate at which the power flow can change. Ramp rate is also known as the slew rate.

Although the current research is aimed at the dynamic behavior of a power network which strongly depend on DG (100% penetration), sizing of the storage is essential. It is important to note that the total energy supplied by DG and the total energy required by the load must always balance. Using the normalized hypothetical data obtained from the Genmin building at the University of the Witwatersrand, the PV installation will need to be over dimensioned by a factor 3.5 to meet the 2 day energy demand without taking inverter efficiency into account. This value is obtained by integrating the normalized load consumed by the Genmin building over 2 days from 16th to 17th of March 2015. The result of the integration was then divided by the integrated normalized PV power over the same period of time. Measurements taken at the university have shown that inverter efficiency of PV inverters varies with insolation power available. In this paper, it is assumed that the efficiency is 90% and the PV installation will be scaled by 3.9 pu. These dimensions do not take into account the efficiency of the solar panels and this means the number of installed solar panels for the real case may be significantly higher. The research will focus mainly on the pattern of the insolation data and not on the cost and the actual sizing of the microgrid system.

In addition, the PV system power must match the power demanded by the load and if there is any power imbalance, storage must supply the power or store the excess power as shown in equation 1.

$$P_{\text{ES}}(t) = P_{\text{PV}}(t) - P_{\text{load}}(t) \tag{1}$$

Figure 5 shows the power difference (i.e. the difference between the potential power generation and power demand profiles). The data used as a representative case was obtained from normalized PV data recorded on the 27th of February 2015 and Genmin building power demand data on the 17th of March 2015 at the University of the Witwatersrand. If the normalized differential power is less than zero, it means the energy storage must supply power to the load. During sunny days, the PV system will produce more power than required by the load. This power is then stored. The study will mainly focus on the dynamic behavior of the system (i.e. region A). This power difference is seldom zero and hence the need for an energy storage system. The graph also shows that using the available data, the energy storage system must have a

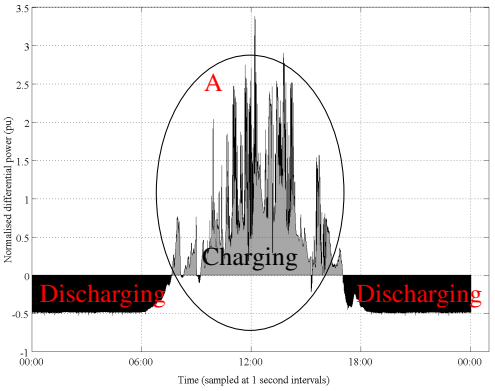


Fig. 5: The calculated power difference between PV power and Genmin building load demand.

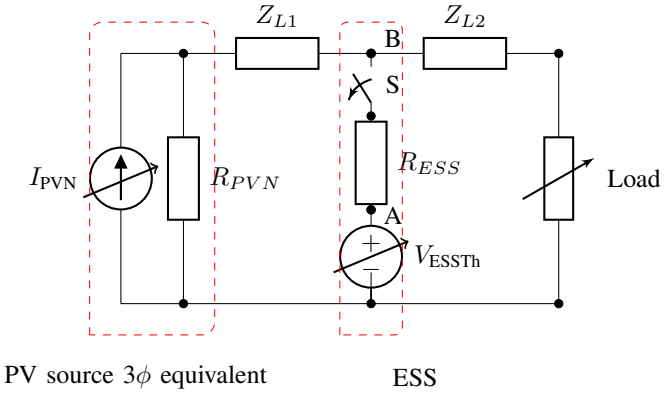


Fig. 6: Simulation circuit for a standalone microgrid with a current and a voltage source modeling a PV source and an energy storage respectively.

ramp rate of 0.4pu/sec. The value was obtained by measuring the largest change of the normalized power over a sampling period of 1 second.

Successful control of a islanded microgrid requires an understanding of the existing inverters that are normally used. Grid-tied inverters use current control as opposed to the voltage-frequency control that is used in off-grid inverters[13]. This is because the microgrid defines the grid frequency and voltage. A microgrid powered from renewable energy sources must have one inverter that specifies voltage and frequency or the inverters must have strict guidelines to follow based on the microgrid voltage and frequency. In this case, each inverter must be able to control its voltage and frequency at the point of common connection [14].

This paper focuses on a grid with inverters that use the conventional voltage-frequency droop control explained in [15]. This control method is used to emulate the behavior of synchronous generators under both normal load and overload conditions [16]. Power systems are considered stable if the real power(P) and the reactive power(Q) can be controlled [17]. The real power is dependent on the power angle and the Q depends on the voltage. By increasing or decreasing the power angle (i.e the frequency), more power can be injected into the microgrid. This technique can be used to avoid overloading inverters without any communication between the power sources and load [17].

Because the objective of this research is to investigate and determine the dynamic power requirements for using controllable energy storage to stabilize three-phase microgrids and ensure power balance, Simulations are conducted for the simplified microgrid to enhance understanding of the problem.

III. Simulations

The simulations are performed in Simulink®, using idealised models to better understand the dynamic requirements for the controlled energy storage. The three phase system can be reduced to a single phase equivalent because of the assumption made of balanced conditions. In these simulations, the PV source is modeled using a Norton equivalent circuit with controlled current sources.

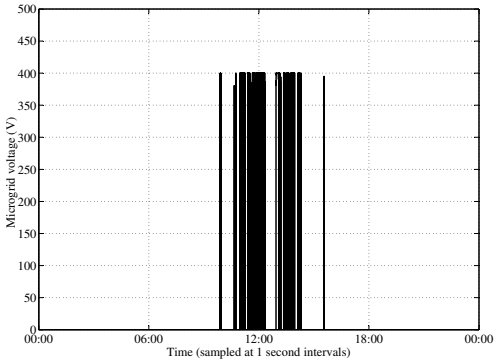


Fig. 7: The voltage of the PV supplied microgrid without storage with a PV inverter voltage controlled to 400V $\pm$10%.

A. Simulations without storage

Figure 6 shows the simulation model used to determine the behavior of an islanded microgrid. When the switch (S) is open, the microgrid simulation operates without the energy storage.

In a microgrid the voltage must be limited to the standardized voltage range of 400V$\pm$ 10% and the acceptable frequency range of 50Hz $\pm$ 2.5% for islanded mode [18]. Drop in voltage is usually a result of too much load and in this case either some of the non-essential loads must be disconnected or the grid will collapse. An increase in grid voltage is a result of more power generation and in this case the grid must throttle the power generation and maintain the voltage at 440V as shown in figure 7. This figure shows that, the absence of energy storage leads to frequent severe blackouts especially for days where there are high fluctuations in insolation.

B. *Simulations with storage*

The microgrid operates with an energy storage when the switch (S) is closed. The energy storage contains the control block that monitors the grid voltage (V_{grid}), the energy storage output AC current (I_{ESS}) and the DC energy storage voltage (V_{ESS}). V_{grid} and I_{ESS} values are used to compute real (P) and reactive (Q) power. The controller uses the power values to estimate the state of the grid and it adjusts the grid voltage (V_{grid}) and grid frequency (f_{grid}). The process is illustrated in figure 9. A flow diagram for the controller is shown in figure 11. It is in the values of voltage (V_{grid}) and frequency (f_{grid}) where other inverters connected to the microgrid get the information about the grid status.

IV. Discussion

Simulations have shown that when stabilizing a standalone microgrid with the power generation and load profiles analyzed in this paper, ideal energy storage must have a power response similar to the one shown in figure 8. This power response has a maximum ramp rate of 0.36 pu/sec. This difference in the ramp rate calculated and the one obtained from the simulations could be because the controller dampens the system. Another possible reason for the difference in the ramp rate is the fact that the controller has a voltage range in which it considers the system stable and the calculated ramp rate assumes only a certain voltage (i.e. it assumes that the grid is only stable at one voltage value not a range).
A controlled energy storage with the response shown in figure 8 will minimize the voltage fluctuations to 400V $\pm$ 5%. The simulations do not yet take into account the state of the energy storage system and assumes that there is an infinite amount of energy stored. This is because the research is focused mainly at the dynamics present in microgrid with large fluctuations.
As part of the future work, an improved model for the energy storage with all the required properties will be developed. More data must be recorded to calculate the ramp rate using many samples. This is useful in determining the size of the energy storage required to compensate for higher ramp rates. It is also useful to record all the PV data ramp rate values and using a frequency histogram will give a detailed knowledge on the type on energy storage required.
Experiments will be conducted on a microgrid testbed to verify the simulation results. The system block diagram shown in figure 10 shows the experimental setup that can be used to carry out the study. Sets of induction machines and variable speed drives will be used to emulate various DGs or energy storage systems as shown in figure 12 depending on the control signal used. Each emulator will receive a control signal that is used to generate a power profile resembling

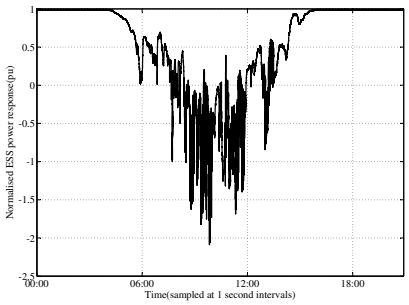


Fig. 8: The required ideal energy storage power response.

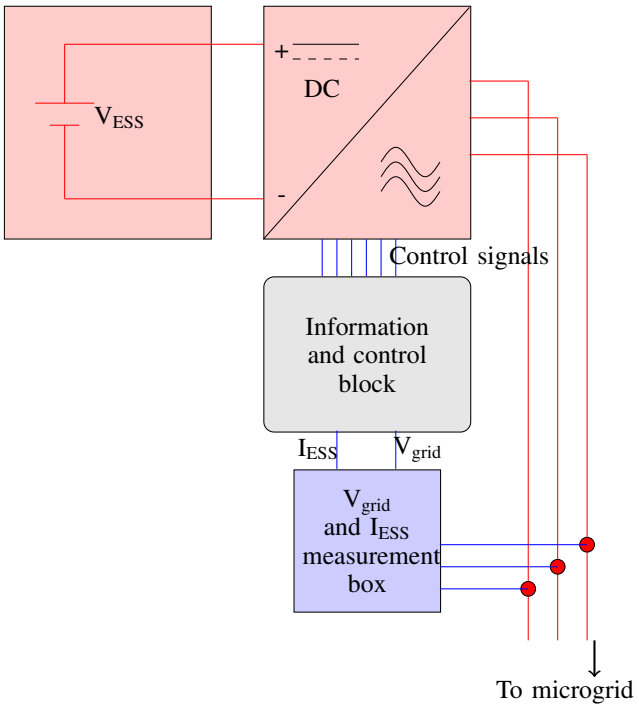


Fig. 9: A controller block diagram showing the required inputs and how it is connected to the microgrid.

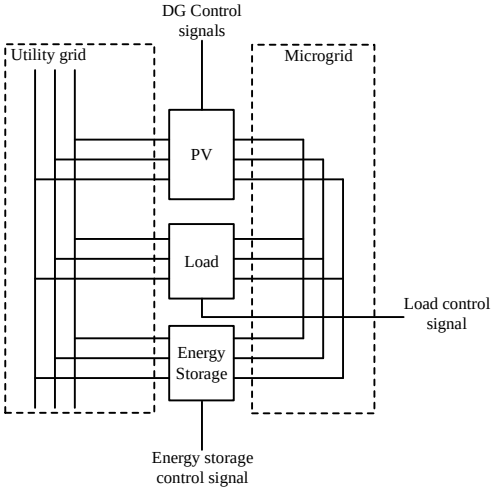


Fig. 10: System block diagram of the microgrid testbed that will be used in this study.

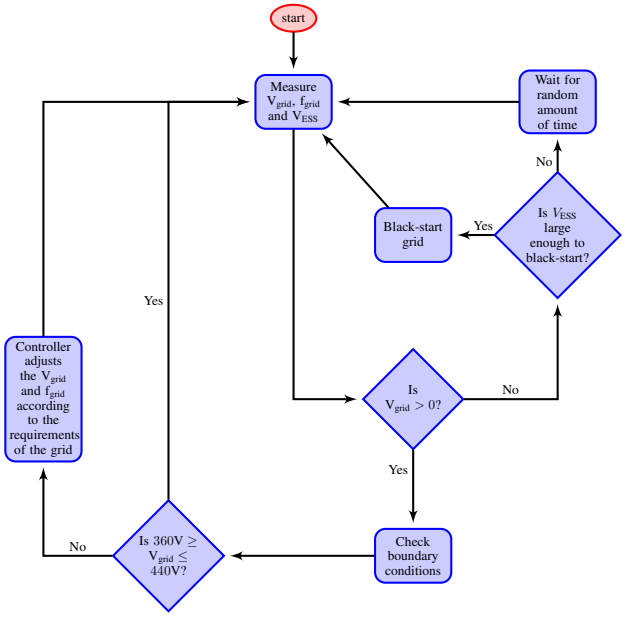


Fig. 11: A flow diagram for the energy storage controller.

DGs or loads or the energy storage system response.

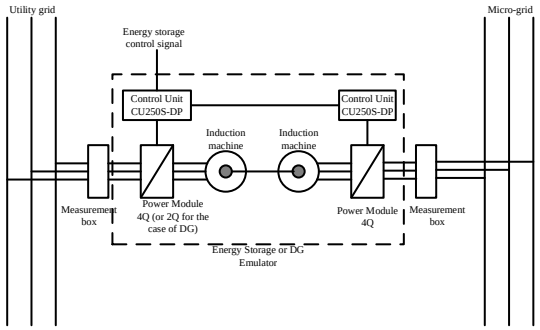


Fig. 12: System block diagram of an emulator that can be used as PV source or load or storage depending on the control signal.

V. Conclusion

The paper has shown that the ramp rate must be 0.4pu/sec to keep the PV microgrid stable. However simulations have shown that even a ramp rate as low as 0.36pu/sec can still also keep the microgrid voltage within the standard voltage range. There is a need for more data and simulations to determine the ramp rate range for this specific example. It is believed that this information if known may significantly reduce the size of the storage required in PV networks.

Acknowledgment

The authors would like to thank the ALSTOM chair for clean energy system technology for funding the research. The authors would also like to thank ACTOM for providing equipment used for the research investigations.

References

[1] X. Vallvé, A. Graillot, S. Gual, H. Colin: *Microgrid and demand side management in distributed PV grid-connected installations*, 9th International Conference on Electrical and power quality and utilization, Barcelona, 9 - 11 October 2007.

[2] Robert G. Ellis: *A Reference Guide to causes, effects and corrective measures*, Power systems harmonics, Rockwell International Corporation, Canada, 2001.

[3] W. Liang: *Determination of power system response during a small load fluctuations*,IEEE, 2009.

[4] Mohd. Hasan Ali, Minwon Park, In-Ken Yu, Toshiaki Murata and Junji Tamura: *Improvement of wind generator stability by fuzzy logic-controlled SMES*,Proceeding of international conference on electrical machines and systems, South Korea, 8 - 11 October 2007.

[5] G. Chen, Q. Yang, T. Zhang, Z. Bao , W. Yan: *Real-time wind power stabilization approach based on hybrid energy storage systems*,Sixth international conference on advanced computational intelligence, Hangzhou, China, 19 - 21 October 2013.

[6] J. Kim, S. Kim and J. Park: *Contribution of an energy storage system for stabilizing a microgrid during standalone operation*,Journal of electrical engineering and technology, Vol. 4, No. 2, pp. 194 - 200, 2009.

[7] R. Hesse, D. Turschner and H. Beck: *Micro grid stabilization using virtual synchronous machine*,International conference on renewable energies and power quality,Spain, 15 - 17 April 2009.

[8] M.G. Molina: *Power flow stabilization and control of microgrid wind wind generation by superconducting magnetic energy storage*,special issue on power electronics for microgrids, IEEE, 2010.

[9] A.A. Solomon, D. Faiman, G. Meron: *Properties and uses of storage for enhancing the grid penentration of very large photovoltaic systems*,Energy policy, Elsevier, 2010.

[10] T.M. Masaud, K. Lee, P.K. Sen: *An overview of energy storage technologies in electric power systems: What is the future*, North American Power Symposium (NAPS), IEEE, 2010.

[11] H. Chen, T.N. Cong, W. Yang, C. Tan, Y. Li, Y. Ding: *Progress in electrical storage systems: A critical review*, Progress in natural science 19, Elsevier Limited and Science in China Press, pp. 291 - 312 , 2009.

[12] Supervised by: B. Espinar, D. Mayer : *The role of energy storage for mini-grid stabilization*,International Energy Agency Photovoltaic Power Systems Program, France, July 2011.

[13] R. Passey, M. Watt, H. Outhred, T. Spoone and M. Snow: *Study of grid-connect PV systems, benefits, opportunities, barriers and strategies*,Centre for energy and environmental markets, Australia.

[14] W.A. Cronje, I.W. Hofsajer, M. Shuma-Iwisi and J. Braid: *Design considerations for rural modular microgrids*, Future energy grids and systems symposium, Second IEEE Energycon conference and exhibition,pp. 743 -748, IEEE, Florence, Sept 2012.

[15] A. Engler, N. Soultanis: *Droop control in LV-Grids*,Future power systems, 2005 International conference, 6pp. - 6, IEEE, Amsterdam, 18 Nov. 2005.

[16] J.A Pecas Lopes, C.L. Moreira and A.G. Madureira: *Defining control strategies for Microgrids Islanded Operation*, Power systems, IEEE transactions , Vol. 21, Issue. 2, pp. 916 - 924, IEEE, May 2006.

[17] Mukul. C. Chandorkar, Deeapkraj M. Divan and Rambabu Adapa: *Control of parallel connected inverters in standalone ac supply systems*, Industrial Applications, IEEE transactions, Vol. 29, Issue. 1,pp. 136 - 142, IEEE, Jan/Feb 1993.

[18] NRS: *Voltage characteristics, compatibility levels, limits and assessment methods*, Electrical supply-quality of supply, NRS 048-2:2003, South Africa, 2003.

DYNAMIC POWER REQUIREMENTS FOR CONTROLLED ENERGY STORE USED FOR STABILIZATION OF THREE-PHASE LOW-VOLTAGE STANDALONE MICROGRID

N. Horonga* **and W. Cronje**

* *Faculty of Engineering and the Built Environment, Private Bag 3, Wits 2050, South Africa. E-mail: nyasha.horonga@students.wits.ac.za and willie.cronje@wits.ac.za*

Abstract: This paper investigates the dynamic power requirements for controllable energy storage systems used for stabilization of standalone three-phase low-voltage microgrids with high penetration of renewable energy. It uses recorded data for fluctuating power sources and fluctuating loads to determine how an ideal controllable energy store can be used to stabilize a microgrid with 100% renewable energy penetration. Simulations incorporating the measured data show that a Proportional Integral Derivative (PID) controller can be used to control the ideal energy storage device to ensure stability of the microgrid.

Key words: microgrids, energy storage emulation, Distributed Generation (DG), Microgrid emulation, remote communities, microgrid control.

1. INTRODUCTION

This paper focuses on understanding the dynamic power requirements for controllable energy storage systems to stabilize standalone three-phase low-voltage microgrids with renewable energy sources. This research is undertaken because in many countries, remote areas are unable to receive power from the utility grid and the use of a standalone microgrid is often considered as one of the solutions that can be used to address the problem. Renewable energy sources with large fluctuations are frequently the source of power for these standalone microgrids. The fluctuating nature of these renewable sources often lead to frequent blackouts.

The remaining sections in this paper will discuss the background, problem statement and methodology for the research. A brief discussion on results for this research is also presented.

2. BACKGROUND

Figure 1 shows an example of a typical standalone microgrid. This standalone microgrid can be powered from Distributed Generation (DG) sources such as Photovoltaic (PV), wind or diesel generators. The renewable sources are influenced by natural conditions such as varying wind speed and cloud movements and cannot produce power continuously and steadily. This is illustrated by the measured insolation data ($P_{\mathrm{PV}}(t)$) in figure 2 recorded on the roof of the Genmin building, University of the Witwatersrand. The insolation data was normalized to the insolation peak of 31.28 W/m^2 for the 5 days. The data was sampled at 5 minute intervals.

Fluctuating loads have always been present in power systems. Figure 3 shows the normalized recorded data for the power demand ($P_{\mathrm{load}}(t)$) of a representative load. The load data was recorded for the Genmin building at

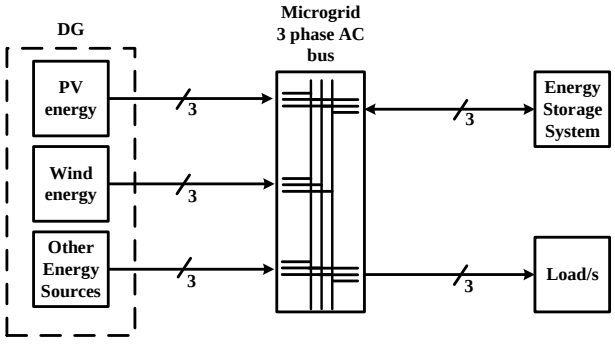


Figure 1. A single line schematic example of a three-phase low voltage standalone microgrid system.

the University of the Witwatersrand. The power demand values were normalized to the Genmin building load peak of 22 kW. The original data was sampled at 30 minute intervals and resampled at 5 minute intervals

Using fluctuating sources on a standalone microgrid

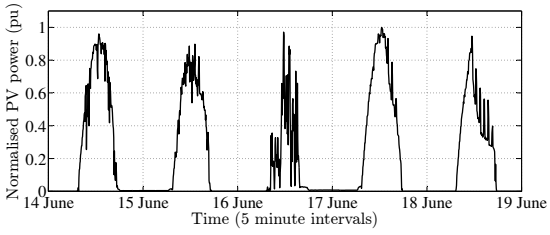


Figure 2. Normalized measured insolation (W/m^2) obtained at the Genmin building (Wits University) during the week of 14 - 20 June 2014.

which already has a fluctuating load can result in significant system power fluctuations. These fluctuations can negatively impact the microgrid operation because

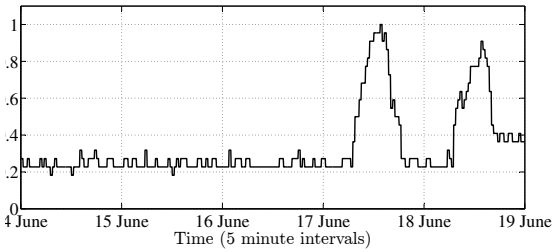


Figure 3. Normalized measured power demand for the Genmin building (Wits University) during the week of 14 - 20 June 2014.

they cause disturbances in the supply voltage. These disturbances includes voltage sags, transients, harmonics, dips and swells that can cause tripping or damage to sensitive appliances [1] [3].

Controllable energy storage can be used to compensate for the microgrid power fluctuations [4–9].

This study will focus on a simplified standalone microgrid that has a single source (in this case a PV source), a single load and a controllable energy store as shown in figure 4 to limit the complexity of the problem.

Depending on the requirements of the microgrid, different types of energy storage systems can be considered. These energy storage systems can be classified into short-term and long-term storage as shown in figure 5. Short-term storage is mainly applied to improve power quality, particularly to maintain the voltage stability during transients [10]. Long-term storage is deployed to contribute towards the energy management, frequency regulation and grid congestion management [10]. Choosing the appropriate energy storage system to stabilize a microgrid requires an understanding of the characteristics of existing energy storage systems. These characteristics includes ramp rate, charge rate, discharge rate, efficiency, energy and power density and response time and are explained in [12]. For the current paper, the most applicable dynamic characteristics are:

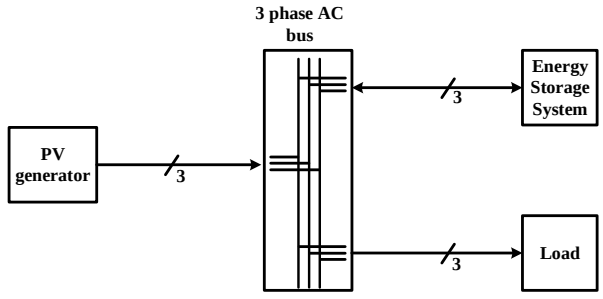


Figure 4. A single line schematic example of a three-phase low-voltage standalone microgrid system with only one power source(PV source).

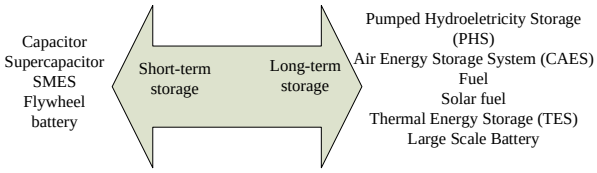


Figure 5. Energy storage classification [11].

- **Response time:** The amount of time the storage system requires to respond to a change in power power demand.
- **Ramp rate:** The rate at which the power flow can change and is sometimes known as the slew rate.

Although the current research is aimed at the dynamic behavior of a power network which strongly depend on DG (100% penetration), sizing of the storage is essential. It is important to note that the total energy supplied by DG and the total energy required by the load must always balance. Using the normalized data obtained from the Genmin building at the University of the Witwatersrand, the PV installation must be scaled by a factor of 1.6 pu for the system to meet the 5 day energy demand of the load. This value is obtained by integrating the normalised load consumed by the Genmin building over 5 days from 14th to 18th of June 2014. The result of the integration was then divided by the integrated normalised PV power over the same period of time. The factor 1.6 calculated above assumes that all the insolation energy is converted into energy required by the load with no losses. This is incorrect in real life and hence efficiency must be taken into account in future studies.

In addition, the PV system power must match the power demanded by the load and if there is any power imbalance, storage must supply the power or store the excess power as shown in equation 1.

$$P_{\mathrm{ES}}(t) = P_{\mathrm{PV}}(t) - P_{\mathrm{load}}(t) \tag{1}$$

Figure 6 shows the overlaid profiles of power generation and load based on the data for the Genmin building on the

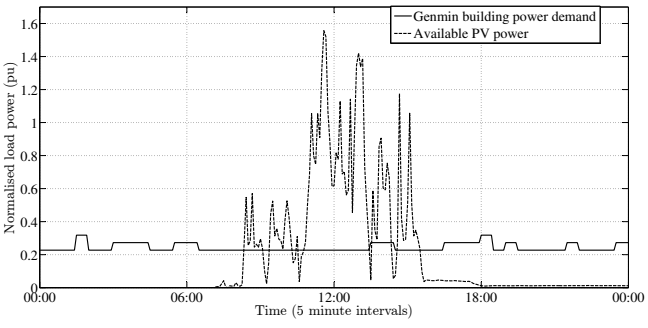


Figure 6. Measured PV and load profiles obtained from Genmin building (University of the Witwatersrand) on the 16th of June 2014

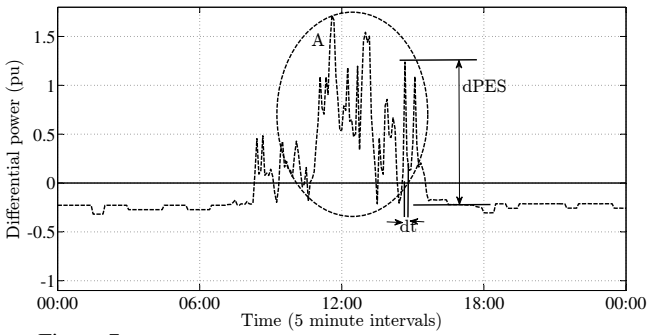


Figure 7. Calculated power difference between PV power and Genmin building load demand.

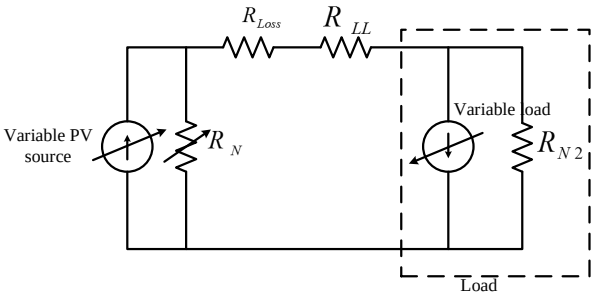


Figure 8. Simulation circuit for a standalone microgrid with 2 current sources modelling the PV source and the variable load respectively.

16th of June 2014. The data recorded on the 16th of June 2014 was selected because the insolation fluctuations were severe. This figure clearly illustrates that power generation does not always match the power demand.

Figure 7 shows the power difference (i.e. the difference between the potential power generation and power demand profiles). The data used as a representative case was obtained from normalized PV and Genmin building power demand data on the 16th of June 2014 at the University of the Witwatersrand. The graph also shows the power to be compensated by energy store and the study will mainly focus on the dynamic behavior of the system (i.e. region A). This power difference is seldom zero and hence the need for an energy storage system. The graph also shows that using the available data, the energy storage system must have a ramp rate (slew rate given by $\frac{dP_{ES}}{dt}$) of 0.1535pu/min. A new set of data with faster sample rate will be used in the future to represent the insolation and load demand data with better resolution and this will provide more accurate ramp rate.

Because the objective of this research is to investigate and determine the dynamic power requirements for using controllable energy stores to stabilize three-phase AC microgrids and ensure power balance, Simulations are conducted for the simplified microgrid in figure 4 to enhance understanding of the problem.

3. SIMULATIONS

The simulations are performed in Simulink®, using idealised models to better understand the dynamic requirements for the controlled energy store. The simulations assume that the microgrid is a balanced three phase system and only one phase needs to be analysed. In these simulations, The PV source and the fluctuating load are modeled using norton equivalent circuits with controlled current sources.

The simulations are done with and without the controlled energy store. In these simulations the current sources representing the PV source and the load are controlled by the pre-recorded data shown in figure 2 and 3.

To better resemble the behavior of a real PV grid-tie inverter, the variable resistor value R_N in figure 8 and figure 11 is varied to keep the grid voltage within the acceptable range ($\pm$ 5V in this case). When the PV source current is high, the resistor value R_N is reduced and this will reduce the voltage on the microgrid. When the PV source current is low resistor value R_N is increased thereby keeping the grid voltage almost constant. If the PV source current is too low to sustain the voltage on the microgrid, the system blackouts.

3.1 Simulations without storage

In the absence of a controlled energy store, the grid voltage will fluctuate and these fluctuations can lead to problems on the microgrid. Figure 8 shows the simulation model for the microgrid without energy storage.

In a microgrid the voltage must be limited to the standardized voltage range. If the voltage is below 210V, the grid collapses and if the voltage is greater than 250V, the microgrid maintains the voltage of 230V $\pm$ 20V as shown in figure 9. This figure also shows that, the absence of energy storage leads to frequent severe blackouts especially for days where there are high fluctuations in insolation.

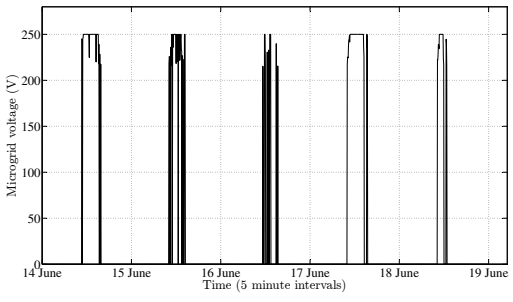


Figure 9. Simulation results for the PV supplied microgrid without storage with a PV inverter voltage controlled to 230V $\pm$ 10 %.

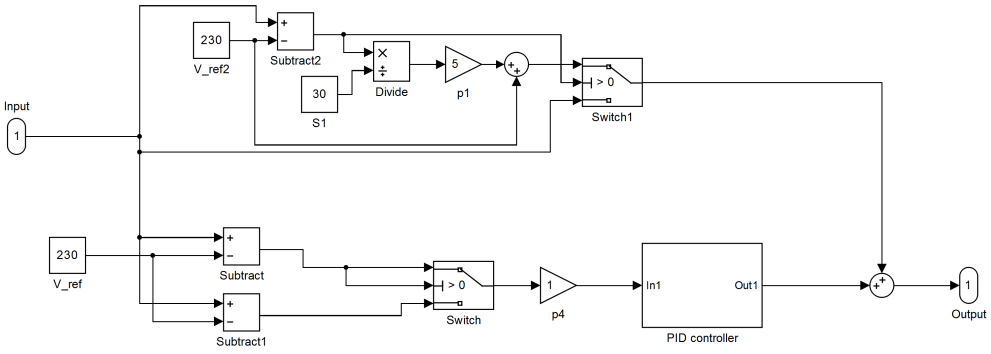


Figure 10. Simulink® circuit showing how the energy storage control signal is generated using the voltage and current signals.

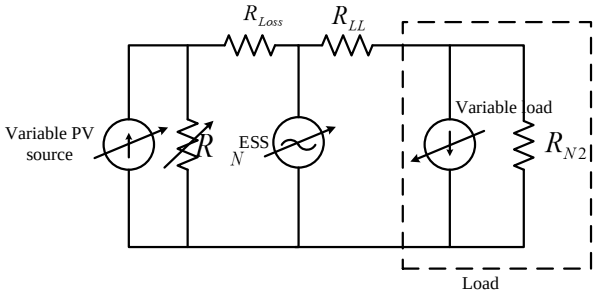


Figure 11. Simulation circuit for a standalone microgrid with current sources modeling PV source and variable load. A controlled voltage source is used to model an ideal energy storage system.

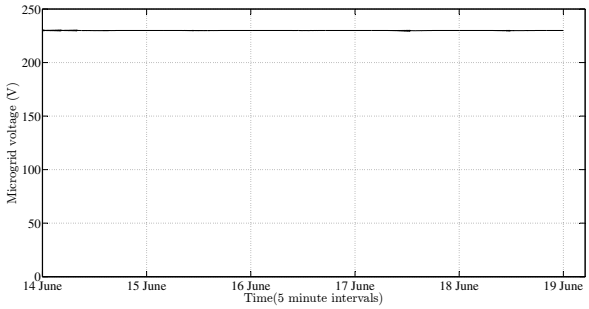


Figure 12. Simulation results of the microgrid with integrated controlled ideal energy storage system.

3.2 Simulations with storage

Subsequent to the simulations for a microgrid without storage, an energy store is introduced. The energy storage system is modeled using a controlled voltage source to regulate the microgrid voltage so that it remains almost constant at all time. By increasing or decreasing the voltage of the energy storage system, the direction of power flow can be changed as required. The energy storage system must maintain the voltage in the range of 230 V $\pm$ 10% [13]. Figure 11 shows the simulation model for the microgrid with ideal controllable energy store.

The block diagram in figure 10 shows how the energy storage control signal is generated in Simulink®. This control block has only one input at present (the microgrid voltage at the point of connection of the energy storage system). A PID controller is used to regulate the voltage. This PID controller uses the microgrid voltage and it assumes that the voltage is equal to the supply voltage of 230V plus an error ΔV (i.e. the difference between the measured microgrid voltage and 230V). The controller then responds to keep ΔV as close to zero as posible.

The results in figure 12 of this simulation for the microgrid with ideal energy storage shows that the voltage can be maintained in the range of 230V $\pm$ 1V, which is acceptable for most appliances.

4. DISCUSSION

The results in figure 12 shows that a controlled ideal energy store can be used to stabilize a microgrid with strongly fluctuating power sources and non-constant loads. The simulations do not yet take into account the state of the energy storage system and assumes that there is an infinite amount of energy stored.

The ramp rate and response time are not yet considered in this paper because of the idealized storage model used in the simulations. As part of the future work, an improved model for the energy store with all the required properties will be developed.

Data used in this paper was recorded at 5 minute and 30 minute intervals. There is a need to record the insolation data and load demand at a much faster sampling rate to establish if there is a change in the ramp rate as the

sampling time increases.
Experiments will be conducted on a microgrid testbed to verify the simulation results. The system block diagram shown in figure 13 shows the experimental setup that can be used to carry out the study. Sets of induction machines and variable speed drives will be used to emulate various DGs or energy storage systems as shown in figure 14 depending on the control signal used. Each emulator will receive a control signal that is used to generate a power profile resembling DGs or loads or energy storage system response.

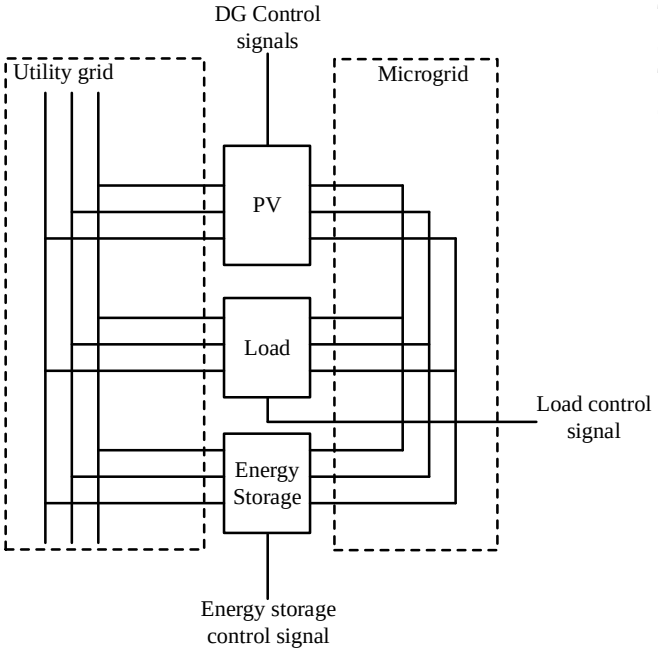


Figure 13. System block diagram of the microgrid testbed that will be used in this study.

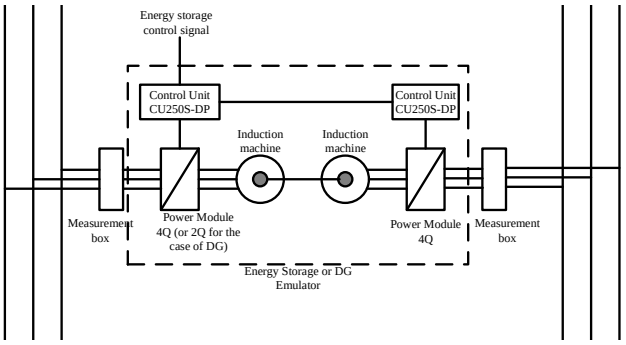


Figure 14. System block diagram of an emulator that can be used as PV source or load or storage depending on the control signal.

5. CONCLUSION

A Simulink® model of a standalone microgrid with and without integrated controlled energy storage was developed. This model can be used to determine the dynamic requirements for stabilizing a microgrid with controlled energy storage. Results from the simulations show that, a PID controlled ideal energy store will be used to stabilize a microgrid with intermittent sources and fluctuating load demand. The model can be further modified to incorporate the properties of a real energy store. Some of these properties include ramp rate and response time and finite energy storage capacity.

ACKNOWLEDGMENTS

The authors would like to thank the ALSTOM chair for clean energy system technology for funding the research. The author would also like to thank ACTOM for providing equipments used for the research investigations.

REFERENCES

[1] X. Vallvé, A. Graillot, S. Gual, H. Colin: *Microgrid and demand side management in distributed PV grid-connected installations*, 9th International Conference on Electrical and power quality and utilization, Barcelona, 9 - 11 October 2007.

[2] Robert G. Ellis: *A Reference Guide to causes, effects and corrective measures*, Power systems harmonics, Rockwell International Corporation, Canada, 2001.

[3] W. Liang: *Determination of power system response during a small load fluctuations*,IEEE, 2009.

[4] Mohd. Hasan Ali, Minwon Park, In-Ken Yu, Toshiaki Murata and Junji Tamura: *Improvement of wind generator stability by fuzzy logic-controlled SMES*,Proceeding of international conference on electrical machines and systems, South Korea, 8 - 11 October 2007.

[5] G. Chen, Q. Yang, T. Zhang, Z. Bao , W. Yan: *Real-time wind power stabilization approach based on hybrid energy storage systems*,Sixth international conference on advanced computational intelligence, Hangzhou, China, 19 - 21 October 2013.

[6] J. Kim, S. Kim and J. Park: *Contribution of an energy storage system for stabilizing a microgrid during standalone operation*,Journal of electrical engineering and technology, Vol. 4, No. 2, pp. 194 - 200, 2009.

[7] R. Hesse, D. Turschner and H. Beck: *Micro grid stabilization using virtual synchronous machine*,International conference on renewable energies and power quality,Spain, 15 - 17 April 2009.